2019•2020

Faculteit Industriële ingenieurswetenschappen

master in de industriële wetenschappen: bouwkunde

Masterthesis

Optimal stiffness of longitudinal stiffeners in girders subjected to patch loading

PROMOTOR :

Prof. dr. ir. Herve DEGEE

PROMOTOR :

Prof. dr. Géze Balázs KOVESDI

Aaron Laenen, Jordi Vanderhoven

Scriptie ingediend tot het behalen van de graad van master in de industriële wetenschappen: bouwkunde

Gezamenlijke opleiding UHasselt en KU Leuven

UHASSELT KU LEUVEN

UHASSELT KU LEUVEN

2019•2020

Faculteit Industriële ingenieurswetenschappen

master in de industriële wetenschappen: bouwkunde

Masterthesis

Optimal stiffness of longitudinal stiffeners in girders subjected to patch loading

PROMOTOR :

Prof. dr. ir. Herve DEGEE

PROMOTOR :

Prof. dr. Géze Balázs KOVESDI

Aaron Laenen, Jordi Vanderhoven

Scriptie ingediend tot het behalen van de graad van master in de industriële wetenschappen: bouwkunde

UHASSELT KU LEUVEN

Deze masterproef werd geschreven tijdens de COVID-19 crisis in 2020. Deze wereldwijde gezondheidscrisis heeft mogelijk een impact gehad op de opdracht, de onderzoekshandelingen en de onderzoeksresultaten.

Preface

This Master's thesis is part of the study program Civil Engineering at the University of Hasselt (Uhasselt) and the Catholic University of Leuven (KU Leuven). This thesis could not have been written without the help of others. Therefore, we would like use this opportunity to thank some people for their help.

First of all, we would like to thank Budapest University of Technology and Economics (BME) for receiving us at their university as Erasmus students, and letting us do our research there. They have provided us the chance to investigate and write an interesting Master's thesis. Additionally, we would like to thank our external supervisor, Prof. dr. Géze Balázs Kovesdi. He was our contact within the university in Budapest. He provided us with some interesting documents to familiarize us with the subject of our thesis. Beside this, he helped us with our research and gave us feedback during the process of documenting it. Furthermore, we want to thank Prof. dr. ir. Herve Degée for supervising the academic aspect of our Master's thesis.

Finally, we are satisfied with the end result of our Master's thesis. It was not easy to provide a balance between answering the research question and achieving a sufficient academic level. However, we have a positive feeling about meeting the expectations of both our supervisors.

Budapest, 8th June 2020

Laenen Aaron, Vanderhoven Jordi

Table of content

Notations and symbols

The notations and symbols used in this thesis are listed and explained here in alphabetical order.

Roman notations and symbols

a	Panel length of the girder
a	length of the longitudinal stiffener, global imperfection
a, b	short span of the subpanels, local imperfection
b_1	Height of the loaded subpanel, clear distance between loaded flange and first stiffener
b_{eff}	Effective width
b_f	Width of the flange
b_{st}	Width of the longitudinal stiffener
C_0	Parameter for calculating the buckling coefficient of a longitudinally stiffened web according to Graciano
C_r	$= 6{,}6 * 10^6$ MPa, when $M_u < M_y\ (LRFD)$ or $1.5\ M_a < M_y\ (ASD)$ at location of the force
C_r	= $3{,}3 * 10^6$ MPa, when $M_u \geq M_y\ (LRFD)$ or $1.5\ M_a \geq M_y\ (ASD)$ at location of the force
D	flexural rigidity of a unit width of the web plate
$\frac{D_i}{D_{max}}$	Relative displacement of the upper and lower subpanel
E	Young's modulus
e_G	displacement, global imperfections
$e_{L,1,2,3}$	displacement, local imperfections
f_s	Correction factor / increasing factor in regression models
f_{yb}	Basic yield strength
f_{yf}	Yield strength of the flange
f_{yw}	Yield strength of the web
F	Force
F_{cr}	Elastic critical buckling load

F_{cr1} Elastic critical buckling load for the upper (directly loaded) panel, patch loading

F_{cr2} Elastic critical buckling load for the whole web panel, patch loading

F_{exp} Ultimate load acquired by tests

F_{Rd} Predicted patch load resistance of longitudinal stiffened girders

F_{R0} Predicted patch load resistance of unstiffened girders

$F_{R,Davaine}$ Predicted patch load resistance of longitudinal stiffened girders, Davaine

F_{Rd} Web buckling criterion for unstiffened girders

F_{Rd2} Web yielding criterion for unstiffened girders

F_{Rd3} Web sidesway buckling criterion for unstiffened girders

$F_{r,exp}$ Experimentally found patch loading resistance

$F_{R,Graciano}$ Predicted patch load resistance of longitudinal stiffened girders, Graciano

$F_{r,num.}$ Numerically found patch loading resistance

F_S Applied load

F_u Ultimate resistance

F_y Yield resistance

G Shear modulus

h Height of the web in specimen

h_{st} Height of stiffener

h_w height of the web

I_f Second moment of inertia, flange

$I_{st,I}$ Second moment of inertia, longitudinal stiffener

k Coefficient

k_{cr} Buckling load coefficient

k_F Buckling load coefficient, patch loading

k_{F1} Buckling load coefficient for the upper (directly loaded) panel, patch loading

k_{F2} Buckling load coefficient for the whole web panel, patch loading

k_{sl} Buckling load coefficient addition for a longitudinally stiffened web

K_{st} Torsional constant

L_b Largest laterally unbraced length along either flange at the point of load

L_{eff} Effective length for resistance to transverse forces

l_y effective loaded length

m_1 contribution of the flange to the patch load resistance of unstiffened girders

m_2 contribution of the web to the patch load resistance of unstiffened girders

M_a Required flexural strength using ASD load combinations

M_e Applied bending moment

M_i Plastic moment resistance, inner plastic hinge in flange

M_o Plastic moment resistance, outer plastic hinge in flange

M_{pf} Plastic moment resistance, flange

M_{pw} Plastic moment resistance, web

M_R Bending moment resistance according to EN 1993-1-5

M_u Required flexural strength using LRFD load combinations, kip-in [N-mm]

M_y Yield moment about the axis of bending, kip-in [N-mm]

N_{cr} Critical load

s_h influence of the horizontal stiffeners, correction factor Bergfelt

s_η modified distance between the outmost plastic hinges in the upper flange

s_s Loaded length

s_v influence of the vertical stiffeners, correction factor Bergfelt

s_y Distance between plastic hinges in loaded flange

t_f Thickness of the flange

t_i Flange thickness, idealized ; correction factor for the flange thickness (Bergfelt)

t_{st} Thickness of the longitudinal stiffener

t_w Thickness of the web

$V_{1(2),s}$ Reaction shear force

Greek notations and symbols

α	Angle
α	Distance between the yield lines in the web
α, α_F	Imperfection factor, reduction function
β	Distance between the plastic hinges
β_1	factor for the slenderness of the flange, SIA
β_2	factor for the slenderness of the web, SIA
β_3	factor for the loaded length, SIA
β_4	factor for the longitudinal stresses, SIA
γ	Boundary condition dependent parameter
γ^t	Transition rigidity of the longitudinal stiffener
γ_M	Partial factor for resistance
γ_M^*	Corrected partial factor for resistance
γ_{M1}	Partial factor for members susceptible to instability
γ_{st}	Relative flexural rigidity of longitudinal stiffener
$\gamma_{st,opt}$	Relative flexural optimal rigidity of longitudinal stiffener, numerically obtained
$\gamma_{st,opt,EC}$	Optimal stiffness of longitudinal stiffener, Eurocode formulation
$\gamma_{st,opt,LBA}$	Optimal stiffness of longitudinal stiffener, LBA formulation
$\gamma_{st,opt,GMNIA}$	Optimal stiffness of longitudinal stiffener, GMNIA formulation
δ	Deformation
δ_w	In-plane deformation of the web
ε	Strain or Material dependent parameter
η	Correction factor for bending moment or imperfection factor
θ	Angle defining deformation of web with yield lines
λ	Slenderness
λ_F	Plate slenderness parameter, patch loading
v	Poisson's ratio, $v = 0{,}3$ if nothing else is stated
σ	Stress
σ_b	longitudinal stress in the flange

σ_c	Compressive stress
σ_{cr}	Critical stress
σ_r	Residual stress
σ_w	Stress in the web
σ_x	Normal stress
φ_F	Slenderness, patch loading
ϕ_{st}	Relative torsional rigidity of longitudinal stiffener
$\chi(\lambda)$	Resistance function
χ	Reduction factor
χ_F	Reduction factor, patch loading
Ψ	Stress ratio

Table list

Figure list

Abstract

Hungarian bridges are usually built using the incremental launching method. This causes large support reactions which need to be considered in the design of the bridge. EN 1993-1-5 gives the patch loading resistance of girders with longitudinal stiffeners, which is known to have a significant underestimation. This formulation is designed for girders with only one longitudinal stiffener, while most bridges are built using two or more stiffeners. The goal of this study is to investigate the patch loading design resistance of the EN 1993-1-5 for stiffened girders and to improve it.

This study is performed using numerical simulations (ANSYS). The effect of four main parameters are examined, which are: the loaded length of the patch load, the length of the girder, the height and the thickness of the web. Afterwards, the effect of the ratio of the height of the loaded subpanel (b_1) over the thickness of the web (t_w), is examined in function of the number of stiffeners.

The results of the numerical simulations are used for a new, improved proposal for a design equation to apply "strong" stiffeners. The previously developed patch loading resistance formula is based on the b_1/t_w ratio and is more accurate and usable for girders with two or more longitudinal stiffeners. However, it needs "strong" stiffeners. The current study checked and developed an improved equation to check if a stiffener can be classified as "strong" or "weak". This is the requirement for the new patch loading resistance formulation.

Abstract Nederlands

Bruggen in Hongarije worden gebouwd met de incrementele lanceringsmethode. Deze zorgt voor een tijdelijke reactiekracht op het steunpunt, wat ingecalculeerd wordt in het ontwerp van de ligger. EN 1993-1-5 geeft een methode om de reactiekracht van longitudinaal verstijfde liggers te berekenen, maar die wordt onderschat. Deze methode is ook ontworpen voor liggers met slechts één verstijver, terwijl de meeste bruggen met twee of meer verstijvers gebouwd worden.

Het doel van dit onderzoek is om de reactiekracht van verstijfde liggers, gegeven door EN 1993-1-5, te onderzoeken en te verbeteren. Dit onderzoek maakt gebruik van een numerieke simulatie in ANSYS. Het effect van de vier belangrijkste parameters voor het berekenen van de reactiekracht van de verstijfde liggers zijn onderzocht. Deze zijn: de belaste lengte, de totale lengte van de ligger, de hoogte en de dikte van het lijf. Ook het effect van de hoogte van het belaste paneel (b_1) ten opzichte van de dikte van het lijf (t_w) is onderzocht in functie van het aantal verstijvers.

De resultaten van het onderzoek zijn gebruikt om een voorstel te doen voor een verbeterde ontwerpmethode voor het gebruik van “sterke” verstijvers. Een eerder ontworpen reactiekrachtformule is gebaseerd op de b_1/t_w ratio en is zowel accurater als bruikbaarder voor longitudinaal verstijfde liggers met meerdere verstijvers. Het gebruik van “sterke” verstijvers hierin is noodzakelijk. Een nieuwe formule wordt voorgesteld om het onderscheid tussen “sterke” en “zwakke” verstijvers te bepalen.

1. Introduction

1.1 Situating

This Master's thesis is performed by two master students from the faculty Civil Engineering of the University of Hasselt (Uhasselt) and the Catholic University of Leuven (KU Leuven). This research was done during an Erasmus exchange in Budapest, Hungary at the Budapest University of Technology and Economics (BME). The performed research investigates the currently available design methods for longitudinally stiffened girders. Eurocode 3 (EN 1993-1-5) [1] formed the base for this research. The design methods are analyzed by using numerical models which are verified based on previous experimental tests.

1.2 Problem statement

The purpose of this investigation is based on the building process of most of the Hungarian bridges. Hungarian bridge erections are performed using a launching technique called "incremental launching". This process is executed in different stages as shown in Figure 1. First, the launching nose is placed and pushed forward to the next pier. In the second phase, the precast segments are pulled over the launching nose. When the cantilever of a part is at its longest point, the patch load onto the I-girder is at his highest value. This patch load can lead to web crippling or web buckling of the I-girder. This can occur due to the use of slender webs for economic reasons. The web buckling is the most common failure mode in Hungarian bridges. Small, vertical stiffeners between the loaded flange and the stiffener are used along the entire bridge to strengthen the longitudinal stiffener. However, this solution causes high manufacturing costs and the structure becomes fatigue sensitive [2]. A more cost efficient solution for this problem is the usage of longitudinal stiffeners [3]. Because of these difficulties, and the widely usage of this method, EN 1993-1-5 [1] describes the design of these stiffeners, despite the fact that the problem is a problem in service state and not in the usage state. The design of these longitudinally stiffened girders is based on the design method described in EN 1993-1-5 [1]. However, there are several problems and voids related to this design method.

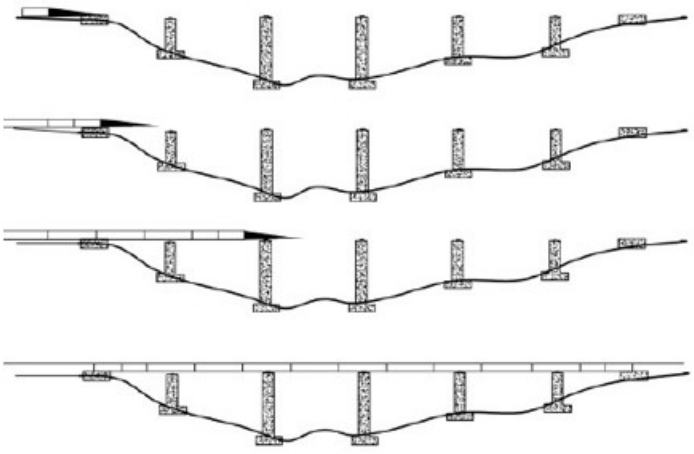

Figure 1: Incremental launching method [4, p. 39]

The first problem with the design method from Eurocode 3 is that the design method is not valid in all geometric ranges. A second problem is the character of the resistance model. This is currently based on one failure mode while there are more failure modes which can occur in reality, depending on the amount and stiffness of the longitudinal stiffener(s) (local buckling of the subpanels, global buckling or an interaction of these failure modes) [2]. Lastly, the design method from EN 1993-1-5 is developed for girders stiffened with only one longitudinal stiffener, while in reality most bridges are built with more than one longitudinal stiffener.

1.3 Goal

The goal of this research is to improve a newly proposed formula for calculating the patch load resistance of longitudinally stiffened girders. In this new formula, a difference has to be made between “weak” and “strong” stiffeners, since this formula is only applicable for “strong” stiffeners. A “strong” stiffener causes a local buckling failure mode, which results in the highest patch loading resistance. Therefore, this investigation is focused on defining a “strong” stiffener. The term “strong” stiffener is based on the stiffness of a longitudinal stiffener. This stiffness is a factor based on the moment of inertia of the composite part of the stiffener and partly of the web of the girder. When making a longitudinal stiffener stiffer, the failure modes will differ and are depending on this value. The optimal stiffness is an important value in this design method because this describes the point from where the stiffener is “strong” and from where there is no further patch load gaining in making the stiffener stiffer. It is important for economic and ecological reasons to describe this point precisely. Therefore, this new design proposal is mostly based on improving the calculation for the optimal stiffness of the longitudinal stiffener.

1.4 Method

Firstly , a theoretical literature review will be done about the research that has already been done about stiffened and unstiffened I-girders. This literature review will also cover the existing designing method from EN 1993-1-5 [1] and will point out the main criticism of this designing method.

Secondly, a numerical model will be created based on the experimental tests conducted by Seitz [5] at the university of Stuttgart. This will be a model with one longitudinally stiffener. This numerical model will be tested and validated based on these experimental test results.

Afterwards, this model will be adjusted to the research domain. This domain includes girders with one, two and three stiffeners. Once these models are completed, a parametrical study will be conducted focusing on four main parameters that can influence the optimal stiffness of a longitudinal stiffener. The aim is to establish a link between the optimal stiffness of a girder and an influencing parameter. If such a link is established, a formula will be created using regression to describe the optimal stiffness of a girder in function of this influencing parameter.

Lastly, the investigation will be documented in this master thesis.

2. Literature review

This chapter describes several methods for determining the patch loading resistance which is available in the literature. Firstly, two models (empirical and mechanical) for determining the patch load resistance of unstiffened girders will be reviewed. Secondly, three different models (direct, regression, reduction factor) for determining the patch load resistance of girders with one longitudinal stiffeners will be reviewed. Afterwards, the standards (British, Swiss, American and European) will be reviewed. Lastly, experimental results from the literature will be discussed.

2.1 Unstiffened girders

The topic of this Master's thesis is the optimal stiffness of longitudinal stiffeners and their influence on the patch loading resistance, hence the patch loading resistance of stiffened I-girders is investigated. However, in many cases this patch loading resistance of longitudinally stiffened girders is determined through the solution of the unstiffened girder. Therefore, it is important to examine this topic as well.

Firstly, there were only empirical methods to calculate the patch loading resistance of unstiffened I-girders. Later, when there were more experiments and studies performed on this subject, more accurate mechanical models emerged. First the empirical methods will be discussed and afterwards the more accurate mechanical models.

2.1.1 Empirical models

Granholm (1960) gave the first formula for calculating the patch loading of unstiffened I-girders. He based his formula on 11 experiments with different geometries. His conclusion was that the patch loading resistance was independent of the height of the web (h_w) and was only depending on the thickness of the web (t_w). The formula for calculating the patch loading resistance based on his experiments is given in eq. (2.1). This formula is significantly in favor of safety, the founded patch load resistance will be lower than it is in reality [6].

$$F_{R0} = 0.85 * t_w^2 \tag{2.1}$$

Bergfelt (1971) on the other hand developed a sizing procedure to estimate the patch loading resistance. He also experimentally investigated the effect of the thickness of the flanges (t_f). This resulted in a new formulation of eq. (2.1) and is given in eq. (2.2) [6].

$$F_{R0} = 0.045 * E * t_w^2 * \left(0.55 + 0.22 * \frac{t_f}{t_w}\right) \tag{2.2}$$

2.1.2 Mechanical models

The mechanical models are based on a yield line mechanism, developed by Roberts and Rockey. This chapter will present the work of Roberts and Rockey (1979), Bergfelt (1979) and Lagerqvist (1994). These models determine the resistance of unstiffened girders. The first

model based on failure mechanisms was developed by Roberts and Rockey. This model was later modified by Lagerqvist and Johansson [7].

2.1.2.1 Roberts and Rockey (1979)

Roberts and Rockey [8] made a proposition for the ultimate resistance of unstiffened I-girders which are subjected to patch loading. This proposal is based on a yield line mechanism which consists of four plastic hinges in the loaded flange and three yield lines in the web (Figure 2).

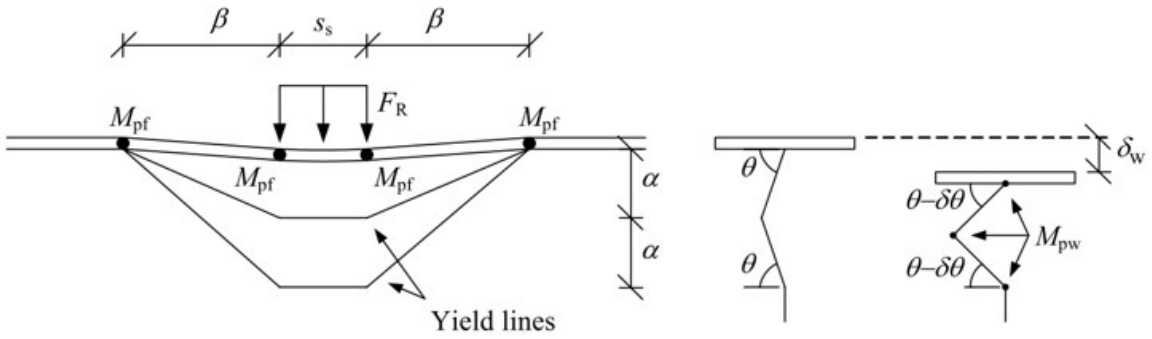

Figure 2: Failure mechanism proposed by Roberts and Rockey [8, p. 1330]

The loaded flange is moved downward, with a value of δ_w, due to the patch loading. This downward movement is described by eq. (2.3).

$$\delta_w = 2 * \alpha * cos\theta * \delta\theta \tag{2.3}$$

The position of the yield lines was assumed to be as shown in eq. (2.4) [8].

$$\alpha = 20 t_w f_{yw} / f_{yf} \tag{2.4}$$

This causes the yield line position to be limited to 2α, which is approximately 40 times the thickness of the web. The parameter θ characterizes the deformation of the web just before failure. The mechanism that is described was used to formulate an expression for calculating the patch load resistance of unstiffened girders. In order to simplify the method, approximations and empirical modifications were used to make it easier to apply this method on hand calculations. The formulation of Roberts and Rockey is presented in eq. (2.5) [6].

$$F_{R0} = f_{yw} * t_w * \left(s_s + 2 * t_f * \sqrt{\frac{f_{yf} * b_f}{f_{yw} * t_w}} \right) \tag{2.5}$$

2.1.2.2 Bergfelt

Bergfelt also used a yield line mechanism to formulate his proposal. The mechanism Bergfelt used is shown in Figure 3. This mechanism shows that there is a plastic hinge formed just below the load which causes the web to flow after the stress limit (f_{yw}) is reached. The positive and negative bending moments generated in the flange will increase and will cause additional plastic hinges to form at the end points of the load. This will result in failure of the structure [6].

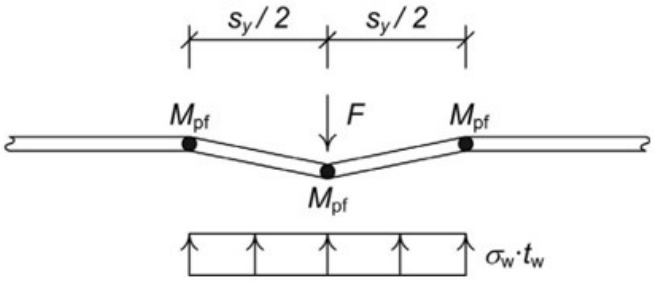

Figure 3: Failure mechanism proposed by Bergfelt [6, p. 1330]

Bergfelt then tried to find a satisfactory correlation with the tension in the web (σ_w) and this mechanism. He formulated the connection between the dent in the flange and the tension in the web as following:

$$\sigma_w = \sqrt{\sigma_{cr} * f_{yw}} \tag{2.6}$$

The proposed solution of Bergfelt for calculating the patch loading resistance of unstiffened girders is given in eq. (2.7).

$$F_{R0} = 0.8 * t_w^2 * \sqrt{E * f_{yw}} * \sqrt{\frac{t_i}{t_w}} * f(s_s, h_w, etc) \qquad if\ \frac{t_f}{t_w} > 2 \tag{2.7}$$

t_i represents the correction factor for the flange width, and is calculated as following:

- $b_f = 25 * t_f \rightarrow\ t_i = t_f$ (2.8a)
- $b_f \neq 25 * t_f \rightarrow t_i = t_f * \sqrt[4]{\frac{b_f}{25 * t_f}}$ (2.8b)

The correction factor $f(s_s, h_w, etc)$ is in function of different geometric parameters, which are presented in detail in the literature [9]. Eq. (2.9) gives a simplified version of this formula:

$$f(s_s, h_w, etc) = f(s_s) * f(h_w) * f\left(f_{yw}\right) * f(M_E) * f(\delta) * f(s_v) * f(s_b) \tag{2.9}$$

2.1.2.3 Lagerqvist (1994)

Lagerqvist performed several experiments and numerical simulations to be able to make a recommendation for a design procedure for calculating the resistance of unstiffened steel girders subjected to patch loading. The model that Lagerqvist used (Figure 4) is very similar to the one that Roberts and Rockey used (see section 2.1.2.1). The difference between the two models is that Lagerqvist also included a part of the web in the plastic hinges of the flange and thus forming a T-section as shown in Figure 4. He came to this conclusion based on his experiments. His experiments showed that when the slenderness of the web was increased, the effective loaded length ($l_y = s_s + 2 * t_f + s_y$) also increased [6].

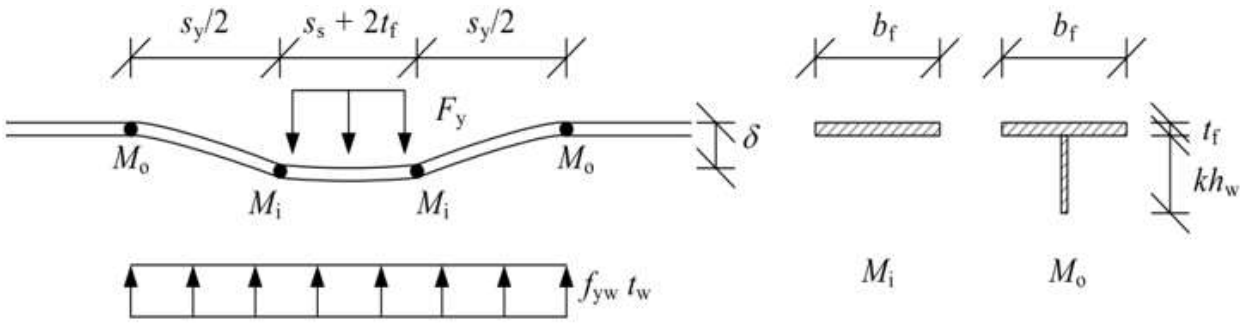

Figure 4: Mechanical model of Lagerqvist [6, p. 17]

The research of Lagerqvist makes use of the yield resistance (F_y), the slenderness parameter ($\lambda = \sqrt{F_y/F_{cr}}$), where F_{cr} is the elastic critical load, and the resistance function ($\chi(\lambda)$) which reduces the yield resistance depending on λ . The patch loading resistance for unstiffened girders (F_{R0}) is given in eq. (2.10) [10] - [11].

$$F_{R0} = F_y * \chi(\lambda) \tag{2.10}$$

With F_y the yield resistance calculated as in eq. (2.11).

$$F_y = f_{yw} * t_w * l_y \tag{2.11}$$

With l_y the effective loaded length calculated as following in eq. (2.12)

$$l_y = s_s + 2 * t_f + \sqrt{m_1 + m_2} \tag{2.12}$$

m_1 and m_2 are dimensionless parameters (m_2 should be taken as zero if $\lambda < 0.5$ and when a welded girder is used)

$$m_1 = \frac{f_{yb} * b_f}{f_{yw} * t_w} \text{ and } m_2 = 0.02 * \left(\frac{h_w}{t_f}\right)^2 \tag{2.13}$$

The resistance function $\chi(\lambda)$ is calculated as in eq. (2.14) and the slenderness parameter as in eq. (2.15).

$$\chi(\lambda) = 0.06 + \frac{0.47}{\lambda} \leq 1 \tag{2.14}$$

$$\lambda = \sqrt{\frac{F_y}{F_{cr}}} \tag{2.15}$$

F_{cr} in eq. (2.15) represents the buckling load (critical load) and is determined by Lagerqvist as in eq. (2.16).

$$F_{cr} = k_F * \frac{\pi^2 * E}{12 * (1 - v^2)} * \frac{t_w^3}{h_w} \tag{2.16}$$

k_F is the buckling coefficient and is given by eq. (2.16).

$$k_F = 5.82 + 2.1 * \left(\frac{h_w}{a}\right)^2 + 0.46^4 * \sqrt{\beta} \text{ with } \beta = \frac{b_f * t_f^3}{h_w * t_w^3} \quad (2.17)$$

Lagerqvist suggests a simplification for both the equations of the resistance function $\chi(\lambda)$ and the buckling coefficient, respectively eq. (2.14) and eq. (2.17). These simplified formulas are given below:

$$\chi(\lambda) = \frac{0.5}{\lambda} \leq 1 \quad (2.18)$$

$$k_F = 6 + 2 * \left(\frac{h_w}{a}\right)^2 \quad (2.19)$$

This design procedure was calibrated to experimental results using a statistical method. They found that the value of the partial safety factor (γ_M^*) is 1,1 [6]. Therefore, the value of the resistance determined by Lagerqvist is as following:

$$F_{R0} = \frac{F_y * \chi(\lambda)}{\gamma_M^*} \quad (2.20)$$

2.2 longitudinally stiffened girders

This chapter will focus on the available models created for calculating the patch loading resistance of longitudinally stiffened girders. There are several different types of models to be found in the literature. The first models that will be discussed are the direct models. These methods try to calculate the patch loading resistance directly. Afterwards, the models using an incremental factor will be discussed. In these methods, the patch loading resistance is calculated for unstiffened girders and then multiplied by an increasing factor (f_s) to add the effect of the longitudinal stiffener and to estimate the resistance of the longitudinally stiffened girder. Lastly, the models using a reduction factor will be discussed. These methods implement the effect of the longitudinal stiffener in the critical load (F_{cr}) and in the buckling coefficient (k_F) by modifying it by an additive factor (k_{sl}).

2.2.1 Direct models

These models attempt to calculate the patch loading resistance of longitudinally stiffened girders directly. Firstly, the genetic programming (GP) method, developed by Cevik (2007) [8], is discussed. Afterwards, a model proposed by Graciano is discussed.

2.2.1.1 Cevik (2007)

The method developed by Cevik (2007) [8] is based on the principle of genetic programming (GP). GP is a technique in which a program is self-developing. It starts with pre-defined variables which are solved and mutated to refine an expressing and to eventually solve an expression, or at least to approximate the solution of an expression. During this process, the program keeps on making new solutions and it keeps the most accurate results and tries to refine the solution. At the end, the best-so-far solution is designated as the result of the genetic programming. Cevik's GP based formulation, applicable for the patch loading resistance of longitudinally stiffened girders, is based on several different experimental results

from the literature. He used 138 experiments with 11 variable geometric and material parameters [6], [8]. The result of this research was an explicit formulation for the patch loading resistance of longitudinally stiffened girders in function of these 11 variable geometric and material parameters. Eq. (2.21) gives a representation of the different parameters used in the GP formulation. The different expressions for this formulation are given in the following units:

$$F_{rl} = (t_w, a, h_w, f_{yw}, t_f, b_f, f_{yf}, S_s, b_l, t_{st}, b_{st}) \tag{2.21}$$

- F_{rl} [kN]
- $t_w, a, h_w, t_f, b_f, S_s, b_l, t_{st}, b_{st}$ [mm]
- f_{yw}, f_{yf} [MPa]

The final form of the GP formulation is given in eq. (2.22).

$$F_{rl} = \left(t_w + \frac{\cos(a^3)*\sqrt{f_{yw}}}{-5\ \ .57*t_{st}+s_s-83.08}\right) * \left(\frac{t_f}{\sqrt{t_f}+1\ \ .97+\frac{184.22}{s_s}}\right) * \left(\frac{f_{yf}}{h_w*b_1+65.81+b_f-98.77*(s_s-f_{yf})}\right) * \left(t_w + \frac{h_w}{t_f^2-1\ \ .42*t_{st}+f_{yf}-34.76-b_{st}}\right) \tag{2.22}$$

The accuracy of this final form is evaluated with the numerical results of the experimental database used for obtaining the formulation itself. The conclusion of this evaluation was that the GP formulation was more accurate than the existing methods, such as the British Standards (see section 2.3.1), the regression model developed by Bergfelt (see section 2.2.2.3) or the mechanical model developed by Roberts and Rockey (see section 2.1.2.1). However, there are still two important issues with this formulation despite the accuracy with the experimental results. Firstly, the proposed GP based equation is complicated which makes it difficult to use it in practical circumstances. The second problem is that this equation is only valid for the same variables used in the research of Cevik [8]. Therefore, this equation may not be dimensionally correct when using other variables than the ones used for the formulation of eq. (2.22).

2.2.1.2 Graciano – model II: Failure mechanism model

Graciano made a direct model for determining the patch loading resistance of longitudinally stiffened girders. He used the four-hinge model from Roberts and Rockey (see section 2.1.2.1) and added the stiffening effect of the longitudinal stiffener.

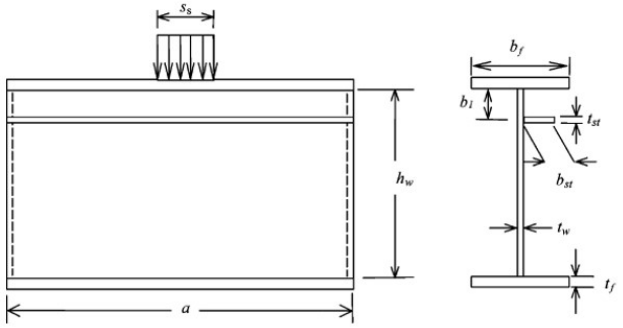

Figure 5: Longitudinally stiffened girder subjected to patch loading [12, p. 566]

He assumed that the yielding of the web and flange was equal ($f_{yw} = f_{yf}$). He formulated his patch loading resistance expression in the following two equations:

$$F_{R1} = 4 * t_w^2 * \sqrt{\frac{E*f_{yw}*t_f}{b_1}} + \frac{24*E*I_f*(s_s+2*t_f-\eta)*M_{pw}^2}{b_1*M_{pf}^2} \qquad if\ \frac{b_1}{t_w} \leq 40 \tag{2.23}$$

$$F_{R1} = 2 * f_{yw} * t_w^2 * \sqrt{\frac{2*E*t_f}{\alpha*f_{yt}}} + \frac{12*E*I_f*(s_s+2*t_f-\eta)*M_{pw}^2}{\alpha*M_{pf}^2} \qquad if\ \frac{b_1}{t_w} > 40 \tag{2.24}$$

The formulas presented above are divided depending on the position of the yield line. Eq. (2.23) is used when $\alpha = \frac{b_1}{2} \leq 20 * t_w$ and eq. (2.24) is used when $\alpha = 20 * t_w * f_{yw}/f_{yf}$. Both formulas use the parameter η, which is describe in eq. (2.25). This parameter assumes that the load at failure is transmitted in the length of the web, which is yielding due to membrane compressive stresses [3], [6].

$$\eta = \frac{M_{pw}*\left(4*\beta+2*\left(s_s+2*t_f\right)\right)}{2*M_{pw}+f_{yw}*t_w*\alpha*\frac{M_{pf}^2}{6*E*I_f*M_{pw}}} \tag{2.25}$$

This method is not usable for hybrid girders since the yielding of the web and the flange is not equal ($f_{yw} \neq f_{yf}$). Therefore, other design methods could be more useful then the model presented above. However, for cases where $f_{yw} = f_{yf}$, this method is suitable.

2.2.2 Incremental factor procedures (regression models)

This chapter will discuss the methods using an incremental factor to calculate the patch loading resistance of longitudinally stiffened girders. The idea of these models is to calculate the patch loading of an unstiffened girder (F_{R0}) and then multiplying this resistance by a correction factor (f_s), as shown in eq. (2.26). This correction factor is usually empirically determined by performing two equal experiments. Once the experiment is performed without the use of a longitudinal stiffener, once the same experiment is performed with the use of a longitudinal stiffener. The difference in the results is then determined as the correction factor [6], [10], [16].

$$F_R = F_{R0} * f_s \tag{2.26}$$

There are multiple proposals available in the literature which describe the correction factor. These will be discussed in the next paragraphs. The discussed methods are the ones of Markovic and Hajdin, Kutmanova and Skaloud, Bergfelt and Graciano's model I.

2.2.2.1 Markovic and Hajdin (1992)

The first proposal to be discussed is the one from Markovic and Hajdin. They developed a formulation based on several tests (133 longitudinally stiffened and 318 unstiffened girders) [6]. They proposed a linear equation for the consideration of the longitudinal stiffener with the use of the mechanism solution presented by Roberts and Rockey (see section 2.1.2.1) [11]. Eq. (2.27) gives the patch loading resistance of the unstiffened girder.

$$F_{R0} = 0.5 * t_w^2 * \sqrt{\frac{E * f_{yw} * t_f}{t_w}} * \left(1 + \frac{3 * s_s}{h_w} * \left(\frac{t_w}{t_f}\right)^{\frac{3}{2}}\right) * \sqrt{1 - \left(\frac{\sigma_b}{f_{yw}}\right)^2} \quad (2.27)$$

Eq. (2.28) gives the proposed correction factor, which is only depending on the relative position of the stiffener. However, it should be noted that this correction factor of Markovic and Hajdin is limited to $1.0 \leq f_s \leq 1.21$.

$$f_s = 1.28 - 0.7 * \frac{b_1}{h_w} \qquad lim: 0.1 \leq b_1/h_w \leq 0.3 \quad (2.28)$$

This formulation has also been incorporated in the 2000 Edition of BS 5400 Part 3 (British Standard, Code of practice for the design of steel bridges) [8], [11], [14].

2.2.2.2 Kutmanova and Skaloud (1992)

Kutmanova and Skaloud also did a proposal for calculating the patch loading resistance of longitudinally stiffened girders with the use of an increment factor. They based their proposal on experiments conducted by Janus in 1988 [15]. The patch loading resistance of unstiffened girders can be calculated using eq. (2.29).

$$F_{R0} = 12.6 * tw^2 * f_{yw} * \left(1 + 0.004 * \left(\frac{s_s}{t_w}\right)\right) * \left(\left(\frac{I_f}{t_w^4}\right) * \sqrt{\frac{f_{yf}}{240}}\right)^{0.153} \quad (2.29)$$

Eq. (2.30) gives the proposed correction factor, which is again only depending on the relative position of the stiffener. However, this correction factor has no limitation on the relative position of the stiffener.

$$f_s = 0.958 - 0.09 * \ln\left(\frac{b_1}{h_w}\right) \quad (2.30)$$

2.2.2.3 Bergfelt

Bergfelt used his own research, given in section 2.1.2.2, to suggest a new method based on the relative position of the stiffener and the distance between the plastic hinges in the loaded flange [11]. He presented a formula for the patch loading of an unstiffened girder in eq. (2.7). He later added a correction factor (f_s) to his research. This correction factor is given in eq. (2.31).

$$f_s = 1 + \left(\frac{1}{3} + \frac{b_1}{h_w}\right) * \sqrt{\frac{s_\eta}{3 * b_1}} \qquad lim: 0.1 \leq b_1/h_w \leq 0.3 \quad (2.31)$$

The factor s_η in eq. (2.31) represents the modified distance between the outmost plastic hinges in the upper flange. The value of s_η lies between the following interval, presented in eq. (2.32) [3]:

$$s_y + s_s \leq s_\eta \leq s_s + \frac{s_s^2}{s_y} \quad (2.32)$$

When considering the correction factor for the flange width (t_i), Bergfelt suggested eq. (2.33) for determining the distance between the outmost plastic hinges in the upper flange [3].

$$s_y = 5.2 * \frac{b_f}{\eta} * \left(\frac{t_f}{t_w}\right)^2 * \sqrt{\frac{t_w}{t_i}} * \frac{f_{yf}}{\sqrt{E * f_{yw}}} \tag{2.33}$$

2.2.2.4 Graciano – model I: Regression analysis of test results

Graciano also [11] developed an incremental factor procedure to calculate the path loading resistance of longitudinally stiffened girders. He used the method of Lagerqvist (see section 2.1.2.3) to determine the patch load resistance of the unstiffened girder. He determined the correction factor by conducting a regression analysis for the relative location of the stiffener (b_1/h_w), the ratio of the flange to web thickness (t_f/t_w) and the ratio of the flange to web yield strength (f_{yf}/f_{yw}). He found out that all three ratios had an influence on the patch load resistance and he thus presented the following formulation for the correction factor. Again, this correction factor is limited for the location of the stiffener.

$$f_s = 0.556 - 0.277 * \ln\left(\frac{b_1}{h_w} * \left(\frac{f_{yf}}{f_{yw}} * \frac{t_w}{t_f}\right)\right) \qquad lim: 0.1 \leq b_1/h_w \leq 0.3 \tag{2.34}$$

This formulation for the correction factor is the most accurate one to be found in the literature. It is the only one that takes the flange to web thickness and flange to web yield strength ratio into account and not only the relative position of the stiffener [6], [8], [10].

2.2.3 Reduction factor and elastic critical load

This chapter discusses the design methods which use buckling reduction factors (χ_F). These methods implement the effect of the longitudinal stiffener in the critical load (F_{cr}) and in the buckling coefficient (k_F) by modifying it by an additive factor (k_{sl}). However, this reduction factor should be evaluated by the same equation for unstiffened and longitudinally stiffened girders. Two methods using a reduction factor will be discussed in this chapter. The first model is from Graciano and second one is from Davaine.

2.2.3.1 Graciano – model III: Post-critical Resistance Approach

Graciano conducted a parametric study using the finite element package ABAQUS. In this study, he proposed an approximative solution for the buckling coefficient (k_F) for longitudinally stiffened girders subjected to patch loading. He started his numerical study on longitudinally stiffened and unstiffened girders and then compared the results with the already discussed methods presented above. He then refined his parametric study to find the significance of the relative position and flexural stiffness of the stiffeners [3], [6], [12].
Graciano used the results of his parametric study to improve the equation (eq. 2.17) found by Lagerqvist (see section 2.1.2.3). He changed this formula by adding an additive factor (k_{sl}). This new formulation is given in eq. (2.35), in which the additive factor takes the effect of the longitudinal stiffener (open or closed section) and the panel aspect ratio of the upper panel (b_1/a) into account [3].

$$k_F = 5.82 + 2.1 * \left(\frac{h_w}{a}\right)^2 + 0.46^4 * \sqrt{\beta} + k_{sl} \qquad \text{with } \beta = \frac{b_f * t_f^3}{h_w * t_w^3} \tag{2.35}$$

The first three terms on the right side of eq. (2.35) are valid for unstiffened girders. Stiffeners are often characterized by two dimensionless parameters: its relative flexural rigidity ($\gamma_{st} = \frac{EI_{st}}{h_w D} = 10.9 \frac{I_{st,l}}{h_w t_w^3}$) and its relative torsional rigidity ($ø_{st} = \frac{GK_{st}}{h_w D}$) . The additive factor takes the effect of the longitudinal stiffener, with its relative bending stiffness (γ_{st}), into account. It also includes a new factor (C_0) which is determined by a regression analysis and which is dependent on the $\frac{b_1}{a}-$ ratio. This is formulated in eq. (2.36) [12].

$$k_{sl} = C_0 * \sqrt{\gamma_{st}} \tag{2.36}$$

C_0 is also dependent on the cross section of the longitudinal stiffener (open or closed section). Therefore, this parameter can be divided into two parts:

$$C_0 = 5.44 * \frac{b_1}{a} - 0.21 \tag{2.37}$$

$$C_0 = 6.51 * \frac{b_1}{a} \tag{2.38}$$

Where eq. (2.37) is valid for open section stiffeners ($ø_{st}/\gamma_{st} < 0.15$) and eq. (2.38) is valid for closed section stiffeners ($ø_{st}/\gamma_{st} \geq 0.15$). Both these equation are valid in the range $0.05 \leq b_1/a \leq 0.3$. When substituting eq. (2.37) and (2.38) into the formulation for the flexural rigidity, one can find the following equation:

$$k_{sl} = 3.3 * C_0 * \sqrt{\frac{I_{st,l}}{h_w * t_w^3}} \tag{2.39}$$

Which should not be larger than:

$$k_{sl} \leq C_0 * \sqrt{\gamma^t} \tag{2.40}$$

Where γ^t represents the transition rigidity of the stiffener. This transition rigidity is the point after which no or only small further increase in k_F is noticeable. This γ^t is defined as following:

$$\gamma^t = 14 * \left(\frac{a}{h_w}\right)^{2.9} + 211 * \left(0.3 - \frac{b_1}{a}\right) \quad for \frac{ø_{st}}{\gamma_{st}} < 0.15 \ (open\ section) \tag{2.41}$$

$$\gamma^t = 45 * \left(\frac{a}{h_w}\right)^{1.3} \qquad for \ \frac{ø_{st}}{\gamma_{st}} \geq 0.15 \ (closed\ section) \tag{2.42}$$

Graciano concluded that these terms take the interaction between the web, the flanges and the longitudinal stiffener into account. Therefore, this formulation takes the transition from the global to the local buckling modes, shown in Figure 6, into account [3].

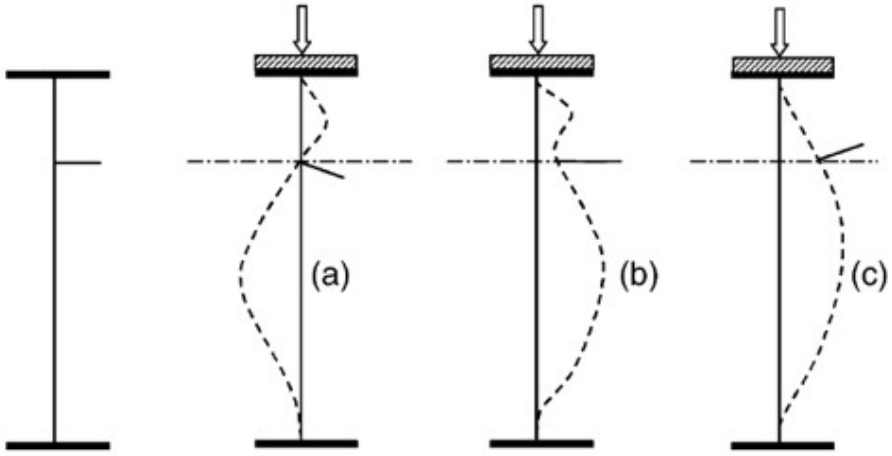

Figure 6: Failure modes, depending on the rigidity stiffness of the stiffener γ_{st}: a) local buckling, b) interaction of local and global buckling, c) global buckling [12, p. 564]

Graciano later continued his research with Mendes in 2014. With the use of a large number of numerical tests, they determined a new critical load amplifier. The proposed equation for determining the values of k_{sl} can be found in eq. (2.43).

$$k_{sl} = -1.87 + 63.94 * \left(\frac{b_1}{h_w}\right) - 62.86 * \left(\frac{b_1}{h_w}\right)^2 - 8.09 * \left(\frac{S_s}{a}\right) + 16.38 * \left(\frac{S_s}{a}\right)^2 - 0.0036 * \gamma_{st} + 0.44 * \left(\frac{t_f}{t_w}\right) + 30.95 * \left(\frac{b_1}{h_w}\right) * \left(\frac{S_s}{a}\right) + 0.031 * \left(\frac{b_1}{h_w}\right) * \gamma_{st} + 0.0035 * \left(\frac{S_s}{a}\right) * \gamma_{st} \quad (2.43)$$

Also eq. (2.35) was simplified and is given in eq. (2.44).

$$k_F = 6 + 2 * \left(\frac{h_w}{a}\right)^2 + k_{sl} \quad (2.44)$$

This model follows the EN 1993-1-5 strategy, however, this formulation is complicated to use in practical cases [2].

2.2.3.2 Davaine (2005)

Davaine developed a methodology which was based on the interaction of two buckling modes. The first mode that is considered is the buckling of the directly loaded subpanel. The second considered mode is the buckling of the whole web (as studied in the work of Graciano and Lagerqvist). In order to consider the buckling of the directly loaded panel, a model, as shown in Figure 7, was proposed by Davaine. This model shows a simply supported panel, asymmetrically loaded on both longitudinal edges [6], [16].

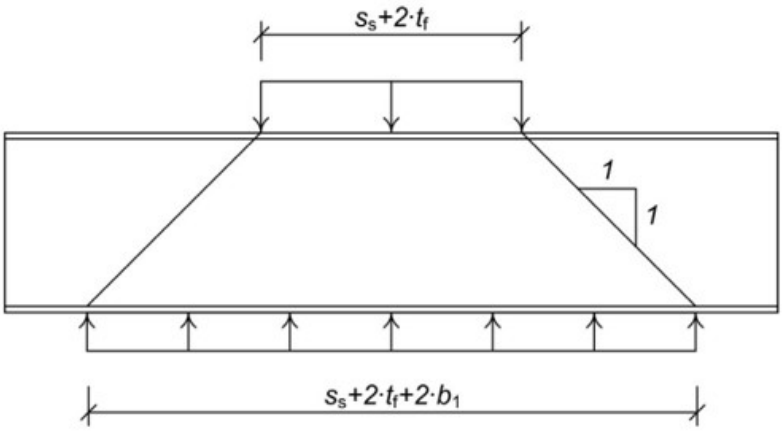

Figure 7: Upper subpanel as suggested by Davaine (2005) [16, p. 4]

He used this model to make a formulation for the buckling coefficient as presented in eq. (2.45). Also a formulation for the critical load of this model is given in eq. (2.46)

$$k_{F2} = \left(0.8 * \left(\frac{s_s+2*t_f}{a}\right) + 0.6\right) * \left(\frac{a}{b_1}\right)^{\left(0.6*\left(\frac{s_s+2*t_f}{a}\right)+0.5\right)} \tag{2.45}$$

$$F_{cr2} = k_{F2} * \frac{\pi^2 * E}{12(1-\nu^2)} * \frac{t_w^3}{b_1} \tag{2.46}$$

As can be seen in Figure 7, the transfer of the load through the upper panel has a slope of one by one. Therefore, eq. (2.45) is only valid in the following case: $s_s + 2 * t_f + 2 * b_1 \leq a$. Davaine also proposed an interaction formula for the two buckling modes that where considered in his research. This formula is given in eq. (2.47) [16].

$$\frac{1}{F_{cr}} = \frac{1}{F_{cr1}} + \frac{1}{F_{cr2}} \tag{2.47}$$

In this formula, F_{cr} is obtained by using eq. (2.16) and eq. (2.35) presented in sections 2.1.2.3 and 2.2.3.1 . The reduction factor (χ_F)was also determined by Davaine:

$$\varphi_F = 0.5 * (1 + 0.21 * (\lambda_F - 0.8) + \lambda_F \tag{2.48}$$

$$\chi_F = \frac{1}{\varphi_F + \sqrt{\varphi_F^2 - \lambda_F}} \tag{2.49}$$

This proposal by Davaine follows the current EN 1993-1-5 strategy. However, it is not applicable for webs with multiple stiffeners [2].

2.3 Standards

This chapter will discuss the different national standards dealing with the patch loading resistance of girders. First, the British (BS), Swiss (SIA) and American (AASHTO) Standards will be briefly discussed to see how other parts of the world handles this problem. Afterwards, the European Standard (EN 1993-1-5) will be discussed more in depth.

2.3.1 British Standard (BS)

Annex D from the British Standard, BS 5400-3: Steel, Concrete and Composite Bridges (2000) [14], describes the patch loading on longitudinally stiffened girders. The design of girders is classified into two categories: beams without longitudinal stiffeners on the web and beams with longitudinal stiffeners on the web. The design of girders without longitudinal stiffeners on the web has 2 criteria which have to be fulfilled. The smallest value of these two gives the patch loading resistance. The first one is the web buckling criterium (this formula is the same as the one presented by Markovic and Hajdin in section 2.2.2.1):

$$F_{Rd1} = 0.5 * t_w^2 * \sqrt{\frac{E * f_{yw} * t_f}{t_w}} * \left(1 + \frac{3 * s_s}{h_w} * \left(\frac{t_w}{t_f}\right)^{\frac{3}{2}}\right) * \sqrt{1 - \left(\frac{\sigma_b}{f_{yw}}\right)^2} \tag{2.50}$$

The second criterion is the web yielding criterium:

$$F_{Rd2} = (s_s * t_w * f_{yw} + 2 * t_f * \sqrt{f_{yf} * f_{yw} * b_f * t_w} * \sqrt{1 - \left(\frac{\sigma_x}{f_{yw}}\right)^2} \tag{2.51}$$

The design for beams with longitudinal stiffeners on the web should be calculated by adding the correction factor from Markovic and Hajdin, presented in section 2.2.2.1: $f_s = 1.28 - 0.7 * b_1/h_w$, which should not be less than 1.0 nor greater than 1.21.

2.3.2 Swiss Standard (SIA)

The Swiss Standard, SIA 263:2003 Constructions métalliques [17], also uses two criteria for calculating the patch loading resistance of unstiffened girders. The smallest value gives the patch loading resistance. These criteria are also the web buckling criterium (F_{Rd1}) and the web yielding criterium (F_{Rd2}). When the resistance of the girder is not enough to resist the patch loading, longitudinal stiffeners are added [18].

$$F_{Rd} = \frac{1}{\gamma_{M1}} * 0.5 * t_w^2 * f_y * \sqrt{\frac{E * t_f}{f_y * t_w}} * \beta_1 * \beta_2 * \beta_3 * \beta_4 \tag{2.52}$$

$$F_{Rd2} = \left(s_s + 10 * t_f\right) * t_w * \frac{f_{yw}}{\gamma_{M1}} \tag{2.53}$$

In eq. (2.52) there are β-coefficients which have to be calculated separately. These β-values correspond to: the slenderness of the flange (β_1), the slenderness of the web (β_2), the loaded length (β_3) and the longitudinal stresses (β_4). The formulas for these coefficients are presented in eq. (2.54):

$$\beta_1 = \sqrt[4]{\frac{b_f}{10 * t_f}} \leq 1.25 \;\; ; \;\; \beta_2 = \sqrt{\frac{60 * t_w}{h_w}} \;\; ; \;\; \beta_3 = 1 + \frac{s_s}{h_w} \leq 1.5 \;\; ; \;\; \beta_4 = 1.5 - \frac{\sigma_{x,Ed} * \gamma_{M1}}{f_{yw}} \leq 1 \tag{2.54}$$

2.3.3 American Standard (AASHTO)

The American standard, AASHTO-AISC-LFRD (2005) [19], calculates the patch loading resistance for longitudinally unstiffened girders by using three criteria, of which the smallest value gives the patch loading resistance. The first two (F_{Rd1} ; F_{Rd2}) represent the same criteria as in the British and Swiss Standard.

$$F_{Rd1} = \text{ø} * 0.80 * t_w^2 * \left(1 + 3 * \left(\frac{s_s}{h_w + 2 * t_f}\right) * \left(\frac{t_w}{t_f}\right)^{0.5}\right) * \sqrt{\frac{E * f_{yw} * t_f}{t_w}} \tag{2.55}$$

$$F_{Rd2} = \text{ø} * \left(s_s + 5 * t_f\right) * t_w * f_{yw} \tag{2.56}$$

The third criterium (F_{Rd3}) takes the lateral displacement of the flanges into account (web sideways buckling). There are two formulas given for calculating this criterium. The first one should be used when the compression flange is restrained against rotation and is only valid for $\frac{h_w}{t_w} / \frac{l}{b_f} \leq 2.3$. The second formula for F_{Rd3} should be used when the compression flange is not restrained against rotation and is only valid for $\frac{h_w}{t_w} / \frac{l}{b_f} \leq 1.7$. This web sidesway buckling should not be taken into account when they are not within their valid area. This means that the web sideways buckling does not apply [19].

$$F_{Rd3} \begin{cases} \frac{C_r * t_w^3 * t_f}{h_w^2} * (1 + 0.4 * \left(\frac{\frac{h_w}{t_w}}{\frac{l}{b_f}}\right)^3 & for: \left(\frac{\frac{h_w}{t_w}}{\frac{l}{b_f}}\right) \leq 2.3 \\ \frac{C_r * t_w^3 * t_f}{h_w^2} * (0.4 * \left(\frac{\frac{h_w}{t_w}}{\frac{l}{b_f}}\right)^3 & for: \left(\frac{\frac{h_w}{t_w}}{\frac{l}{b_f}}\right) \leq 1.7 \end{cases} \tag{2.57}$$

All formulas presented in this paragraph determine the limit state for the required strength of the girder. When the load on the girder exceeds this strength, stiffeners will be provided and will be sized for the difference between the required strength and the available strength for the applicable limit state [19].

2.3.4 European Standard (EN 1993-1-5)

Nowadays, EN 1993-1-5 [1] is the most widely used design procedure. Researches that are investigating this topic are mostly starting from this design method. However, there are certain criticisms on this design method. In Figure 8, the most relevant cross section notations, used in EN 1993-1-5 [1], are presented.

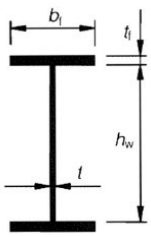

Figure 8: Cross section notations [1, p. 22]

In EN 1993-1-5 [1], section six is dedicated to the resistance of transverse forces (patch loadings) on I-girders. This section six includes a check for the buckling resistance, which was originally designed by Lagerqvist and Johansson [20]. This design method makes use of a parameter that defines the patch loading resistance for an unstiffened/stiffened I-girder. This parameter is shown in equation (2.58).

$$F_{Rd} = \frac{f_{yw}\, L_{eff}\, t_w}{\gamma_m} \tag{2.58}$$

This equation makes use of the yield strength of the web (f_{yw}), the thickness of the web (t_w), the partial safety factor (γ_m) and the effective length for resistance to transverse forces (L_{eff}). This last parameter can be calculated using equation (2.59).

$$L_{eff} = \chi_F\, l_y \tag{2.59}$$

l_y in this equation is the effective loaded length and should be calculated using equation (2.60).

$$l_y = s_s + 2\, t_f\, (1 + \sqrt{m_1 + m_2}\,) \tag{2.60}$$

s_s is the parameter which represents the length of stiff bearing on the flange. This length should be taken as the length where the load is applied and effectively distributed at a slope one by one. m_1 and m_2 are dimensionless parameters.

$$m_1 = \frac{f_{yf}\, b_f}{f_{yw}\, t_w} \tag{2.61}$$

In equation (2.61), m_1 represents the contribution of the flange on the resistance of unstiffened girder webs. f_{yf} represents the yield resistance of the flange and f_{yw} is the yield resistance of the web. b_f is the length of the cross section of the flange and t_w is the thickness of the web.

$$m_2 = 0{,}02\, \left(\frac{h_w}{t_f}\right)^2 \tag{2.62}$$

In equation (2.62), m_2 represents the contribution of the web on the resistance of unstiffened girder webs. h_w represents the height of the web and t_f is the thickness of the flange. For welded girders $m_2 = 0$ if $\lambda < 0{,}5$. This restriction was obtained by Davaine [21] after conducting a numerical study. Here, there was founded that there is a better correlation between the computed resistances and theoretical predictions when the contribution of the web was neglected and m_2 was chosen to be zero. This conclusion is sustained by a study done by Gozzi [9]. The slenderness parameter λ used to determinate if the restriction on m_2 is necessary, can be calculated using equation (2.63).

$$\lambda = \sqrt{\frac{l_y\, t_w\, f_{yw}}{F_{cr}}} \tag{2.63}$$

F_{cr} represents the elastic critical buckling load. The reduction factor χ_F, that was used in equation (2.59) to calculate the effective length for the resistance to the transverse forces, can be obtained from equation (2.64).

$$\chi_F = \frac{0{,}5}{\lambda} \tag{2.64}$$

The elastic critical buckling load can be obtained using equation (2.65).

$$F_{cr} = 0{,}9\, k_F\, E\, \frac{{t_w}^3}{h_w} \tag{2.65}$$

k_F is the buckling coefficient and depends on whether the girder is stiffened or unstiffened with longitudinally stiffeners and on the position of the load onto the girder. The most relevant load position for this research is type a, described in EN 1993-1-5 [1] as shown in Figure 9. Both of the equations (2.64) and (2.65) are simplified versions of the formulas represented by Graciano and Lagerqvist based on a finite element analysis [22].

This load type a transfers the load through the flange and is resisted by shear forces in the web, as can be seen in Figure 9.

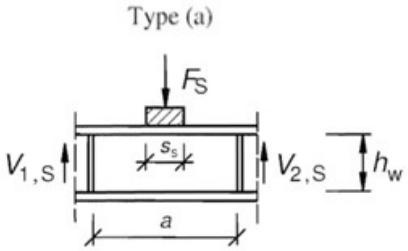

Figure 9: Load type a for an unstiffened I-girder [1, p. 26]

The buckling coefficient k_F for this load application type is given by equation (2.66).

$$k_F = 6 + 2\left(\frac{h_w}{a}\right)^2 \tag{2.66}$$

Equation (2.66) is obtained after a rounding off and by taking the rotational restraint of the flanges as a constant value [16].

In the case of a girder with longitudinally stiffeners, another formula should be used to calculate the buckling coefficient.

$$k_F = 6 + 2\left(\frac{h_w}{a}\right)^2 + \left[5{,}44\,\frac{b_1}{a} - 0{,}21\right]\sqrt{\gamma_{st}} \tag{2.67}$$

In equation (2.67) that represents the buckling coefficient for a longitudinally stiffened girder, it is clearly visible that the third part of the formula is the contribution of the longitudinally stiffener. b_1 in this formula stands for the depth of the loaded subpanel taken as the clear distance between the loaded flange and the stiffener.

γ_{st} is the relative flexural rigidity of the longitudinally stiffener and is described in equation (2.68).

$$\gamma_{st} = 10{,}9\frac{I_{sl,I}}{h_w\, {t_w}^3} \leq 13\left[\frac{a}{h_w}\right]^3 + 210\left[0{,}3 - \frac{b_1}{a}\right] \quad (2.68)$$

$I_{sl,I}$ is the second moment of area of the stiffener that is the closest to the loaded flange.
To summarize the design method in EN 1993-1-5, it can be stated that equations (2.58) – (2.65) are used to calculate the resistance of the longitudinally stiffened girder, while equations (2.66) – (2.68) are used to obtain the buckling coefficient of an unstiffened or stiffened girder.

2.3.4.1 Criticism on EN 1993-1-5

This chapter will discuss some concerns about the widely used design method presented in EN 1993-1-5 (see section 2.3.4).

In general, several studies have pointed out that the current design method in EN 1993-1-5 [1] leads to a significant underestimation of the resistance against the patch load.

The next thing to point out is that the design method, as it is now in EN 1993-1-5 [1], only considers an I-girder with one longitudinally stiffener. In practice, this type of setting is rarely used. In fact, there are almost none bridges designed with one longitudinally stiffened I-girder. The more common used number of stiffeners is two or more. The model in EN 1993-1-5 [1] only covers the web crippling resistance of the upper and lower part and the interaction between these two in one mechanical model. Therefore, these models cannot be used for I-girders with two or more longitudinally stiffeners explicitly [16].

Thirdly, the current design method does not deal correctly with the placement of the longitudinally stiffener of the I-girder regarding to the patch load resistance. Davaine [21] proposed a solution for this manner, but his solution was still only applicable for one longitudinal stiffener and still underestimated the resistance of the stiffener. This problem will be further discussed in the next section about the analysis of the parameters [16].

The last remark is about the calculation of the additional strength of the longitudinal stiffener. The additional strength, generated by this stiffener, is implemented in the calculation of the buckling coefficient k_F as pointed out before. This implies that by increasing the strength of the stiffener, the buckling coefficient will increase. Because of the increase of the buckling coefficient, the critical load F_{cr} will also increase accordingly. This argumentation comes from the mechanical model where there is a global buckling and the stiffener can have a positive influence on the buckling resistance. But when the stiffener is rigid enough to separate the buckling shapes into the buckling of the lower and upper part, the further increase of the rigidity of the stiffeners does not affect the buckling resistance anymore. This rule thus only applies until the moment that the buckling shape is a global buckling of the whole web. Research done by B. Kövesdi shows that with a relatively small rigidity of the stiffeners, the buckling shape already changes from global buckling of the whole web to local buckling of the subpanels. From this point on, the increasing of the size of the stiffeners does not affect the patch load resistance anymore. The analysis of this phenome is missing from the current design method in EN 1993-1-5 [1] [16].

2.4 Experimental results

This chapter will discuss some experimental results found in the literature. A large number of previous (experimental and numerical) investigations have studied the behavior of longitudinally stiffened girders subjected to patch loading. These investigations are mostly performed with girders having only one longitudinal stiffener, which can have a closed- or open stiffener type. Some of these researches are presented in Table 1. The number of tests, the used cross-sections of the stiffeners and some geometrical domains are also given in this table.

Table 1: Characteristic data from the experiments and simulations found in the literature [3, p. 46]

Author	No. of tests	Open/Closed stiffener	a/h_w	h_1/h_w	s_s/h_w
Rockey et. Al (1978)	4	open	1	0,20-0,21	0,05
Bergfelt (1979)	9	open	0,75-3,24	0,2	0,05-0,06
Bergfelt (1983)	6	open	1,50-4,08	0,20-0,34	0,05-0,16
Galea et. Al (1987)	2	open	1,4	0,21-0,26	0,54
Shimizu et. Al (1987)	1	open	1	0,2	0,3
Janus et. al (1988)	101	open	1,00-2,00	0,10-0,50	0,10-0,20
Dubas and Tschamper (1990)	24	12 open 12 closed	1,76-2,48	0,15-0,20	0,04-0,24
Dogaki et. Al (1990)	2	open	1	0,2	0,1
Carretero and Lebet (1998)	6	closed	1,31-2,25	0,20-0,38	0,25-0,38
Walbridge and Lebet (2001)	5	3 open 2 closed	1,43	0,11-0,23	0,29
Kuhlmann and Seitz (2004)	4	closed	2	0,25-0,30	0,58
Davaine (2005) (FEA)	366	open	1,33-4,00	0,10-0,40	0,20-1,00

The results of the researches presented in the table above are compared to EN 1993-1-5. Mind that the validation statement, regarding eq. (2.66) in paragraph 2.3.4 of EN 1993-1-5, is not followed for this comparison with the test results. All results were plotted in three different figures, in order to be able to evaluate all test results with respect to EN 1993-1-5. There were 540 tests results compared to EN 1993-1-5, including 140 cases having open cross-sectional stiffeners (Figure 10), 24 cases having closed cross-sectional stiffeners (Figure 11) and 366 cases having open cross-sectional stiffeners. This was done using numerical FE simulations (Figure 12) [3].

All researches mentioned in Table 1 come to the conclusion that adding a longitudinal stiffener to the web of a girder results in an increase of the patch loading resistance. This increase is even more significant when closed section stiffeners are used. The stiffness of the stiffener also has an influence on the patch loading resistance. When increasing the stiffness of the stiffener, the patch loading resistance also increases. However, the gain of patch loading resistance, due to the adding of a longitudinal stiffener, only depends on the cross-section of the girder, the placement of the stiffener and the cross-section of the stiffener [3].

Figure 10 shows the comparison of the results of the experiments using an open type stiffener with the predicted resistance of EN 1993-1-5. Most of these test are on the safe side, which means that the Eurocode underestimates most of these cases. However, there are a few, less slender, specimens which are overestimated by the Eurocode design method. These overestimated tests are excecuted by Janus et. al (1988) and have a slendernes of $\lambda_F \sim 0.6$. A large scatter in the results is also noticable. For the slender cases, with a slenderness of $\lambda_F > 2$, a rise of the resistance curve of EN 1993-1-5 would be favorable [3].

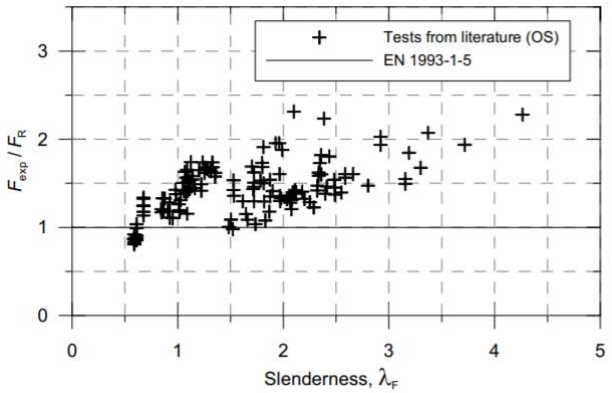

Figure 10: The 140 specimens with open section longitudinal stiffeners. Ultimate experimental load, F_{exp} compared to the EN 1993-1-5 recommended design procedure [3, p. 63].

Figure 11 shows the comparison of the results of the experiments using a closed type stiffener with the predicted resistance of EN 1993-1-5. All cases are on the safe side, which means that the Eurocode underestimates all of these cases. Though, there is one case which has exactly the same value as predicted by the Eurocode (test by Carretero and Lebet). The prediction of the resistance of the girders by EN 1993-1-5 is on the conservative side. A rise of this curve would result in a more accurate prediction. Again, a large scatter in the results can be seen [3].

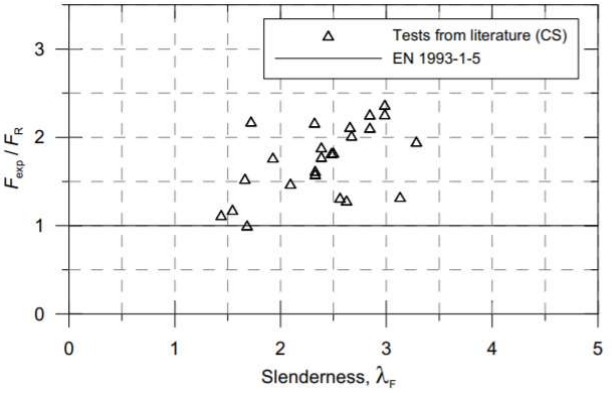

Figure 11: The 24 specimens with closed section longitudinal stiffeners. Ultimate experimental load, F_{exp}compared to the EN 1993-1-5 recommended design procedure [3, p. 63].

Figure 12 shows the comparison of the numerical results of Davaine with the predicted resistance of EN 1993-1-5. There is less obvious scatter noticable in these results, most of the cases are concentrated in one area. However, there are still some cases showing a significantly larger resistance than predicted by EN 1993-1-5. A rise of the curve, representing the

prediction resistance of EN 1993-1-5, would be recommended for the cases with a slenderness higher than $\lambda_F > 1.5$ [3].

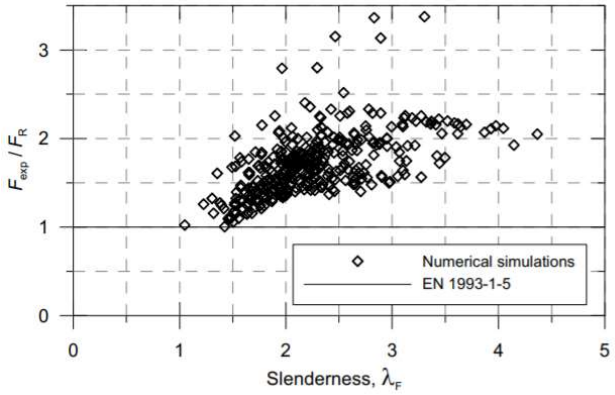

Figure 12: The 366 numerical simulations with open section longitudinal stiffeners. Ultimate experimental load, F_{exp} compared to the EN 1993-1-5 recommended design procedure [3, p. 64].

When looking at all these results, one can conclude that overall all results would be better predicted by EN 1993-1-5 when the calculation of the patch loading resistance would be changed to better fit the more slender cases. Two things have to be improved in the EN 1993-1-5 design method. Namely, the prediction must fit better for the more slender specimens and the patch loading resistance must be better calculated to reduce the scatter in the results [3].

Test results from B. Kövesdi et al. were also examined and compared to different patch loading resistance models. The compared models were from Davaine, Graciano (2015) and EN 1993-1-5. The patch loading behavior, of longitudinally stiffened girders, was numerically examined in the research conducted by B. Kövesdi et al. [25]. The most important parameters in this research were the imperfection shape and magnitude of the specimens. The test results of this research, and the three existing models, are presented in Table 2. The second column of each resistance model gives a percentual comparison with the experimentally determined resistance. These results are also plotted in Figure 13 to compare the experimental and numerical results with the predicted resistance of EN 1993-1-5. In Figure 14, the experimental results with the different resistance models are compared.

Table 2: Comparison of different resistance models to test results, [kN] [25, p. 204].

Specimen	f_{exp}	f_{num}	$F_{R,EN1993-1-5}$		$F_{R,Davaine}$		$F_{R,Graciano}$	
1	206,4	204,6	124,1	0,60	-	-	-	-
2	258,4	254,8	163,5	0,63	173,7	0,67	184,6	0,71
3	271,0	266,8	151,9	0,56	187,9	0,69	178,2	0,65
4	320,4	268,2	166,9	0,52	198,2	0,62	180,9	0,56
5	180,2	176,5	108,4	0,60	-	-	-	-
6	214,3	207,9	142,9	0,67	142,1	0,66	156,7	0,73
7	218,4	191,6	125,3	0,57	146,7	0,67	144,2	0,66
8	223,8	208,9	139,8	0,62	156,2	0,69	148,6	0,66

In Figure 13, it can be see that the numerical model, using standard imperfection magnitudes and considering local or global imperfections shapes, is in close vicinity of the experimentally determined patch loading resistance. However, all numerical results are slightly on the safe side. When looking at the predicted resistance of EN 1993-1-5, one can see that these values are underestimating the real situation [25].

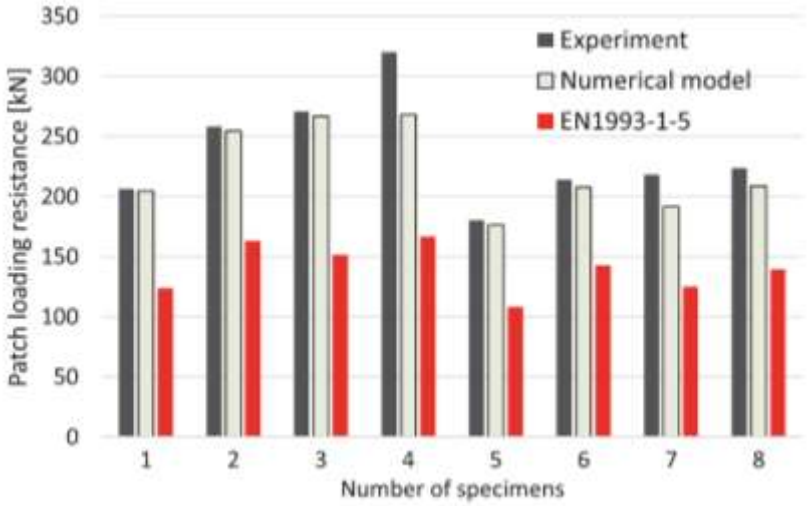

Figure 13: Comparison of the experimental, numerical and analytical resistance models [25, p. 204].

In Figure 14 it can be seen that all resistance models underestimate the real patch loading resistance of the conducted experiments. However, the improvements made by Davaine and Graciano, on the widely used resistance model of EN 1993-1-5, are seeable in this figure. Therefore, the resistance model of EN 1993-1-5 is the most conservative with ratios varying between 52-67 %, while the resistance model of Davaine varies between 62-69 % and the resistance model of Graciano between 56-73 %. This proves that the design method of EN 1993-1-5 must be improved to better predict the real patch loading resistance of longitudinally stiffened girders. Also, the models proposed by Davaine and Graciano still have some room for improvement [16], [25].

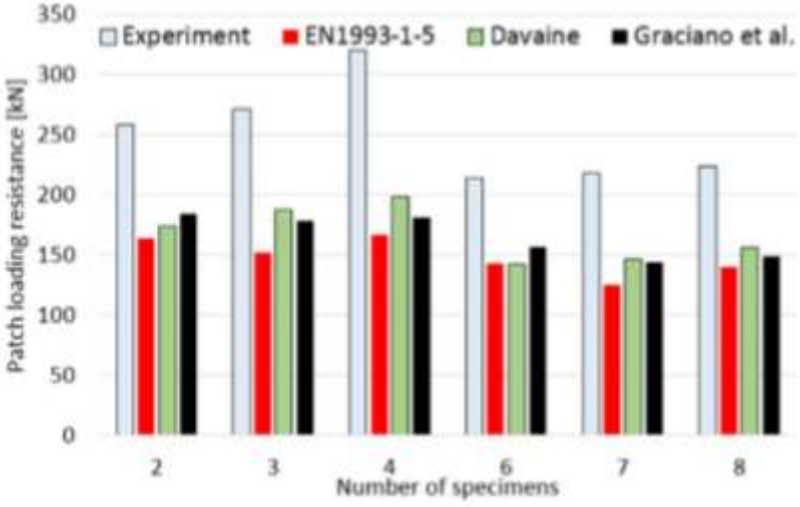

Figure 14: Comparison of different resistance models to test results [25, p. 204].

2.5 Analysis of the most relevant factors

Several investigations showed that there are multiple factors which are relevant in designing longitudinally stiffened I-girders. The first, and most common used in the literature, is the relative position of the stiffener. This factor is described as b_1/h_w. The second one is the rigidity of the longitudinal stiffener γ_{st} [24] [25]. Lastly, the ratio of the directly loaded panel b_1/t_w is a relevant parameter. This parameter is referred to as the slenderness of the directly loaded panel. In Table 3, a summarizing table of these parameters can be seen while in figure 15 a notion of different parameters is presented.

Table 3:The most relevant parameters

	Factors
1	b_1/h_w
2	γ_{st}
3	b_1/t_w

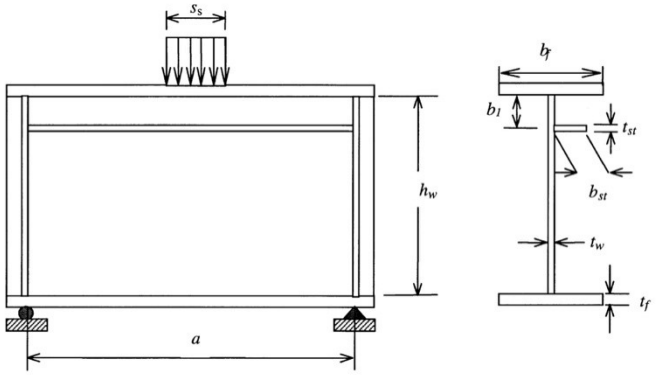

Figure 15: Parameter notation of longitudinally stiffened girders under patch loading [28, p. 1234]

2.5.1 Relative position of the stiffener

In order to obtain a maximum capacity for a longitudinally stiffened I-girder under patch loading, the placement of the longitudinally stiffener is of high importance. Carlos Graciano [22] did research about the validity of the EN 1993-1-5 [1] design method towards the relative position of the stiffener. He compared the results of experimentally tests, done by Wallbridge and Lebet [26]. They tested four girders with open section stiffeners. The experiments showed a significant increase in the resistance of the girders for the patch load when the longitudinal stiffener was placed rather close to the loaded flange. Carlos Graciano [22] found out that there was an anomaly between these test results and the results that were obtained using EN 1993-1-5 [1]. Using EN 1993-1-5 [1], the critical load should increase when the longitudinal stiffener is placed further from the loaded flange. This is in contrast with the experimental test results. Carlos Graciano [22] thus observed that with the approach proposed by Davaine [21], the weakness in EN 1993-1-5 [1], in regards to the stiffener location, could be overcome. As stated before, this is still only for a girder with one longitudinal stiffener and also still underestimates the resistance of the stiffener [27].

2.5.2 Rigidity of the longitudinal stiffener

By increasing the cross section of the stiffener, the rigidity of the stiffener will also increase. This increase of stiffness was observed in comparison to the buckling coefficient k_F by Carlos Graciano [27]. Here it was observed that k_F would only increase until a certain point. This was expected because of the reasoning stated in section 2.3.4.1, "criticism on EN 1993-1-5 design method". After a certain rigidity of the stiffener, the buckling shape will reform to local buckling of the subpanels and thus will no longer contribute to the patch load resistance of the girder. The most efficient way to design the rigidity would be to do it just under the point that would make the loaded sub panel buckle. Further research has to acknowledge this statement.

2.5.3 Slenderness of the directly loaded panel

The stiffeners are in practice always placed in the compression zone of the web of the I-girder. In order to withstand a shear force, research has founded that the stiffener needs to be placed at half the girder depth. For bending, it is found that the stiffeners are best placed at one fifth of the girder web, in the compression zone. [28]. In practice, this value for bending is often also used for an I-girder under patch loading. Experimental and laboratory studies, done by many researchers [28], show that an I-girder can withstand more patch loading when the stiffener is closer to the loaded flange than one fifth of the girder web. By placing the stiffener closer to the loaded flange, the slenderness of the upper part of the web decreases and the stresses are more uniformly distributed through the web of the girder. In the literature, the placement of the stiffener is most of the times described as the relationship between the length of the loaded subpanel (b_1) and the total height of the girder between the flanges (h_w). This relationship is called the relative position of the stiffener. Graciano and Edlund [28] researched the relationship between b_1 and the thickness of the web (t_w). This is called the slenderness of the directly loaded part. In this way, they tried to find new insights in the best placement of the stiffener by not only looking at the placement, but also the slenderness of the directly loaded part.

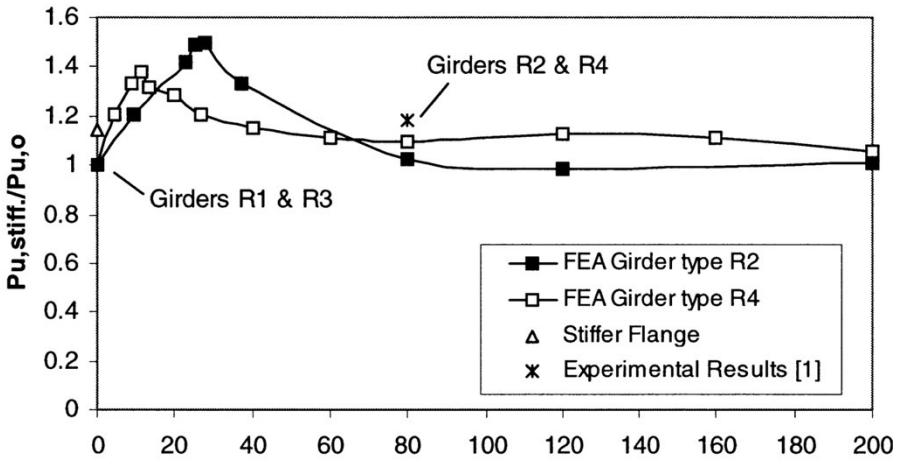

Figure 16: Load carrying capacity versus slenderness ratio of the directly loaded sub panel

They conducted a finite element study on two plate girders with two extreme values of the ratio flange to web thickness. For both of these situations, it was found that the optimal position of the stiffener was less than 40 times the thickness of the web. This can be seen in Figure 16, where the horizontal axis gives the ratio of the extra created load capacity due to the stiffener over the vertical axis that gives the slenderness ratio of the directly loaded web panel (b_1/t_w). The two different plate girders are both represented by the relationship between the load carrying capacity and the slenderness ratio.

If the stiffener is located below the position that there is no buckling possible in the loaded part, the maximum value for the load carrying position should be found there. Due to the limited number of tests conducted (2), these results and findings are not yet conclusive, but they give a good indication of where the stiffener should be best and most efficiently placed.

3. Numerical model

3.1 Geometry of the verified model

The numerical model, used for this research, must be verified to its accuracy. This was done based on the experiments conducted by Seitz in 2005. The experiments conducted by Seitz were observed as to be the closest to the set of parameters which will be researched in this paper. Therefore, these experiments were used to verify this model [5].

Seitz carried out a total of 7 experiments on patch loading. One of the experiments used no stiffeners, two experiments used two stiffeners and the remaining four experiments used one stiffener, some of which contained a moment [5].

The first three tests were chosen to conduct the model validation. These experiments were conducted by applying a transverse force onto the test models. The three different test models can be seen in Figure 17.

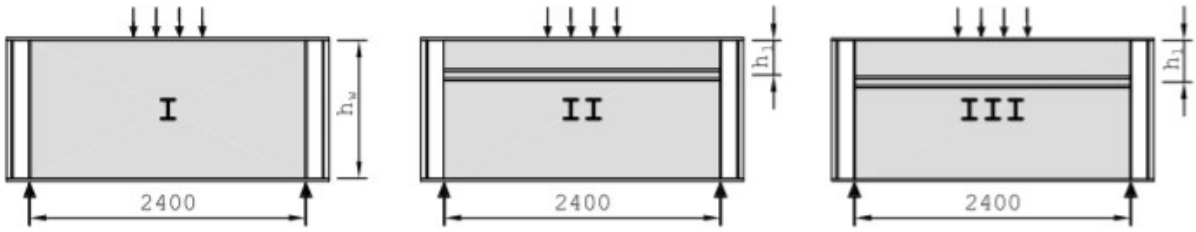

Figure 17: Experiment I, II ($h_1/h_w = 0.25$) and III ($h_1/h_w = 0.30$)

The geometrical properties of these experiments are shown in Figure 18. The h_1/h_w ratio is 0.25 and 0.30 for respectively experiments II and III. This dimension gives the location of the stiffener, calculated as the distance between the loaded flange and the stiffener. The thickness of the web is $t_w = 6\,mm$ and the height is $h_w = 1200\,mm$. The length of the girder is $a = 2400\,mm$ up to the support. However, there is an extra overlength of 240 mm on each side of the specimen to allow the girder to be simply supported during the experiment. Both flanges have a width of $b_f = 260\,mm$ and a thickness of $t_f = 20\,mm$. The stiffeners consists of a hollow trapezoidal shape and are $t_{st} = 4\,mm$ thick. The other geometrical properties are shown in Figure 18.

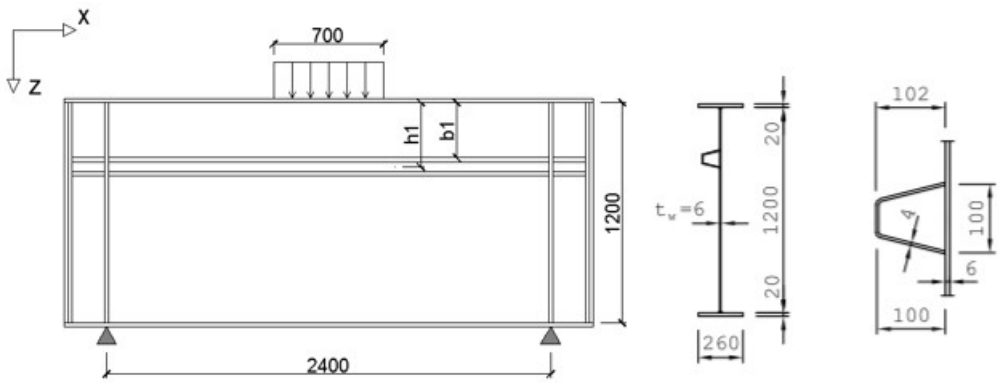

Figure 18: Geometrical properties of the experiments

3.2 Applied numerical model

The numerical model was constructed using Ansys v17.2 finite element software [29]. A visualization of the created model is shown in Figure 19. This figure shows the plotted areas used in the ANSYS model.

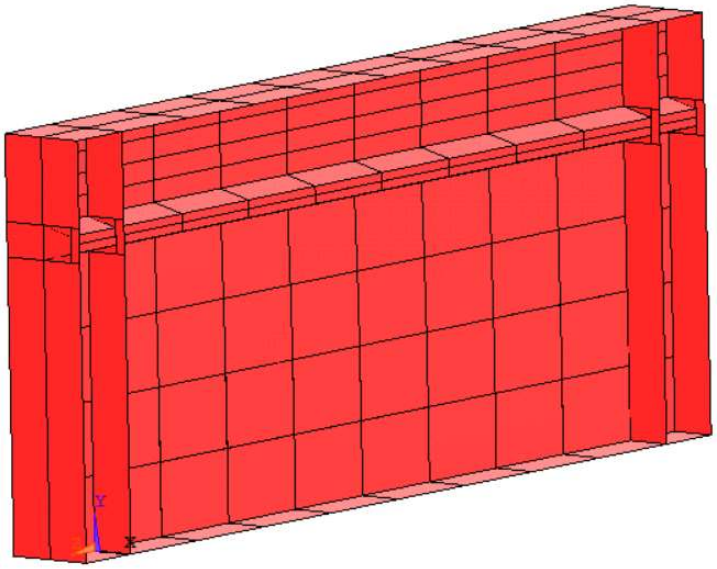

Figure 19: Visualization of the created finite element model in ANSYS

A basis numerical model was constructed by B. Kövesdi, this model was examined and adjusted to match the experiments carried out by Seitz [5].

The elements that are used in the mode are all shell181 elements, as can be seen in Figure 20. The shell181 element is a four-node element with six degrees of freedom at each node. The six degrees of freedom exist of translations in the x, y, and z direction and rotations around the x, y, and z axis. This element is well suited for linear and non-linear applications. It also allows large rotations and large deformations. The numerical model takes, when needed, the material and geometrical non-linearities into account.

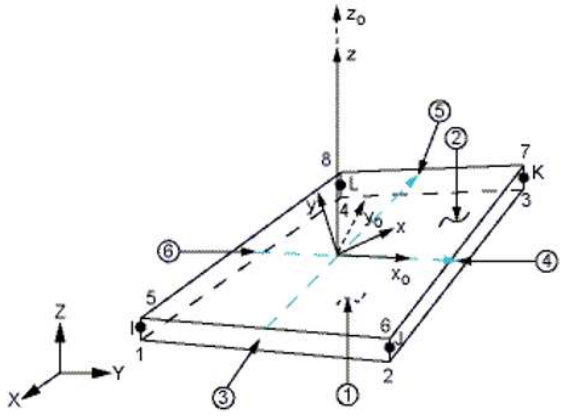

Figure 20: Shell181 element

3.3 Model properties

Certain material properties were assigned to the numerical model. These properties correspond to the ones used in the Seitz [5] experiments. Table 4 gives a summary of the properties for the flange, web and stiffener for each used experiment. The yield strength (f_y), tensile strength (f_u) and Young modulus (E) were experimentally determined by Seitz [5] and are given for each element of the girder for each separate test.

Table 4: Material properties of Seitz experiments

Experiment	Structural element	f_y [N/mm²]	f_u [N/mm²]	E [N/mm²]
I	Flange	378	604	192 800
	Web	357	541	202 500
II	Flange	378	604	192 800
	Web	357	541	202 500
	Stiffener	386	538	200 100
III	Flange	363	596	192 800
	Web	357	541	202 500
	Stiffener	386	538	200 100

For the verification of the numerical model, the values of Table 4 were used. However, for the numerical parametric study, the steel grades of steel type S355, with the corresponding characteristic values for the yield strength, tensile strength and Young modulus, were used.

Figure 21 shows the linear material model which was used for the numerical parametric study in ANSYS [27].

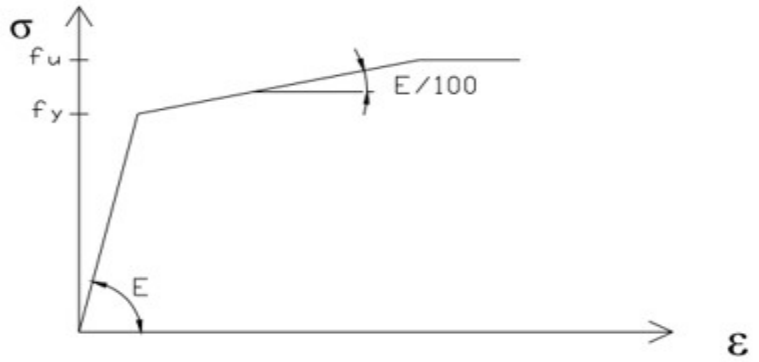

Figure 21: Applied material model

3.4 Linear buckling analysis and geometrically and materially nonlinear imperfection analysis

First of all, a linear buckling analysis (LBA) was performed. LBA is a method that only includes a failure based on buckling. This model does not include any non-linearities of the material nor of the geometry. It also does not include imperfections. Therefore, this is a simplified version which can only fail due to buckling, not due to material failure.

Secondly, a geometrically and materially non-linear imperfection analysis (GMNIA) was performed. In this analysis, non-linearities of the material and of the geometry are included. The imperfections of the subpanels (local imperfections) and of the longitudinal stiffener (global imperfection) are included as well. The failure in the GMNIA can occur due to buckling and due to failure of the material.

3.5 Finite element mesh sensitivity testing

Before the parametrical study on this model is performed, it needs to be verified which mesh size is the most efficient for this model. This is done by running the model for test setup two and three, with combination five as the applied imperfections (see section 3.7.2 and 3.7.3), with each time a different mesh size. This is done until there is less than 1% difference between the load carrying resistances. This is performed for the geometrically and materially non-linear imperfection analysis (GMNIA) and for the linear buckling analysis (LBA). Figure 22 and 23 shows the results for test setup two, once for the linear and once for the non-linear analysis. The red lines represent the 1% offset of the mesh size that is chosen. Figure 24 and 25 are presenting the same but for test setup three.

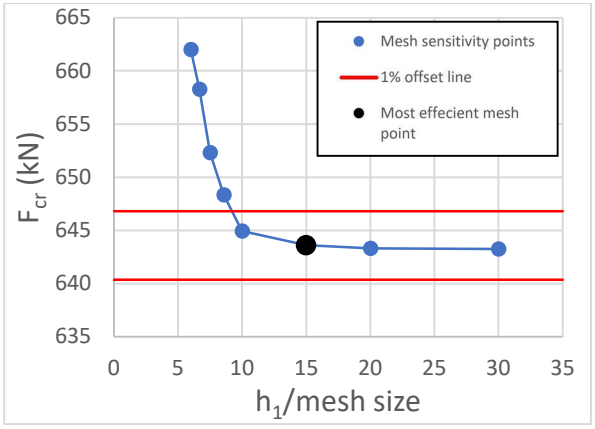

Figure 22: LBA model mesh sensitivity analysis for test setup 2

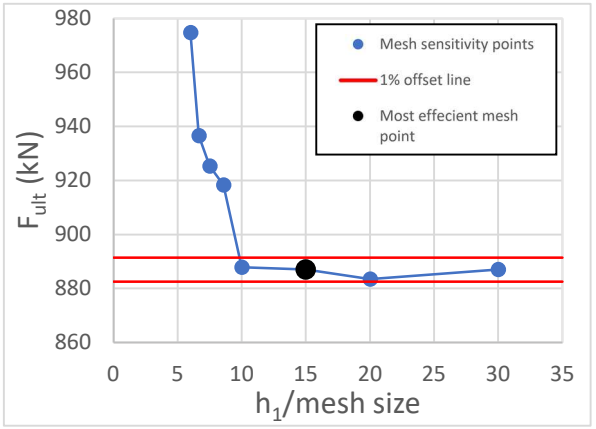

Figure 23: GMNIA model mesh sensitivity analysis for test setup 2

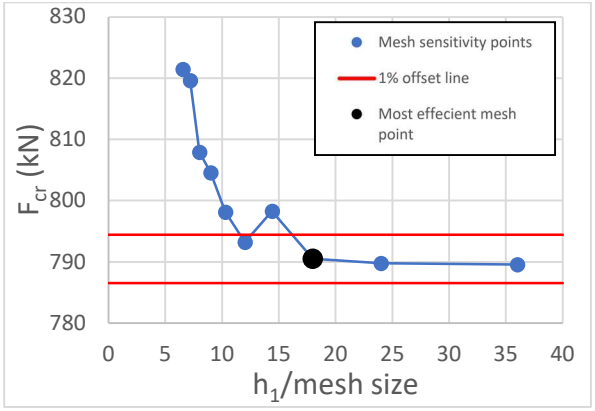

Figure 24: LBA model mesh sensitivity analysis for test setup 3

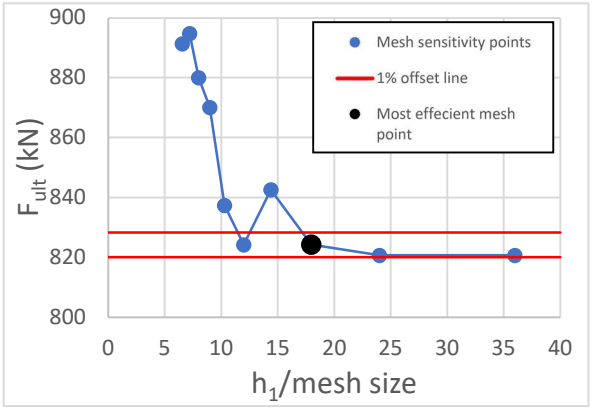

Figure 25: GMNIA model mesh sensitivity analysis for test setup 3

It can be seen that for test setup two, the ideal mesh size, with an error margin of 1% for the linear and non-linear analysis, is at h_1/mesh size = 15. This corresponds with a mesh size of 20mm. For test setup three, the ideal mesh size with an error margin of 1% for the linear and non-linear is found at h_1/mesh size = 18. This also corresponds with a mesh size of 20mm. This mesh size will thus be applied, for both LBA and GMNIA, in the further parametrical study.

3.6 Applied imperfections

Annex C5 of EN1993-1-5 [1] gives a guidance for the usage of finite element analysis. The Eurocode provides the possibility to use eigenmodes as the imperfections of an element. However, the model that was used for this research showed significant differences for the load carrying capacity when comparing it with the results founded by Seitz [5]. Therefore, the model was changed to a model where the imperfections were added manually following the recommendations of annex C5 of EN1993-1-5 [1]. There are several different types of imperfections to be found in the model. The first type is the global imperfection on the longitudinal stiffener with length a. It has a magnitude of $\min\,(a/400\,;\,b/400)$ and it forms the shape of a bow. The remaining imperfections containing the model are the local imperfections of the subpanels with a short span a or b. These imperfections have a magnitude of $\min\,(a/200\,;\,b/200)$ and form a buckling shape. Both types of imperfections are respectively shown in Figure 26 and 27.

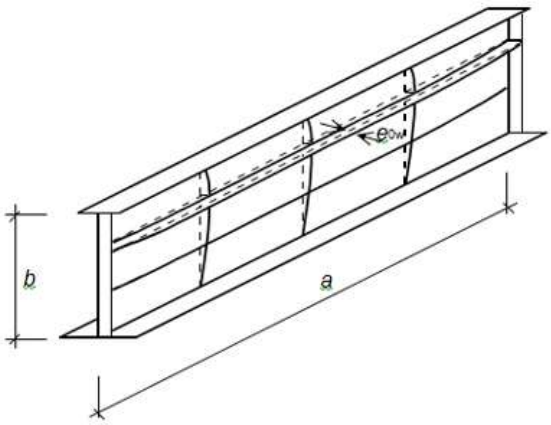

Figure 26: Global imperfection of longitudinal stiffener with length a

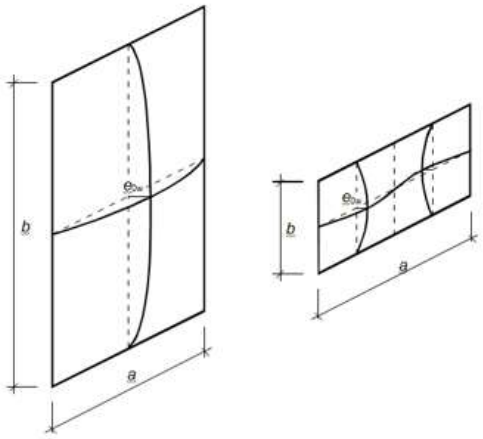

Figure 27: Local imperfections of web-(sub)panel

By meshing the model, all of the finite element nodes were shifted out of its plane to create an imperfection. A mesh size of 20 mm was used. Previous research of A. László [6] showed that a mesh size of 20 mm would be the most efficient combination of accuracy and running time for the used model. This was also confirmed in section 3.5. Therefore, this mesh size was reused in this research for the model validation. After all the imperfections are defined, a combination of all these imperfections has to be made to be able to find the most accurate and most critical combination for each test set-up. For test set-up 1, there is only one imperfection (local imperfection of the web). However, for test set-up 2 and 3 there are four imperfections (one global imperfection of the longitudinal stiffener, and three local imperfections of the web-(sub)panels) for each case. The local imperfections for test set-up two and three are defined as following:

- Local imperfection 1: subpanel 1 between the loaded flange and the stiffener
- Local imperfection 2: subpanel 2 at the location of the stiffener
- Local imperfection 3: subpanel 3 between the stiffener and the bottom flange

Each imperfection can have a positive and a negative value. Therefore, there are two combinations for test set-up one, and 16 combinations for test set-up two and three. For the validation of the model, the most accurate value will be used that is the closest to the experimental values of Seitz [5].

3.7 Performed tests

3.7.1 Test set-up 1

Test set-up 1 has only one imperfection (local imperfection of the web). Therefore, only two different cases must be validated, one with a positive sign for the imperfection and one with a negative sign for the imperfection. Figure 28 gives a visualization of the applied imperfections. Table 5 gives the results of the numerical analysis compared to the experimental load carrying resistances obtained by Seitz [5].

Table 5: Combinations of imperfections for test set-up 1

Test set-up 1	#1	#2
imp. (lok.)	+	-
R_{num}/F_{exp}	97,8%	97,8%

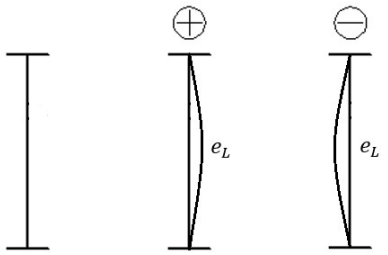

Figure 28: Local imperfection of the web

The numerical results of test set-up 1 have an accuracy of 97,8 % when comparing them with the experimental values obtained by Seitz [5]. Both the cases with a positive and a negative imperfection result in the same value. This can be explained by the fact that both combinations are perfectly similar due to symmetry of the specimen. Therefore, the failure will be exactly the same in both cases.

3.7.2 Test set-up 2

Test set-up 2 has 16 different combinations of imperfections. Figure 29 to 33 give a visualization of all the different imperfections for test set-up 2. Table 6a and 6b presents the used imperfections for each case and it gives the matching value of the numerical results compared to the experimental results obtained by Seitz [5] for test set-up 2.

Table 6a: Combinations of imperfections for test set-up 2

Test set-up 2	#1	#2	#3	#4	#5	#6	#7	#8
imp. (glob.)	-	-	-	-	-	-	-	-
imp. (lok. 1)	-	-	-	+	-	+	+	+
imp. (lok. 2)	-	-	+	-	+	-	+	+
imp. (lok. 3)	-	+	-	-	+	+	-	+
R_{num}/F_{exp}	92,8%	86,5%	90,6%	103,1%	85,8%	97,9%	106,1%	94,5%

Table 6b: Combinations of imperfections for test set-up 2

Test set-up 2	#9	#10	#11	#12	#13	#14	#15	#16
imp. (glob.)	+	+	+	+	+	+	+	+
imp. (lok. 1)	-	-	-	-	+	+	-	+
imp. (lok. 2)	-	-	-	+	+	+	+	-
imp. (lok. 3)	-	-	+	+	+	-	-	+
R_{num}/F_{exp}	85,4%	85,8%	84,4%	83,3%	86,2%	101,9%	97,6%	102,1%

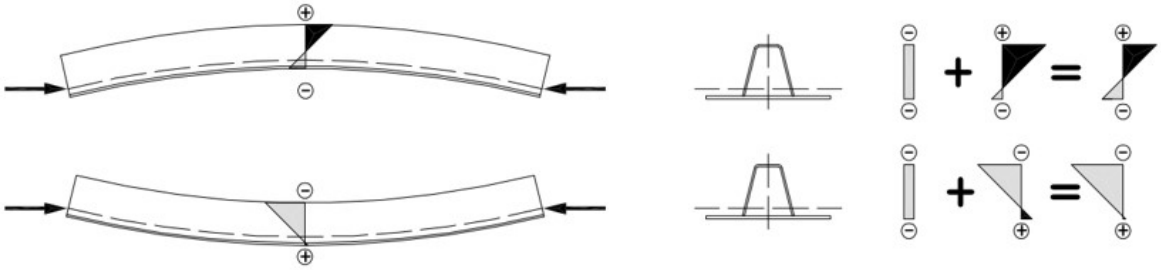

Figure 29: Imperfection of the longitudinal stiffener, positive and negative

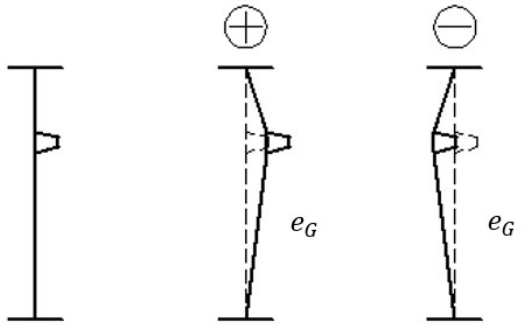

Figure 30: Global imperfection of the stiffener

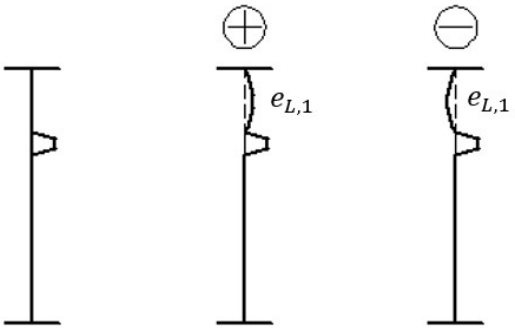

Figure 31: Local imperfection of subpanel 1

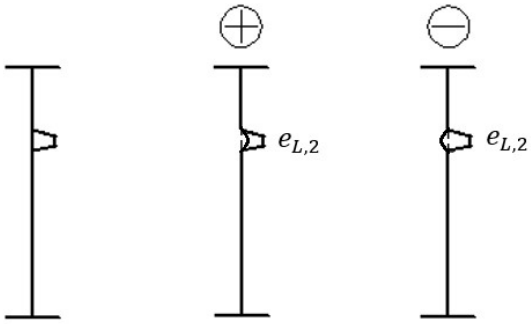

Figure 32: Local imperfection of subpanel 2

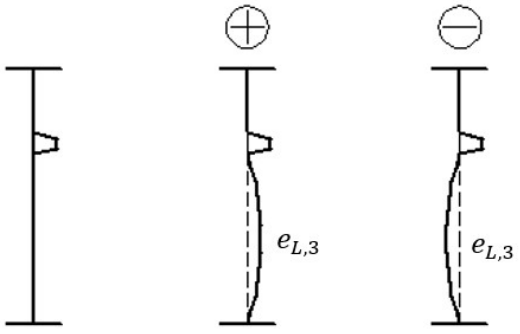

Figure 33: Local imperfection of subpanel 3

Table 6a/b shows that the accuracy of the numerical model is between 83,3 % and 101,9 %. The total deviation of the results is 18,6 %. This is a significant scatter, further research could give an explanation for this observation. However, this will not be discussed further because it is not in the scope of this research. For the validation of the model, combination 14 will be used because it is the most accurate one.

3.7.3 Test set-up 3

Test set-up 3 is similar to test set-up 2. The only difference is the placement of the stiffener. Therefore, this case will be examined in the same way as test set-up 2. Figure 29 to 33 give a visualization of all the different imperfections for test set-up 3. Table 7a,b are giving the used imperfections for each case and it gives the matching value of the numerical results compared to the experimental results obtained by Seitz [5] for test set-up 2.

Table 7a: Combinations of imperfections for test set-up 3

Test set-up 3	#1	#2	#3	#4	#5	#6	#7	#8
imp. (glob.)	-	-	-	-	-	-	-	-
imp. (lok. 1)	-	-	-	+	-	+	+	+
imp. (lok. 2)	-	-	+	-	+	-	+	+
imp. (lok. 3)	-	+	-	-	+	+	-	+
R_{num}/F_{exp}	87,7%	92,9%	86,5%	99,5%	86,9%	95,5%	94,9%	96,2%

Table 7b: Combinations of imperfections for test set-up 3

Test set-up 3	#9	#10	#11	#12	#13	#14	#15	#16
imp. (glob.)	+	+	+	+	+	+	+	+
imp. (lok. 1)	-	+	-	-	+	+	-	+
imp. (lok. 2)	-	-	-	+	+	+	+	-
imp. (lok. 3)	-	-	+	+	+	-	-	+
R_{num}/F_{exp}	92,7%	93,1%	91,5%	90,7%	93,7%	94,7%	92,0%	92,7%

Table 7 shows that the accuracy of the numerical model is between 86,5 % and 99,5 %. The total deviation of the results is 13 %. For the validation of the model, combination 4 will be used because it is the most accurate one.

In Figure 34 until 37, the cross sections of the different shapes of imperfections is shown for test setup 2 and 3. For test setup 2 combination 12 and 14 is represented, respectively the most critical and most accurate imperfection shape. For test setup 3 combination 3 and 4 is represented, respectively the most critical and most accurate imperfection shape. At last, combination 5 is showed for test setup 2 in Figure 38. This is showed because this imperfection shape gives the most critical values overall. This shape will be used in the parametrical analysis that will be conducted in this paper. The horizontal lines represent the position of the longitudinal stiffener.

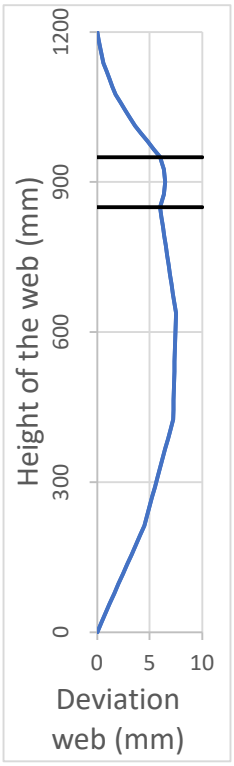

Figure 34: Test setup 2 combination 12

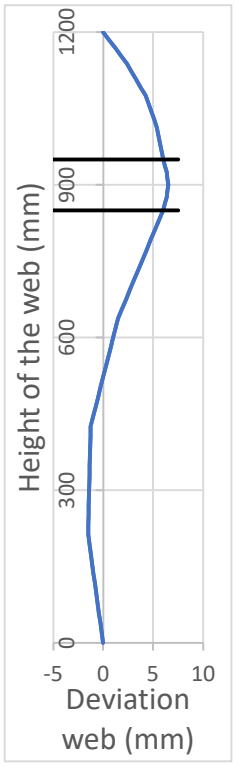

Figure 35: Test setup 2 combination 14

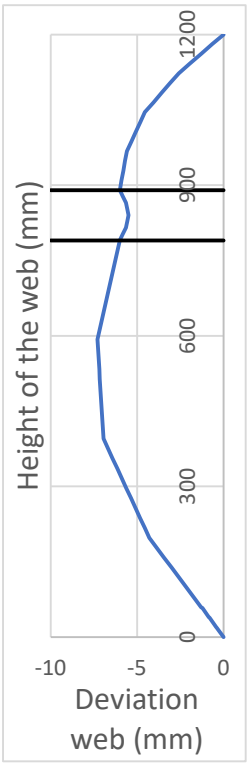

Figure 36: Test setup 3 combination 3

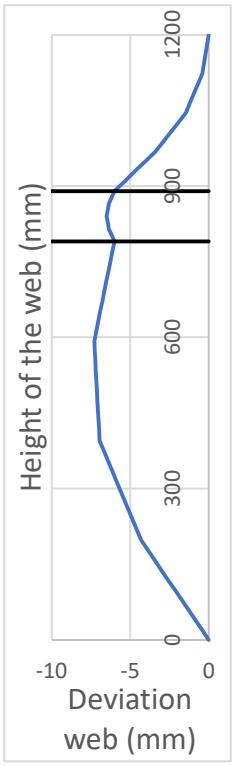

Figure 37: Test setup 3 combination 4

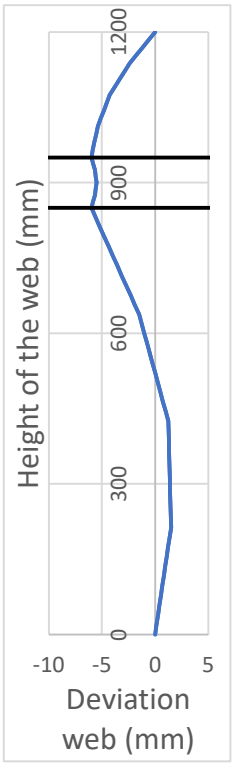

Figure 38: Test setup 2 combination 5

3.8 Model verification

The numerical model calculates the ultimate load capacity using the appropriate imperfections in such a way that it meets up with the conditions of the experiments conducted by Seitz [5]. The program calculates this ultimate load capacity by using a geometric and material non-linear imperfection analysis. The geometric imperfections are as described above and the material non-linearities are as described in Table 4. The program uses the Newton-Raphson algorithm (tangent method) to solve the non-linear analysis. This method makes a linearization of the problem at each iteration step. This is performed until the deviation between the linear solution and the non-linear solution is small enough (Figure 39).

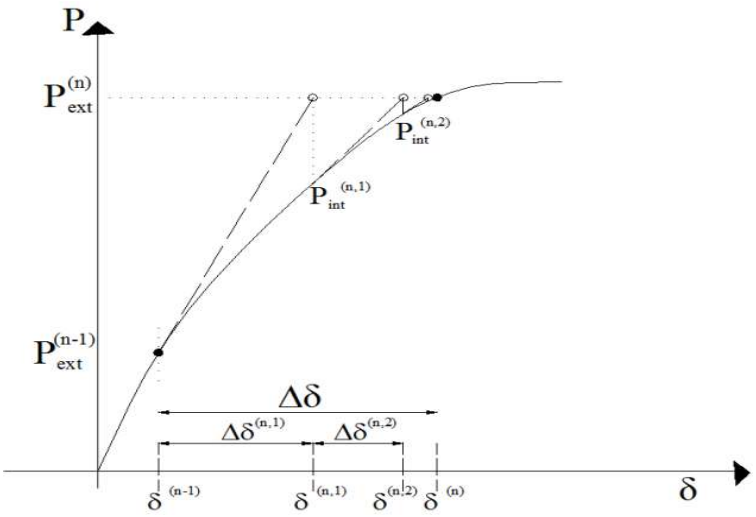

Figure 39: Newton-Raphson procedure [6, p. 48]

A comparison of the results of the three experiments conducted by Seitz [5] and the numerically found results of the model are shown in Table 8. This table shows the values of the limit load capacities of the experimental ($F_{r,exp}$) and numerical ($F_{r,num}$) results. It can be seen that the numerical results are giving a good approximation compared to the values obtained by the experiment. The difference is between 0,5-2,5% for the 3 experiments. The 2,5% deviation belongs to the experiment without a longitudinal stiffener. In the case of experiments with a longitudinal stiffener, which is also the main topic of this research, the deviation is between 0,5 and 2%. These are good approximations which prove that the model, used for the parametric study, is correct.

Table 8: Comparison of experimental and numerical results

Test set-up	Location-stiffener	$F_{r,exp}$ (kN)	$F_{r,num}$ (kN)	$F_{r,num}/F_{r,exp}$
Test set-up 1	/	659	645	97,8%
Test set-up 2	$h_1/h_w = 0{,}25$	1034	1054	101,9%
Test set-up 3	$h_1/h_w = 0{,}3$	949	944	99,5%

The finite element model shows different failure behavior as the one observed by Seitz [5] in his experiments (Figure 40).

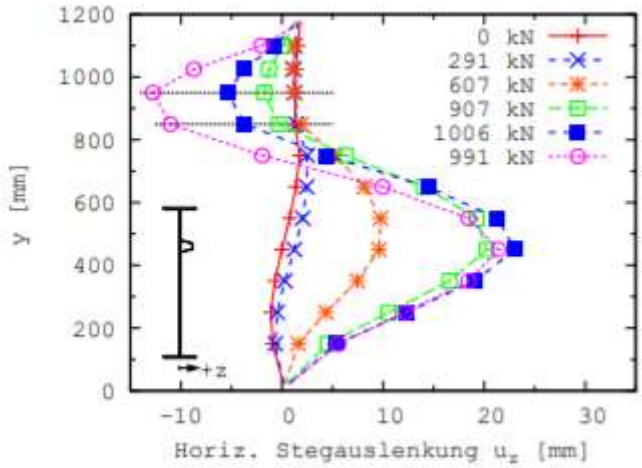

Figure 40: Displacement of the web perpendicular to the web plane obtained by Seitz

However, for the parametric study further on in this research, the most critical imperfection combination will be used. Table 6a/b and Table 7a/b shows that respectively combination 12 and combination 4 are the most critical values. However, these combinations will not be used. Instead, the values of combination 5 will be used because this combination is for all cases nearly the most critical one. This decision is also made because this combination shows similar failure behavior as the one observed by Seitz [5] in his experiments.

4. Numerical parametric test

In this chapter, the results of the parametric study of all of the changing parameters will be discussed. There will also be an investigation on two and three stiffener cases.

4.1 Numerical test Design

The purpose of the numerical testing is to verify if the limited value of the stiffness of the longitudinal stiffener, formulated by formula 6.6 in chapter 6 of EN 1993-1-5 [1], is correct. This formula describes a limitation on the stiffness of a longitudinal stiffener of a girder. This limitation point of the stiffness will be further referred to as the optimal stiffness of the stiffener. This optimal stiffness is the limit value of which there will be no further patch loading resistance gaining when further increasing the stiffness of the stiffener. The Eurocode provides this formula for cases with one longitudinal stiffener. But in practice, this limit value is also commonly used for girders with multiple stiffeners.

The first thing to do is to evaluate this formula for the optimal stiffness given by the Eurocode. Eq. (4.1) represents the equation stated in EN 1993-1-5 [1].

$$\gamma_{st} = 10{,}9\frac{I_{st,l}}{h_w\, {t_w}^3} \leq 13\left[\frac{a}{h_w}\right]^3 + 210\left[0{,}3 - \frac{b_1}{a}\right] \tag{4.1}$$

The left part of this equation shows how the stiffness of a certain longitudinal stiffener is defined. As can be seen, the stiffness of a longitudinal stiffener depends on the moment of inertia of a hybrid system between a part of the web and the actual longitudinal stiffener. This parameter is defined as $I_{st,l}$. Further, the height of the web (h_w) and the thickness of the web (t_w) are characterizing this stiffness parameter. The right side of the equation is the optimal stiffness as described by the Eurocode [1]. The calculation of the optimal stiffness exists of three parameters. The total length of the girder (a), the height of the web (h_w) and the length between the loaded flange and the first stiffener on the web (b_1). In the parametrical study, the influence of these parameters will be studied on the optimal stiffness together with the loaded length of the patch load (s_s). This study is performed for a non-linear material and geometry analysis (GMNIA) with imperfections and for a linear buckling analysis (LBA). All of the tests are performed on situations with rigid end posts on both sides and with rectangular closed-section stiffeners.

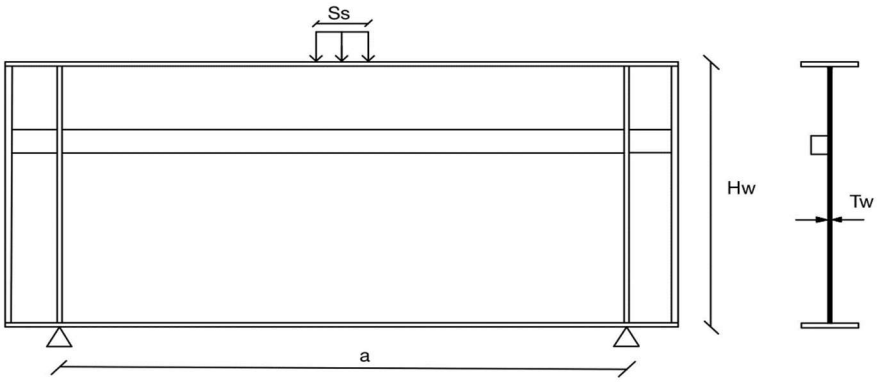

Figure 41: The four investigated parameters

In the next section, the general test setups will be explained for the one stiffener cases, the changing parameters will be identified and their range will be set.

Afterwards, the influence of these four parameters on the optimal stiffness will be discussed. First, the four parameters for the one stiffener cases will be investigated. If a certain link between this parameter and the optimal stiffness is observed, further research is done using two and three stiffeners.

4.2 Numerical test setup – one stiffener

4.2.1 General

A parametric study was performed on girders with one longitudinal stiffener to analyze the influence of the stiffness of the stiffener on the patch loading resistance. The optimal stiffness of the longitudinal stiffener was determined for each changing parameter.

For each of the four changing parameters, there were two types of failure modes tested. At first, the stiffener was placed at a distance of 15% of the height of the web of the loaded flange. With this placement, a failure in the lower subpanel was triggered. The second failure type that was investigated was a failure in the upper subpanel. This failure happened when the stiffener was placed at 30% of the height of the web of the loaded flange. Both failure types are shown in Figure 42.

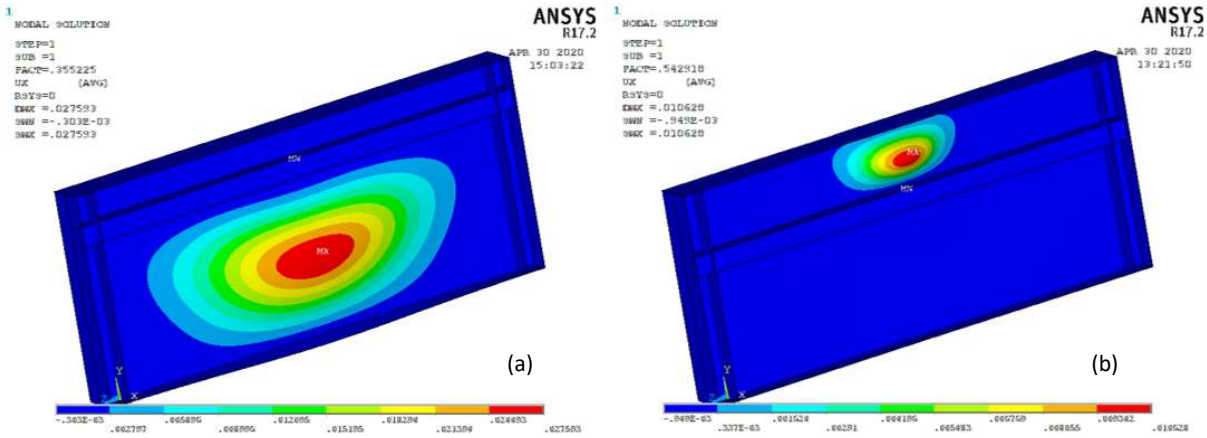

Figure 42: Illustrative example of failure in lower (a) and upper (b) subpanel

4.2.2 Range of the changing parameters

The range of the used parameters can be found in Table 9. The geometry of the girder was kept constant for each changing parameter. The different kinds of geometries used for each parameter can be found in Table 10. This table also shows the b_1 value for both failure types. The first b_1-value was used when failure occurred in the lower subpanel. The second b_1-value was used when failure occurred in the upper subpanel.

Table 9: Changing parameters (1 stiffener)

Changing parameters	Range of the parameters (mm)
t_w	6 – 9 – 14 – 16 - 18
s_s	400 – 800 – 1000 - 1200
a	2500 – 3500 – 4500 – 5500 - 6500
h_w	1500 – 1800 – 2100 – 2500 - 2900

Table 10: Geometries for each parameter

Parameter	t_w	s_s	a	h_w	b_f	t_f	F_{yf}	F_{yw}	b_{st}	b_1
t_w		800	4000	2700	400	16	355	355	180	405/810
s_s	10		4500	2100	400	16	355	355	140	315/630
a	10	800		2700	400	16	355	355	180	405/810
h_w	10	800	4500		400	16	355	355	180	$0.15h_w/0.3h_w$

The optimal stiffness was determined for the four different parameters shown in the tables above, each time for five (or four) different geometries as can be seen in Table 9. This was done for failure in both the upper and the lower subpanel. For example for the thickness of the web, the optimal stiffness of the stiffener was searched for the following values of the thickness of the web: 6, 9, 14, 16 and 18 mm. To find this optimal stiffness, the tests were performed by starting with a low stiffness of the stiffener and gradually increasing this by changing the thickness of the stiffener (t_s). The height of the stiffener (h_{st}) was kept constant. This was done for the non-linear material and non-linear geometry analysis (GMNIA) with imperfections and for the linear buckling analysis (LBA). After performing the tests, different patch loading resistances were obtained and linked with a specific stiffness of the longitudinal stiffener. These values were plotted on a graph for the GMNIA and for the LBA. Out of these graphs, the optimal stiffness for each case was determined.

4.2.3 Determination process of the optimal stiffness

This paragraph will explain how the optimal stiffness of the longitudinal stiffeners was determined. The optimal stiffness was determined for both the LBA and GMNIA. This was done to be able to compare the results for both analyses. The process which was followed to determine the optimal stiffness will be clarified by using two examples of our parametric study. Example one is for the case where the length (a) is 3500 mm and example two is the case where the height of the web (h_w) is 2100 mm. The two main principles which the determination process of the optimal stiffness is based on, are the relation between the critical buckling load (for LBA), or the ultimate load (for GMNIA), and the stiffness of the longitudinal stiffener. The second principle which the optimal stiffness is based on, is the relation between the relative displacement of the upper subpanel and the stiffness of the longitudinal stiffener. First, the LBA method for determining the optimal stiffness will be explained followed by the explanation of the GMNIA method.

4.2.3.1 LBA method

The first principle for determining the optimal stiffness is shown in Figure 43. The load-stiffness curve for example one can be seen based on the LBA. This represents the stiffness of the longitudinal stiffener with the corresponding patch load resistance of the girder. In Figure 44, the same curve can be seen for example two.

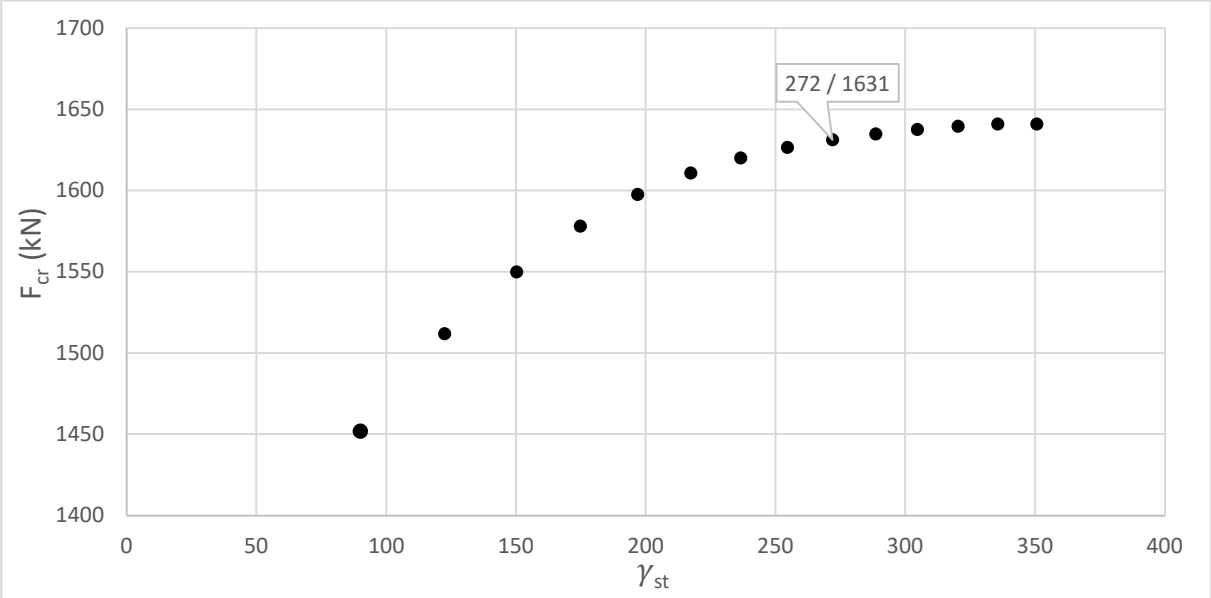

Figure 43: Load-stiffness curve, example one (LBA)

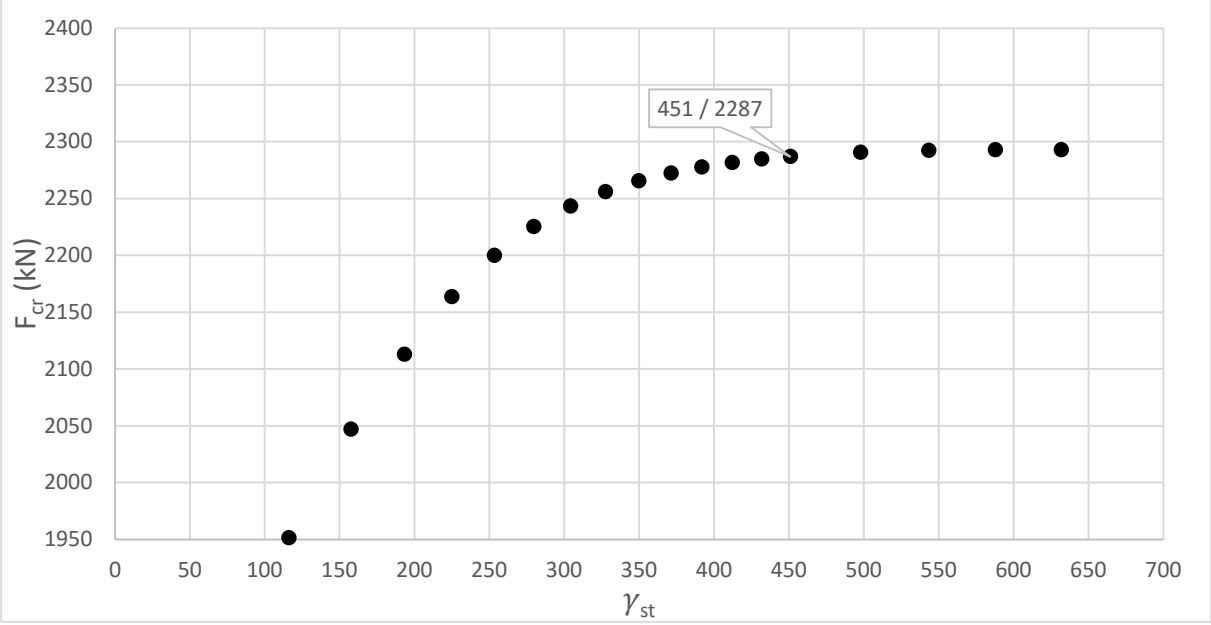

Figure 44: Load-stiffness curve, example two (LBA)

When observing these curves, one can see that these curves have a steep inclination in the beginning and are going to a maximum value at the end of the curve. The optimal stiffness is chosen as the point from whereon there is no significant increase anymore in the patch load resistance. For example one, this point is where the stiffness is 272 and where the patch load resistance is at 1631 kN. For example two, this point can be observed as where the stiffness is 451 and where the patch load resistance is at 2287 kN.

The second main principle for determining the optimal stiffness is via the relative displacement of the upper subpanel. The relative displacements for both subpanels can be seen in Figure 45 for example one and in Figure 46 for example two based on the LBA. The trend of the lower subpanel for both examples will also be discussed.

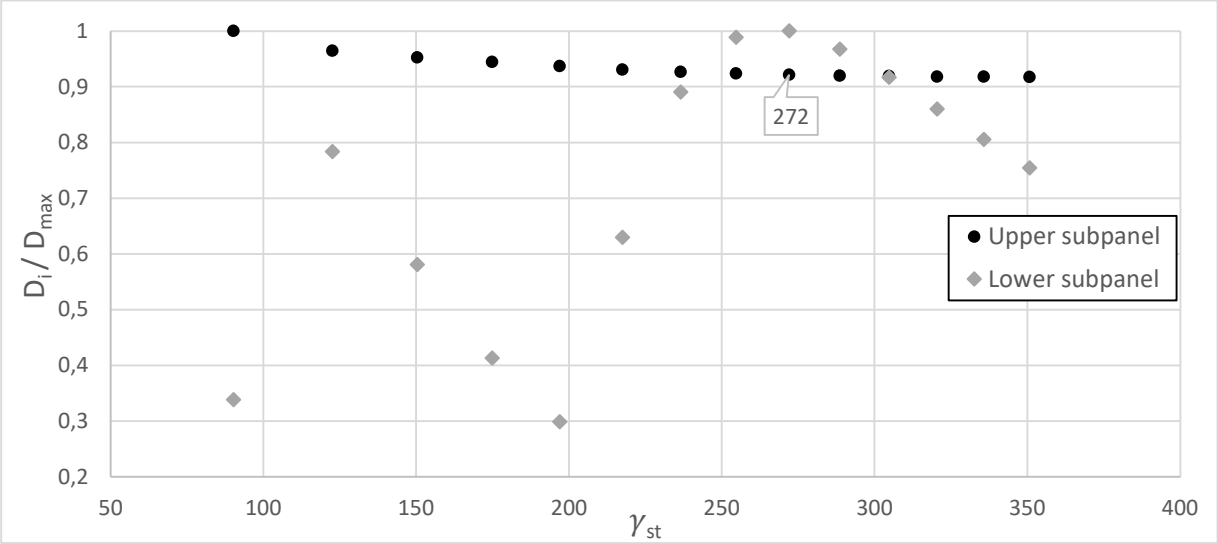

Figure 45: Relative displacement of the upper and lower subpanel, example one (LBA)

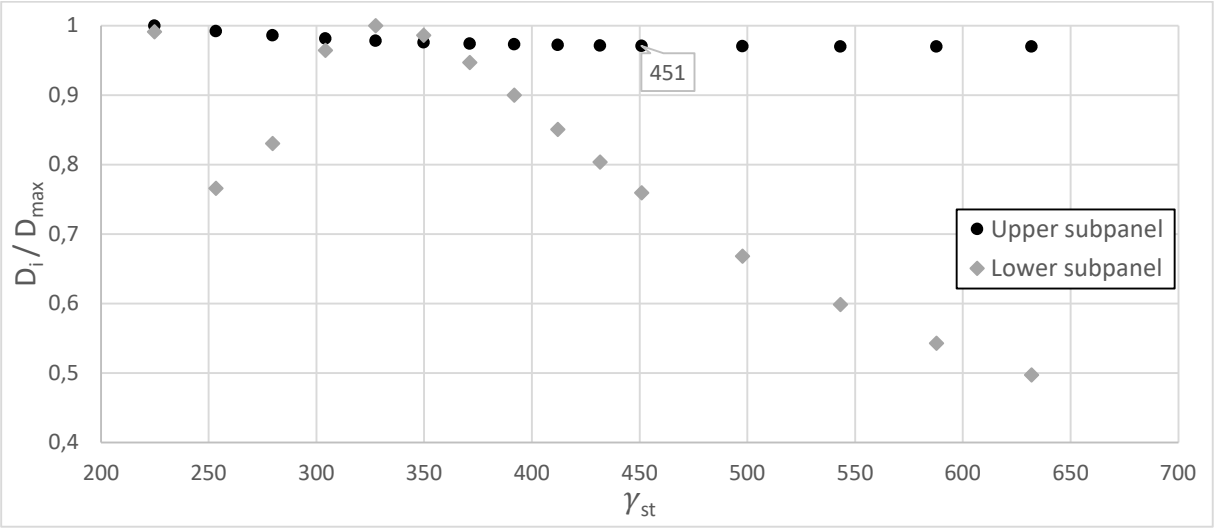

Figure 46: Relative displacement of the upper and lower subpanel, example two (LBA)

The horizontal axis gives the stiffness of the longitudinal stiffener, while the vertical axis gives the displacement of the upper and lower subpanel relative to the maximum displacement in the upper or lower subpanel. When observing the upper subpanel, it can be seen that when the stiffness is low, the displacement of this subpanel is at its highest point. This is because this part is still very flexible because of the low stiffness of the stiffener. The failure mode that is occuring here is a global buckling mode (Figure 6c). The stiffener is unable to separate the failure into multiple buckling shapes due to its low stiffness. Therefore, this stiffener can be reffered to as a “weak” stiffener. This “weak” stiffener causes larger displacements in the upper subpanel.

When making the stiffener stiffer, the maximum displacement in the upper subpanel goes to a minimum. In the process of changing the stiffness, the occuring failure mode will change from a global failure mode to an interaction failure mode (Figure 6b).

From a certain stiffness on, the maximum displacement will remain constant at a minimal value. At this point, a local failure mode will occur (Figure 6a). The stiffener now has the ability to separate the global buckling shape into multiple local buckling shapes. Therefore, this stiffener can be refferd to as a “strong” stiffener. The stiffness from where the maximum displacement in the upper subpanel remains constant, results in the optimal stiffness of the longitudinal stiffener.

A next, minor, thing to observe is the displacement in the lower subpanel. In the LBA method, the lower subpanel goes to a maximum displacement before decreasing and going to a minimal displacement.

To give some context to these graphs, three points are chosen to be pointed out (before, at and after the optimal stiffness) with their corresponding displacement figures. These displacement figures can be found in Figure 47 until 49.

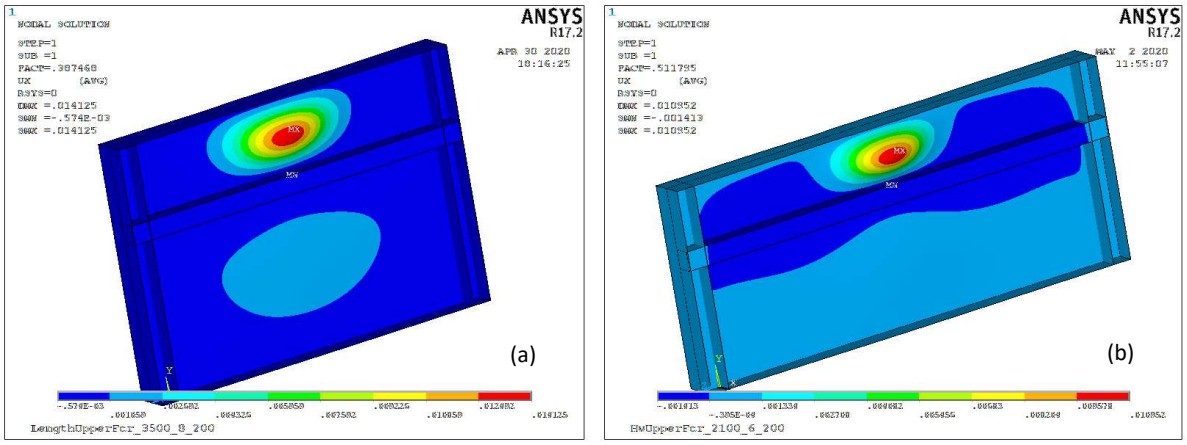

Figure 47: LBA displacement; a) example one: point (150/1550), b) example two: point (157/2047)

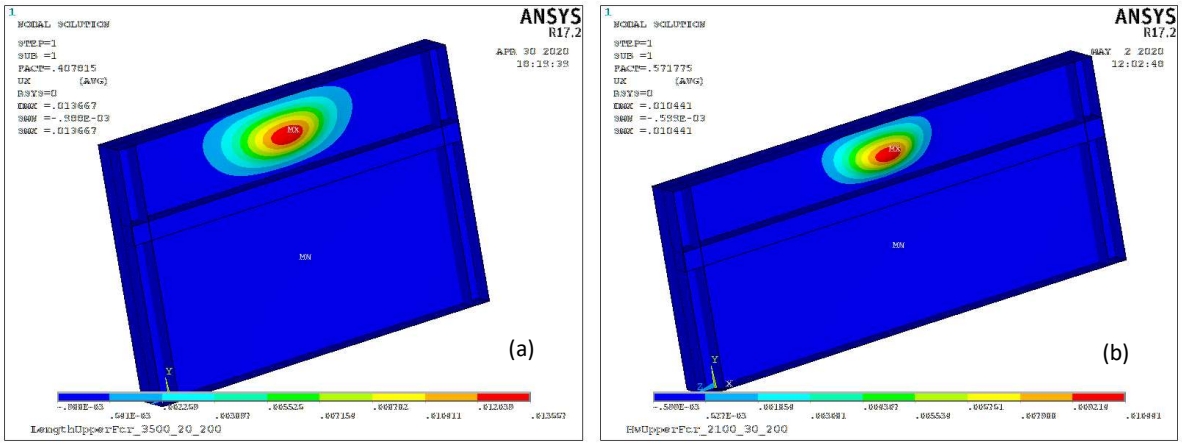

Figure 48: LBA displacement; a) example one: point (272/1631), b) example two: point (451/2287)

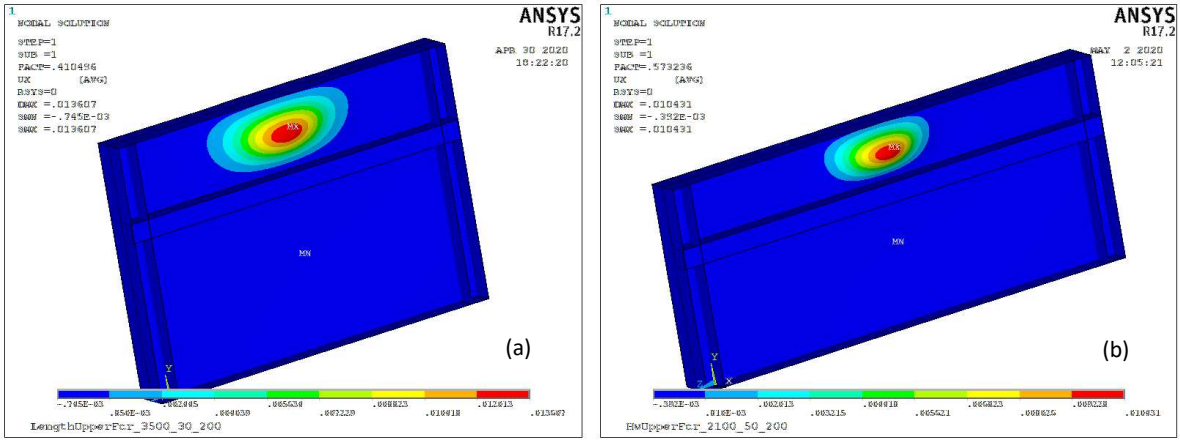

Figure 49: LBA displacement; a) example one: point (351/1641), b) example two: point (632/2293)

4.2.3.2 GMNIA method

The first principle for determining the optimal stiffness in the GMNIA is shown in Figure 50. The load-stiffness curve for example one can be seen based on the GMNIA. This represents the stiffness of the longitudinal stiffener with the corresponding patch load resistance of the girder. In
Figure 51, the same curve can be seen for example two.

The trends, visible in Figure 50, are similar to the ones that were observed in Figure 43 for the LBA method. The optimal stiffness is chosen as the point from whereon there is no significant increase anymore in the patch load resistance. For example one, this point is where the stiffness is 255 and where the patch load resistance is at 1561 kN. For example two, this point can be observed as where the stiffness is 451 and where the patch load resistance is at 1705 kN.

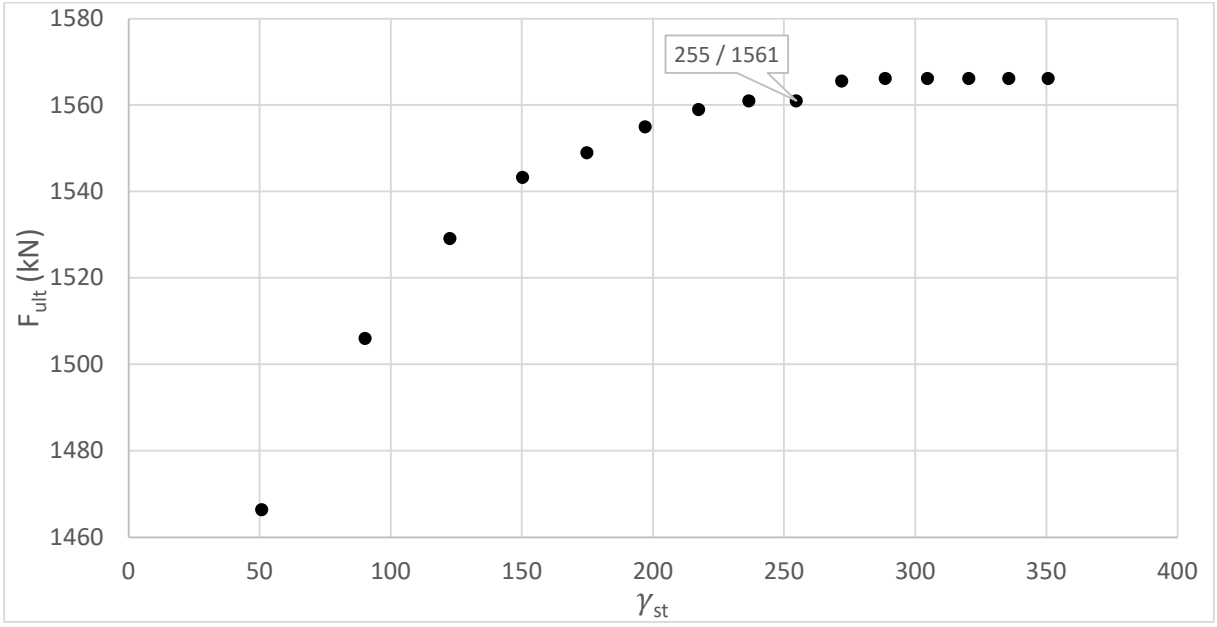

Figure 50: Load-stiffness curve, example one (GMNIA)

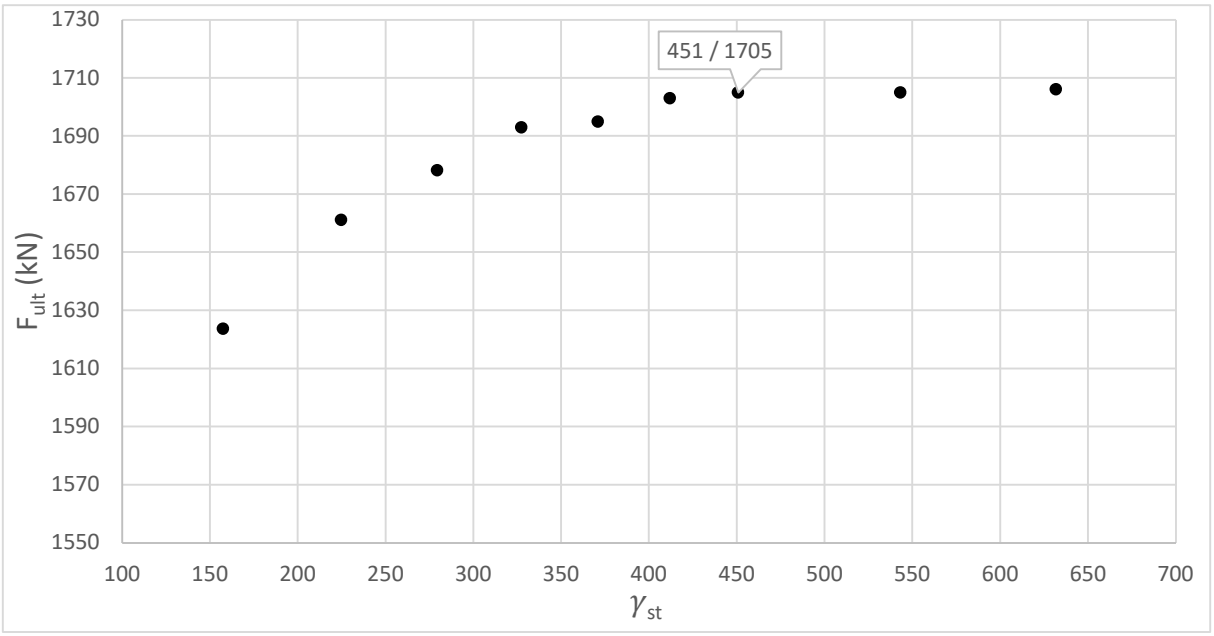

Figure 51 Load-stiffness curve, example two (GMNIA)

The second main principle for determining the optimal stiffness is via the relative displacement of the upper subpanel. The relative displacements for both subpanels can be seen in Figure 52 for example one and in Figure 53 for example two, based on the GMNIA. The trend of the lower subpanel for both examples will also be discussed.

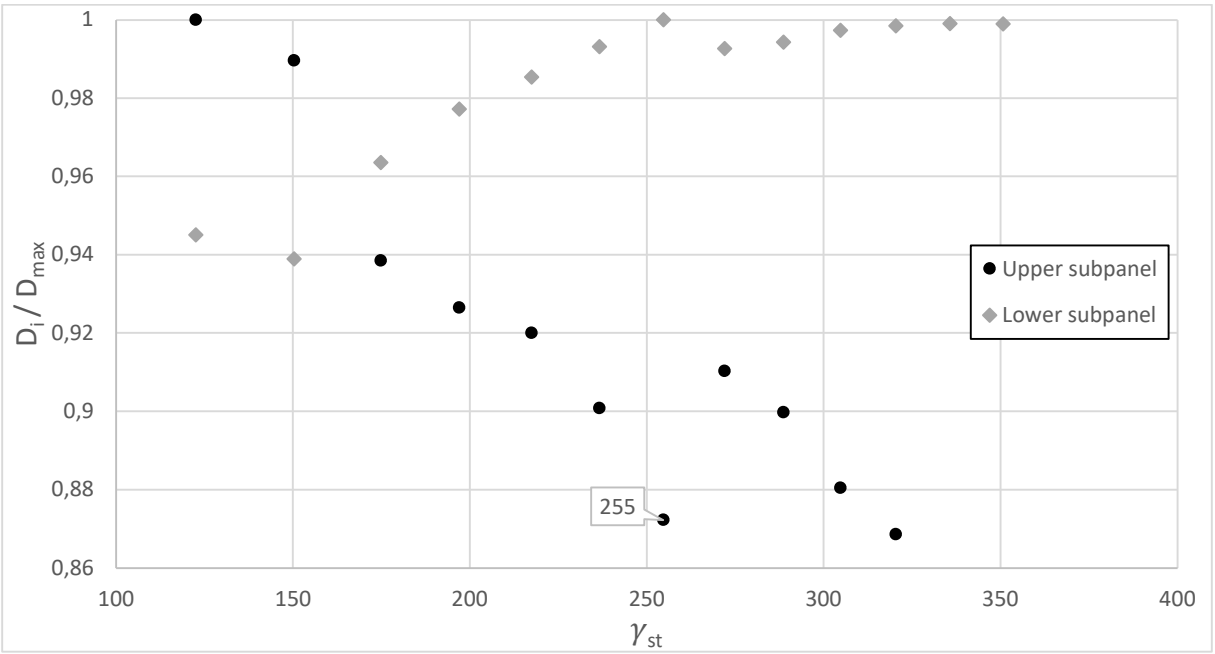

Figure 52: Relative displacement of the upper and lower subpanel, example one (GMNIA)

The data that is shown in Figure 52 is more inconsistent than in Figure 45. This can be explained via the load-slip curves, generated per investigated point. For the LBA, this curve is a continuous linear function. When there is an uncertainty on the failure load, this results only in a minor decrease or increase of the according displacement. For the GMNIA, this curve is a linear function in the beginning, but is deflecting to a maximum value at the end. If there is an uncertainty on the GMNIA failure load, this results in a significant decrease or increase of the according slip. This is the reason why there is a sudden change in relative displacement visible in Figure 52 after the investigated point with a stiffness of 255.

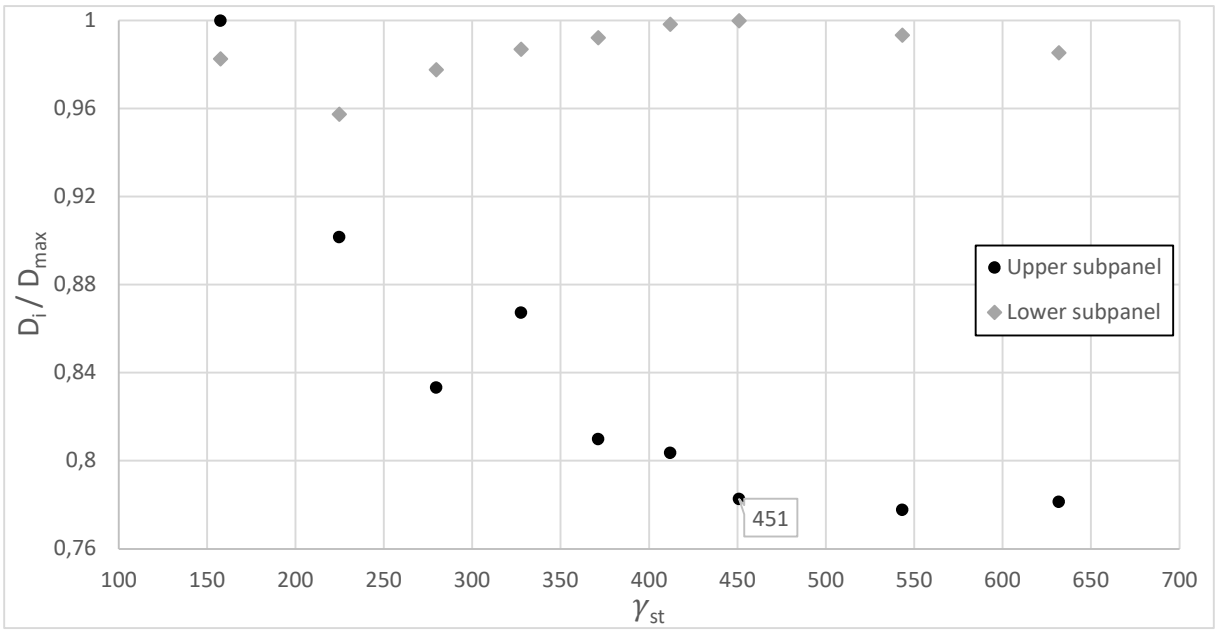

Figure 53: Relative displacement of the upper and lower subpanel, example two (GMNIA)

Although, some similar trends can be observed. The three different failure modes that were observed in the LBA method are also visible here. When the displacement in the upper subpanel is at its highest point, a global buckling failure mode occurs (“weak” stiffener). Between this point and the optimal stiffness, the failure mode changes to an interaction buckling failure mode. From the optimal stiffness on, a local buckling failure mode can be observed (“strong” stiffener)

A next, minor, thing to observe is the displacement in the lower subpanel. In the GIMNIA method, the lower subpanel goes to a maximum displacement and stays at a constant value. This is in contradiction with the observed trend in the LBA method.

To give some context to these graphs, three points are chosen (before, at and after the optimal stiffness) with their corresponding displacement and von Mises stresses figures. These figures can be found in Figure 54 until 59.

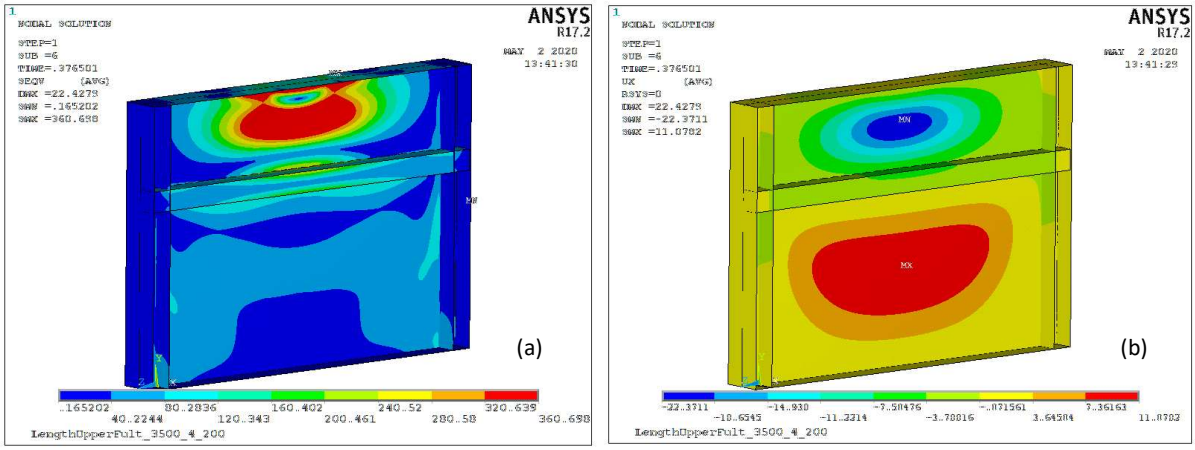

Figure 54: Example one: point (157/1624), a) von Mises stress, b) GMNIA displacements

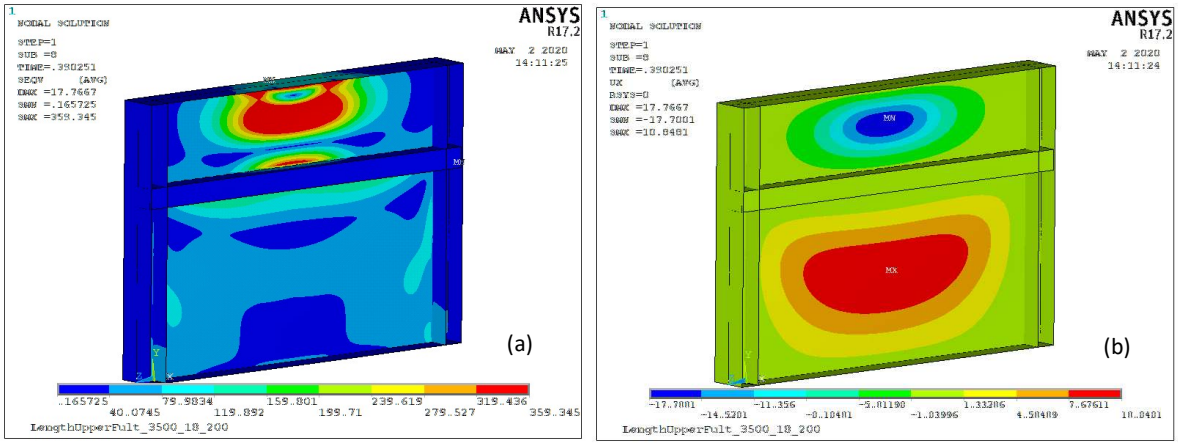

Figure 55: Example one: point (255/1561), a) von Mises stress, b) GMNIA displacements

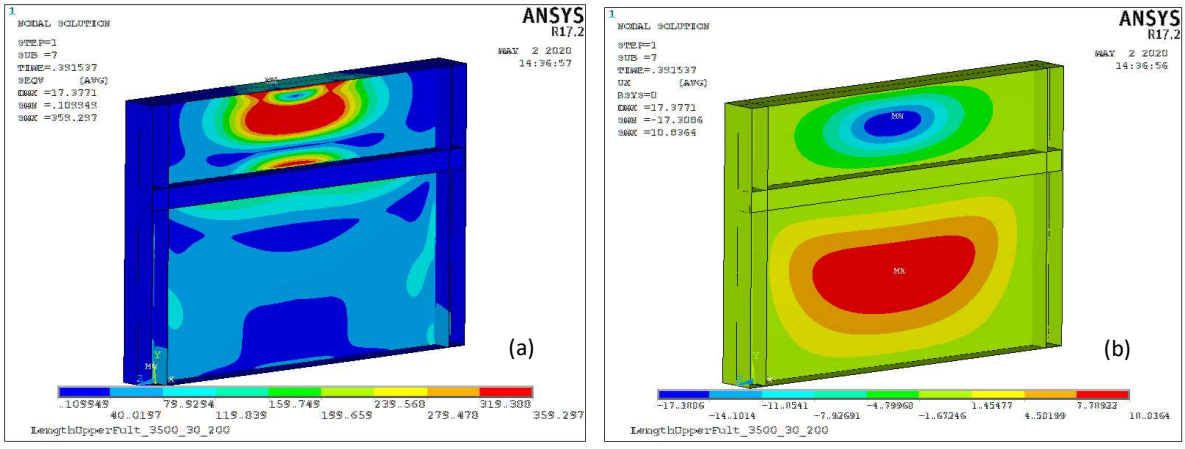

Figure 56: Example one: point (351/1566), a) von Mises stress, b) GMNIA displacements

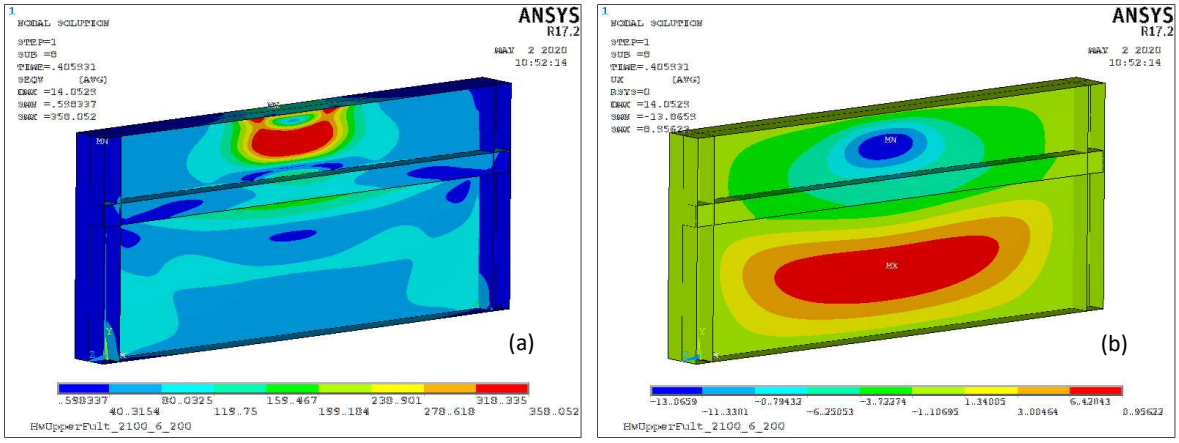

Figure 57: Example two: point (157/1624), a) von Mises stress, b) GMNIA displacements

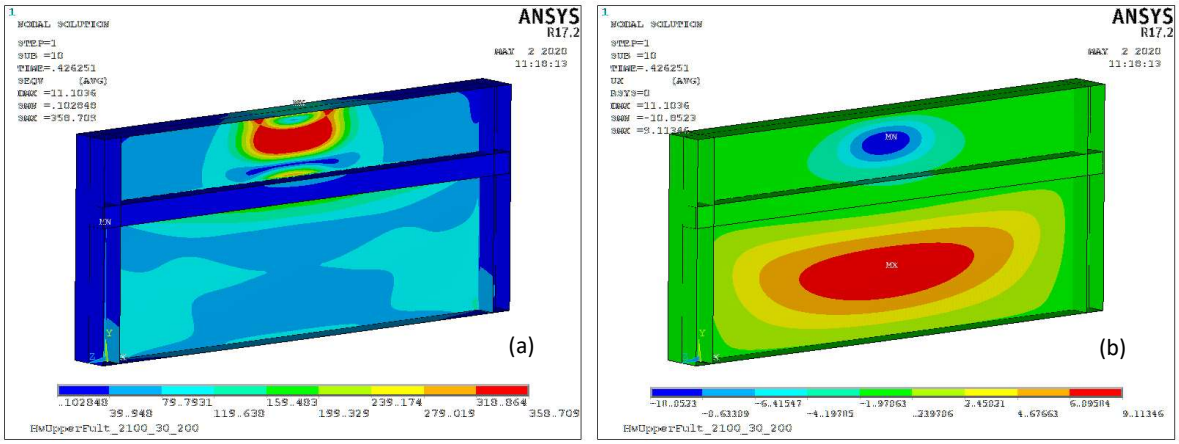

Figure 58: Example two: point (451/1705), a) von Mises stress, b) GMNIA displacements

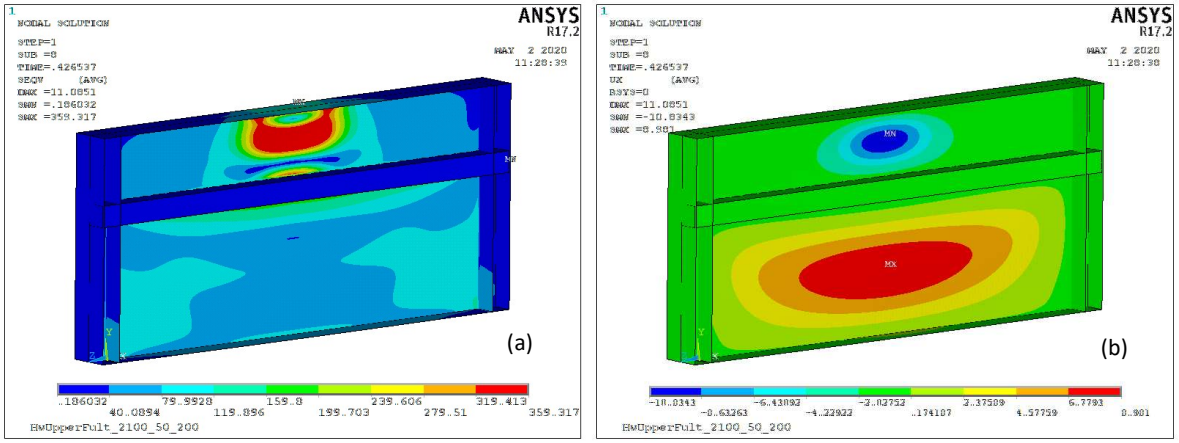

Figure 59: Example two: point (632/1706), a) von Mises stress, b) GMNIA displacements

4.2.4 Eurocode formula range

To be able to compare the numerical test results with the optimal stiffness prescribed by the Eurocode formula (eq. (4.1)) [1], our investigation should be within the limits set by the Eurocode. These limitations are described for the buckling coefficient k_F, which includes γ_{st}. It is stated that eq. (2.67) and eq. (2.68) of section 2.3.4 are only valid for the following criteria:

$$0.05 \leq \frac{b_1}{a} \leq 0.3 \text{ (criteria 1) and } \frac{b_1}{h_w} \leq 0.3 \text{ (criteria 2)} \tag{4.2}$$

The values of this research are well within this range, except for one outlier (a = 2500 mm). This outlier will be taken into account when reviewing the results. This outlier only accounts for the calculation of its optimal stiffness via the formula of the Eurocode. The numerical results are not limited by these criteria. The values for the two criteria used in our cases can be found in Table 11a/b.

Table 11a: Range of criteria 1

Parameter	Failure upper subpanel: b_1/a	Failure lower subpanel: b_1/a
t_w	0.20	0.10
s_s	0.14	0.07
a_{2500}	0.32	0.16
a_{3500}	0.23	0.12
a_{4500}	0.18	0.09
a_{5500}	0.15	0.07
a_{6500}	0.12	0.06
$h_{w,1500}$	0.10	0.05
$h_{w,1800}$	0.12	0.06
$h_{w,2100}$	0.14	0.07
$h_{w,2500}$	0.17	0.08
$h_{w,2900}$	0.19	0.09

Table 11b: Range of criteria 2

Parameter	Failure upper subpanel: b_1/h_w	Failure lower subpanel: b_1/h_w
t_w	0.3	0.15
s_s	0.3	0.15
a	0.3	0.15
h_w	0.3	0.15

4.3 Test results and discussion – one stiffener

4.3.1 Interpretation of the results

The results of the research should be interpreted while bearing the following things in mind. First of all it is very difficult to compare the exact absolute values for the optimal stiffnesses found with the Eurocode formulation and with the numerical testing. This is the case because there is not an exact definition of the optimal stiffness described in the literature. Therefore, it is more accurate to evaluate the trend described by the Eurocode and the one found with the numerical testing. For the absolute values, the conclusions are based on the fact if the two descriptions for the optimal stiffness are in close vicinity and in the same order of magnitude.

4.3.2 Main comment for one stiffener cases

In the one stiffener cases, there were two failure modes investigated. During the observations of the cases with a failure in the lower subpanel, a discrepancy in the data could be observed. From a certain point on, the increase of the patch loading resistance became a linear function instead of a deflecting curve going to an optimal stiffness. An example for both the critical buckling load and the ultimate failure load is given in Figure 60 and 61.

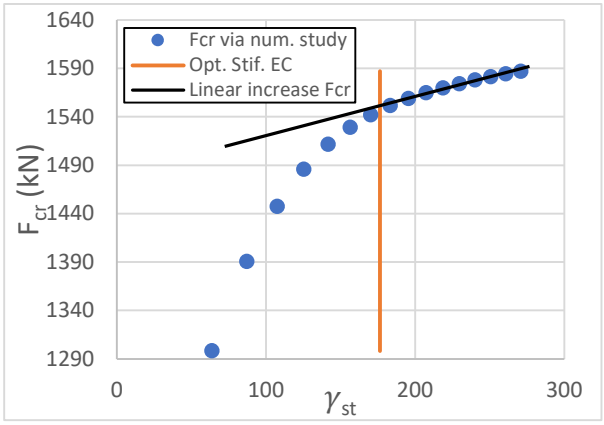

Figure 60: Optimal stiffness determination for critical buckling load (LBA) (Ss=1200)

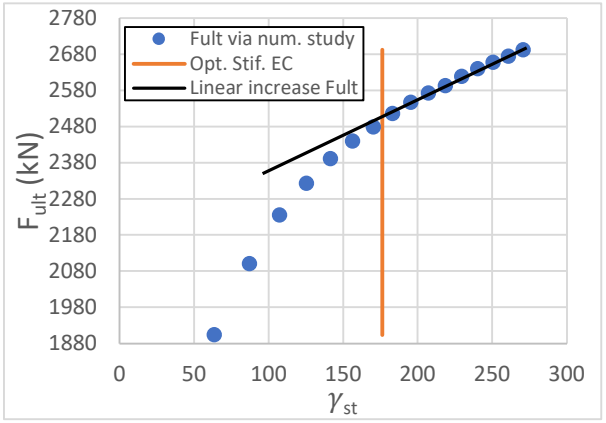

Figure 61: Optimal stiffness determination for ultimate failure load (GMNIA) (Ss=1200)

This phenomenon can be explained by the fact that all of the buckling problems have some post buckling reserve. In these cases, the lower subpanel fails, but the upper subpanel still has some reserve and thus some extra resistance. Because of this extra resistance, the curve keeps inclining instead of deflecting to an optimal stiffness. There will be found a maximum for this inclining curve at the point where both the lower and the upper subpanel fail. In order to still have a useful point for the research, the stiffness right before the curve goes to a linear form is chosen as the optimal stiffness of that configuration. This discrepancy only occurred for the cases with a failure in the lower subpanel.

4.3.3 Effect of change of the loaded length (S_s)

4.3.3.1 Effect according to Eurocode

The second part of eq. (4.1) represents the optimal stiffness of a longitudinal stiffener, this second part of eq. (4.1) is given below:

$$\gamma_{st,EC} = 13\left(\frac{a}{h_w}\right)^3 + 210\left(0{,}3 - \frac{b_1}{a}\right) \tag{4.3}$$

In total, there are four parameters which are being investigated. Of these four parameters, the loaded length is not included in the Eurocode formulation for the definition of the optimal stiffness. This means that according to the Eurocode, the loaded length does not have an influence on the optimal stiffness of a longitudinal stiffener. The value of the optimal stiffness will remain constant while changing the loading length. This link between the loaded length and the optimal stiffness is shown in .

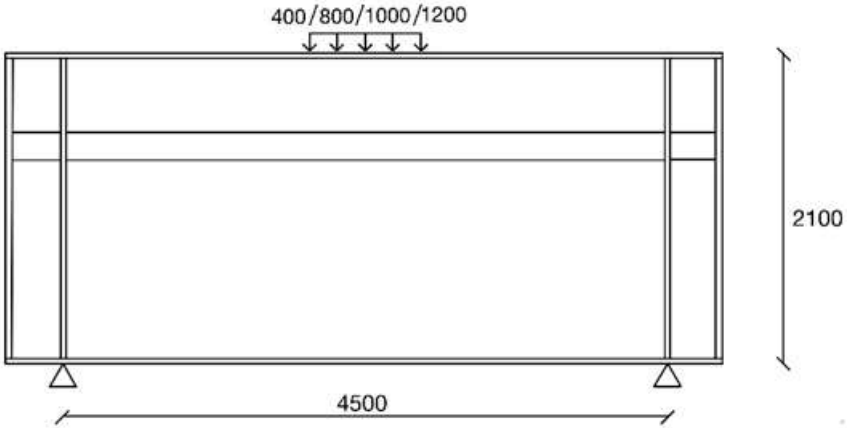

Figure 62: Visualization of changes of parameter Ss (in mm)

4.3.3.2 Effect according to numerical results for one stiffener cases

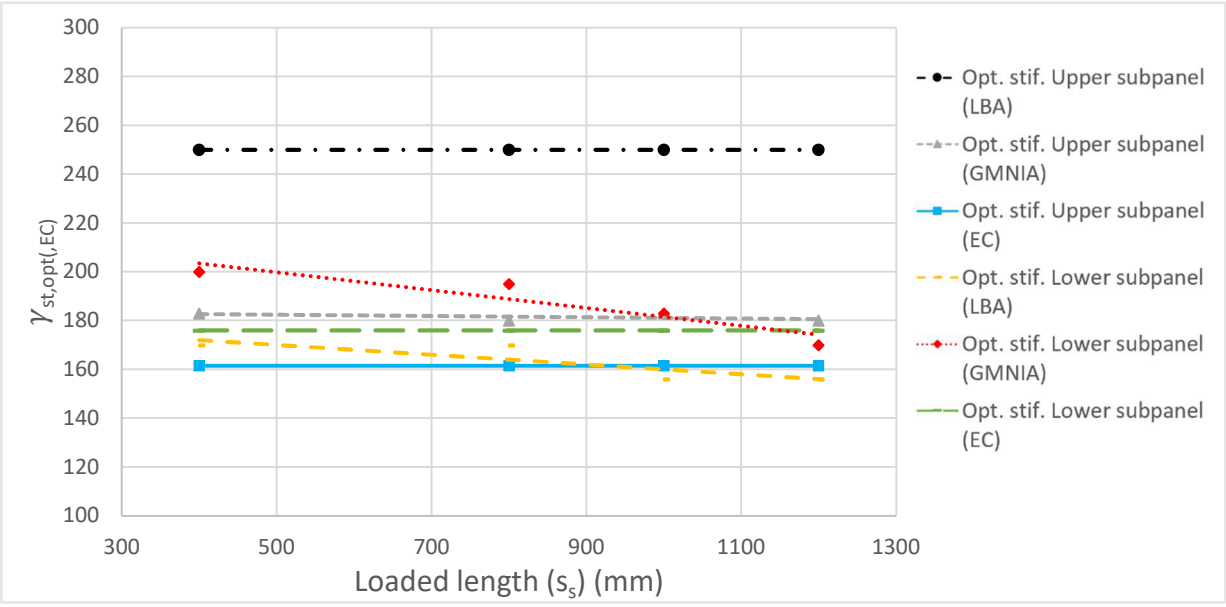

Figure 63: Optimal stiffness in function of the loaded length

A constant line can be observed for the optimal stiffness when the failure occurred in the upper subpanel for both the GMNIA and the LBA. This is in agreement with the Eurocode formulation. Hereby, it can be stated that for failure in the upper subpanel, the Eurocode describes the right trend. The absolute values of the optimal stiffness are for both analyses within an acceptable range and the closest to the GMNIA.

For the second failure mode in the lower subpanel, a slightly declining trend can be observed. This accounts for both the critical buckling load analysis as for the GMNIA. All of the investigated points for the critical buckling load analysis are below the Eurocode formulation, while three out of four of the GMNIA points are above this formulation. But in general all of the points are very close to the Eurocode formulation. The declining trend may be explained by the discrepancies in the data that were described above.

It can thus be stated that the Eurocode formulation describes the right trend when changing the loaded length. The loaded length has no influence on the optimal stiffness of a longitudinal stiffener.

4.3.4 Effect of change of the length of the girder (a)

4.3.4.1 Effect according to Eurocode

According to eq. (4.3), the length of the girder should have an $1/a$ increasing type of influence. This means that when increasing the length of the girder, the optimal stiffness also increases exponentially. This link between the length of the girder and the optimal stiffness is shown in Figure 65.

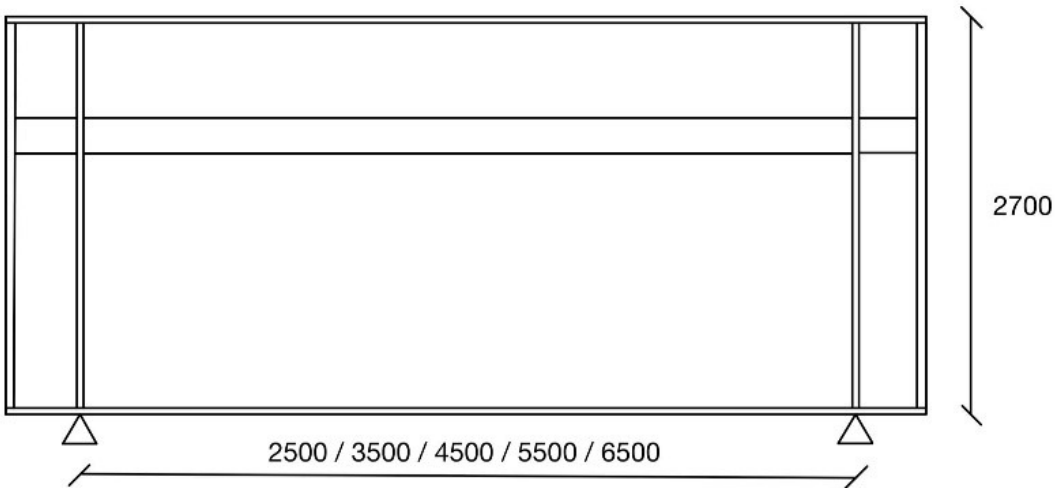

Figure 64: Visualization of changes of parameter a (in mm)

4.3.4.2 Effect according to numerical results for one stiffener cases

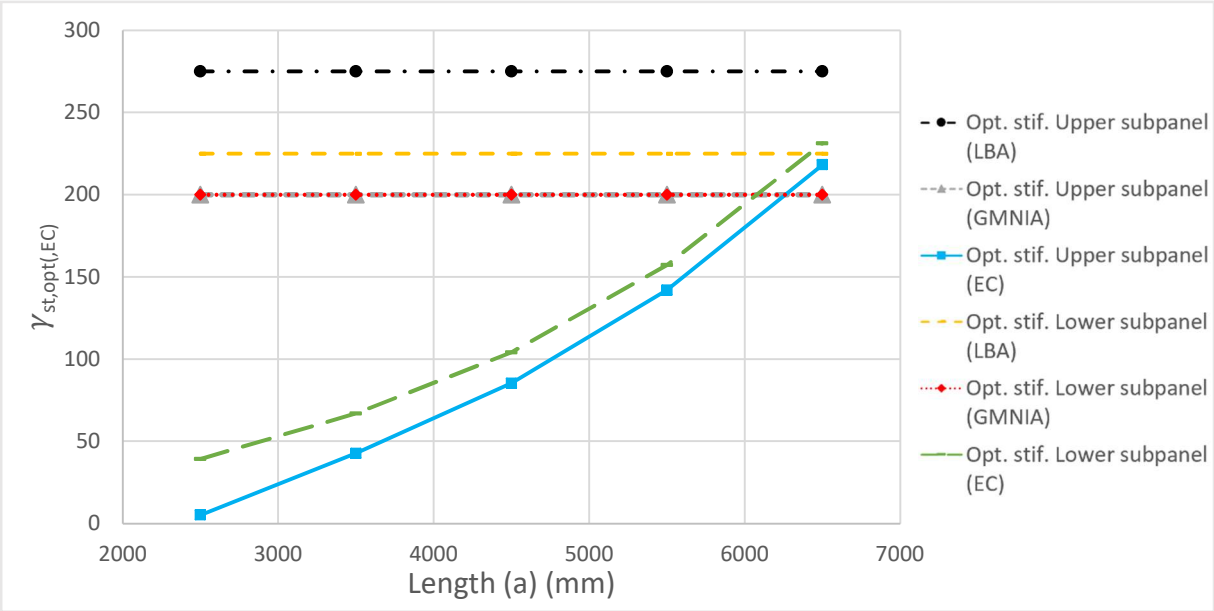

Figure 65: Optimal stiffness in function of the length of the girder

When the failure happens in the upper subpanel, a $1/a$ trend is described by the Eurocode formulation. For the numerical results, both for the LBA and for the GMNIA, a constant value for the optimal stiffness is obtained. For the LBA, overall higher values were found for the optimal stiffness compared to the GMNIA. This observed trend is in contradiction with the Eurocode formulation. Thus there can be stated that when the failure happens in the upper subpanel, the total length of the girder has no influence on the optimal stiffness value of the longitudinal stiffener. As stated before, the point situated at a length of 2500 mm is out of the range of the Eurocode formulation. This is the reason why the trend is slightly off at this point, compared to the Eurocode formulation when the failure happens in the lower subpanel. But this point has no influence on the trend based on the numerical results an can therefore be included in our research results.

The Eurocode formulation describes slightly higher values for the optimal stiffness when the failure is located in the lower subpanel, but the trends remain the same. For this failure type it also applies that the length of the girder has no influence on the optimal stiffness of the longitudinal stiffener.

Thus there can be stated that the length of the girder should be excluded from the calculation of the optimal stiffness of the stiffness, for both failure in the upper and lower subpanel. This since it has no influence, according to the numerically obtained results.

4.3.5 Effect of change of the height of the web (H_w)

4.3.5.1 Effect according to Eurocode

In eq. (4.3), the parameter h_w has a $1/{h_w}^3$ decreasing type of influence. This means that for lower heights of the web, a higher optimal stiffness must be obtained, in an exponential way. This link between the height of the web and the optimal stiffness is shown in Figure 66.

4.3.5.2 Effect according to numerical results for one stiffener cases

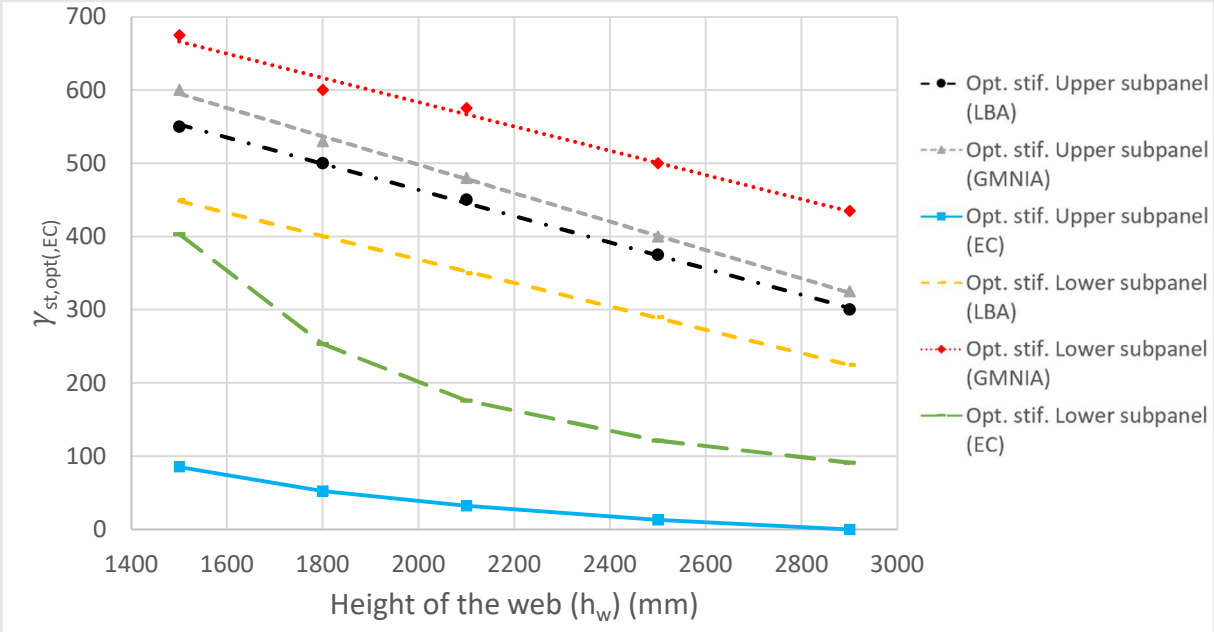

Figure 66: Optimal stiffness in function of the height of the web

For the failure mode occurring in the upper subpanel, a $1/h_w$ decreasing type of trend is described by the Eurocode formulation. When reviewing the numerical results, a linear decreasing trend is obtained, which states that the optimal stiffness declines, following a linear trend, when the girder length increases. This accounts for both the GMNIA method and for the linear buckling analysis method. It can be stated that, despite the $1/h_w$ decreasing trend versus the linear decreasing trend, the global trend described by the Eurocode, is close to the one obtained via the numerical analysis. However, the influence of the change of the height of the web should be more significant than described by the Eurocode. The difference of the absolute values between the Eurocode formulation and the numerical test results is significant. In order to describe the optimal stiffness better when changing the length of the girder, the influence of the length of the girder should be noticeable higher on the optimal stiffness formulation than it is now.

The values of the numerical testing for the failure mode in the lower subpanel are showing the same linear trends that could be observed with the failure mode in the upper subpanel. The $1/h_w$ decreasing trend, described by the Eurocode, is more explicit here. This means that the increase for the lower values of the height of the web are steeper than they were for the failure in the upper subpanel. This effect is not visible in the numerical results. In these numerical results, the linear trends are the same for both the failure in the upper and in the lower subpanel.

4.3.6 Effect of change of the web thickness (t_w)

4.3.6.1 Effect according to Eurocode

Eq. (4.3) shows that the thickness of the web has no influence on the determination of the optimal stiffness of a longitudinal stiffened girder according to the Eurocode. The optimal stiffness should thus remain constant when only changing the thickness of the web. This can be seen on Figure 67. Once for the upper and once for the lower subpanel failure mode.

4.3.6.2 Effect according to numerical results for one stiffener cases

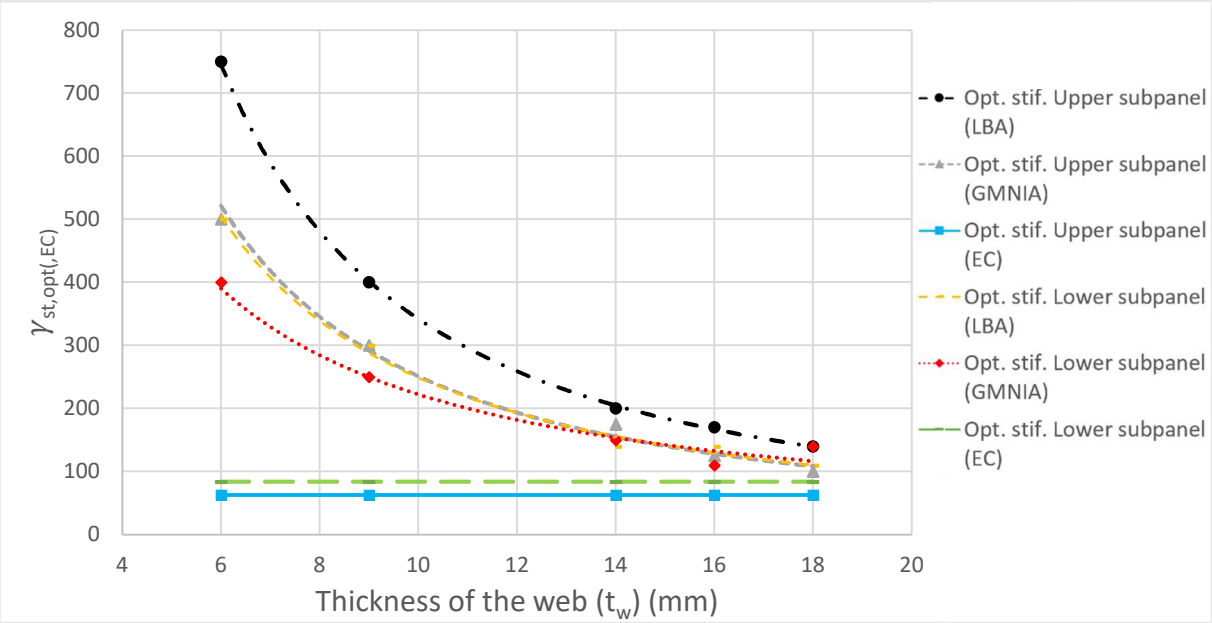

Figure 67: Optimal stiffness in function of the thickness of the web

If the failure happens in the upper subpanel, a $1/t_w$ decreasing type of trend can be observed when reviewing the numerical results. This means that for a lower thickness of the web, a higher optimal stiffness can be found. This can be stated for both the GMNIA method as for the LBA method. These two types of methods are also in close range to each other regarding their absolute values. It can be clearly observed that the trend, described by the Eurocode formulation, is totally in contradiction with the trend gained by the numerical investigation.

For the failure mode in the lower subpanel, the same trends can be observed as described in the section above, but with different absolute values.

The thickness of the web is the parameter where the Eurocode formulation is the least accurate. It describes the trend wrong and the absolute values are also not within an acceptable range. This is the reason why this parameter is chosen to be investigated more in depth. This is done by finding a link between these values and the values that are obtained by numerical testing on girders with two and three stiffeners. The goal is to find a new formulation, via a regression, where the optimal stiffness is a function of a certain ratio that describes the right optimal stiffness for the one, two and three stiffener cases.

First, the test setup and the range will be defined that was used to investigate the two and three stiffener cases. Next, a link will be established between the one, two and three stiffener cases. This is done to be able to describe the optimal stiffness independently of the amount of stiffeners.

In the next section, the test setup for the two and three stiffener cases will be described. Afterwards, a ratio will be found, that includes t_w, which describes the same optimal stiffness for the one, two and three stiffener cases. Using this ratio, and via regression, a new formulation for the optimal stiffness will be produced based on this ratio.

4.4 Numerical test setup – two and three stiffeners

As stated before, the use of longitudinal stiffeners is in practice mostly performed with two or more stiffeners, instead of only one stiffener. This is done because of the fact that most of the used girders for steel bridges have a significant height of the web and are exposed to high patch loadings, which causes the girder to be extremely vulnerable for buckling. In order to be able to make a new formulation for the optimal stiffness of a stiffener, that is applicable for two or three stiffeners, the research is made more widely than only the one stiffener cases. This is done since EN 1993-1-5 only describes the patch load resistance of one stiffener cases. In order to meet the requirements of the work field, a proposal is made for the criteria of a "strong" stiffener, independent of the amount of stiffeners.

Firstly, a ratio has to be found which describes the two and three stiffener cases with the same optimal stiffness. The hypothesis was that the amount of stiffeners, that is present in a test setup, only influences the amount of patch load favorably. However, it only has a minimal or a negligible influence on the optimal stiffness of each stiffener. This means that for two identical test setups with a constant value of the depth of the loaded subpanels, the value of the optimal stiffness for each individual stiffener, should remain the same. The only varying parameters between the two test setups are thus the amount of stiffeners and the height of the web. The height of the web is changing due to the fact that the dept of the subpanels remain constant. The stiffeners were uniformly placed along the web. The train of thought behind this hypothesis is the following. When placing the stiffeners uniformly along the web, the failure will happen in the directly loaded subpanel. In the test setup this refers to the upper subpanel. When the variables of this part of the girder are untouched (such as the b_1 value and the t_w value), the optimal stiffness for the stiffeners that divides the web into these subpanels, remains the same. The critical force although will become larger when varying the amount of stiffeners and the height of the web. In Figure 68, a visualization can be seen for one test configuration with two and three stiffeners.

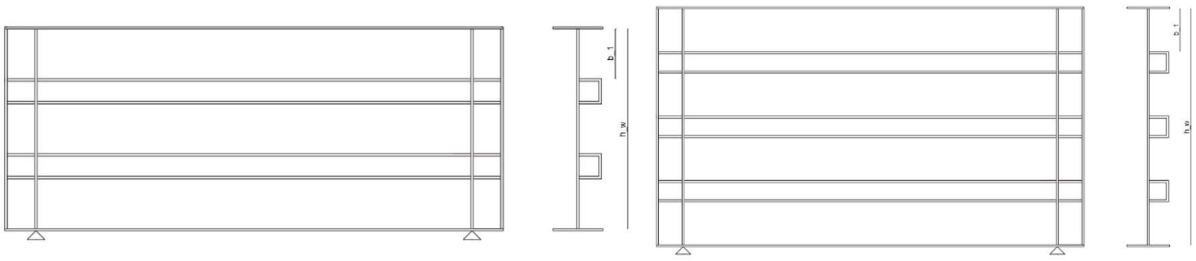

Figure 68: Configuration with constant b_1 - value (2 and 3 stiffeners)

In total there were four different values of b_1 tested, each time for two and three stiffeners. This process was repeated also for the three different values of the thickness of the web. Thus in total there were 24 cases investigated for their optimal stiffness value. TTable 12 shows a summary of these 24 cases.

Table 12: Investigated cases for b_1

b_1 (mm)	Number of stiffeners	Tw (mm)
400	2 / 3	6 / 9 / 18
500	2 / 3	6 / 9 / 18
600	2 / 3	6 / 9 / 18
800	2 / 3	6 / 9 / 18

4.5 Test results and discussion – two and three stiffeners

First of all, the analysis and investigations will be done only for the LBA.. There will be a formulation suggested for the optimal stiffness, via regression, for the LBA method. Afterwards, the same will be done but for the GMNIA method to verify the obtained formulation on its validity and accuracy.

4.5.1 Effect of number of stiffeners on optimal stiffness, numerical results

After conducting the LBA, a total of twelve pair of points were compared with each other. These pair of points are visualized in Figure 69.

As can be seen on Figure 69, the points for the same cases of two and three stiffeners are mostly overlapping. In order to simplify the further research and to make a formulation for both two and three stiffener cases, the assumption is made that the amount of stiffeners has no influence on the optimal stiffness of a stiffener when keeping b_1/t_w constant.

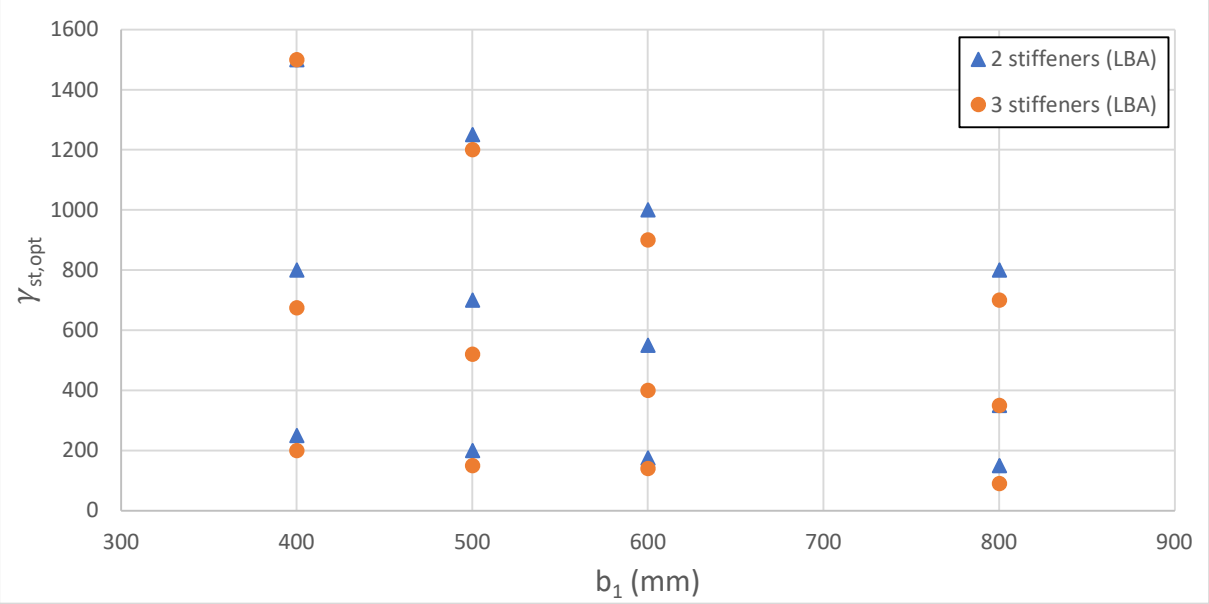

Figure 69: Comparison of the pairs for each b_1 value for the linear buckling analyses test's

4.5.2 Effect of number of stiffeners on optimal stiffness, Eurocode formulation

After computing and calculating the optimal stiffnesses of the 24 cases via the numerical investigation, the same was done for all of the 24 cases, but now using the formula suggested by the Eurocode. The formula that is stated in the Eurocode, eq. (4.3), only depends on the b_1 value, not on the thickness of the web (t_w). Using this calculation resulted in eight unique values. One unique value per b_1-value and depending on if the case had two or three stiffeners since there is a change of height of the web between these two. This value remains the same when changing the thickness of the web. These eight values can be found in Table 13.

Table 13: Optimal stiffness according to EC for b_1 (2 and 3 stiffeners)

b_1	Number of stiffeners	$\gamma_{s,opt,EC}$
400	2	245
400	3	120
500	2	158
500	3	84
600	2	110
600	3	62
800	2	59
800	3	36

A clear trend can be observed when this equation is used for the two and three stiffeners cases. If you fill in the equation for these specific cases, one can notice that for the same b_1-value, the optimal stiffness is more or less half the value for the three stiffener case than for the two stiffener case. This is in contradiction with the previous finding where was stated that the amount of stiffeners only had a neglectable influence on the optimal stiffness.

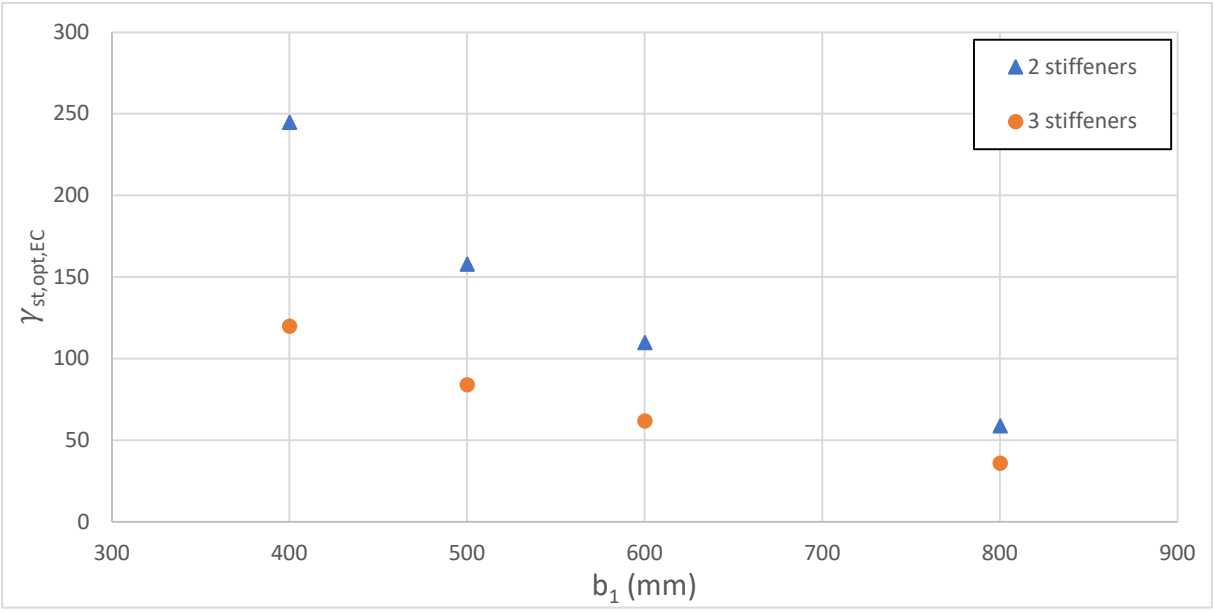

Figure 70: Optimal stiffness according to EC for b_1 (2 and 3 stiffeners)

As can be seen in Table 12 and in Figure 70 and in eq. (4.3), the Eurocode formulation does not include an influence caused by the change of the thickness of the web. However, in Figure 70, one can clearly see an influence on the numerical results for the optimal stiffness when changing the thickness of the web. This aspect will be further investigated in the section below. Instead of investigating this simply for t_w, a research was done for the ratio of b_1/t_w. In this way, one optimal stiffness can be assigned to multiple configurations. This can be done since we made the simplification of the influence of the amount of stiffeners on the optimal, stiffness as stated before.

4.5.3 Effect of b_1/t_w ratio on the optimal stiffness, numerical results

As stated before, a clear influence of the thickness of the web on the optimal stiffness could be noticed in our results. To further research this parameter, a graph was made to show the link between the optimal stiffness and the ratio of b_1/t_w. This graph is presented in Figure 71

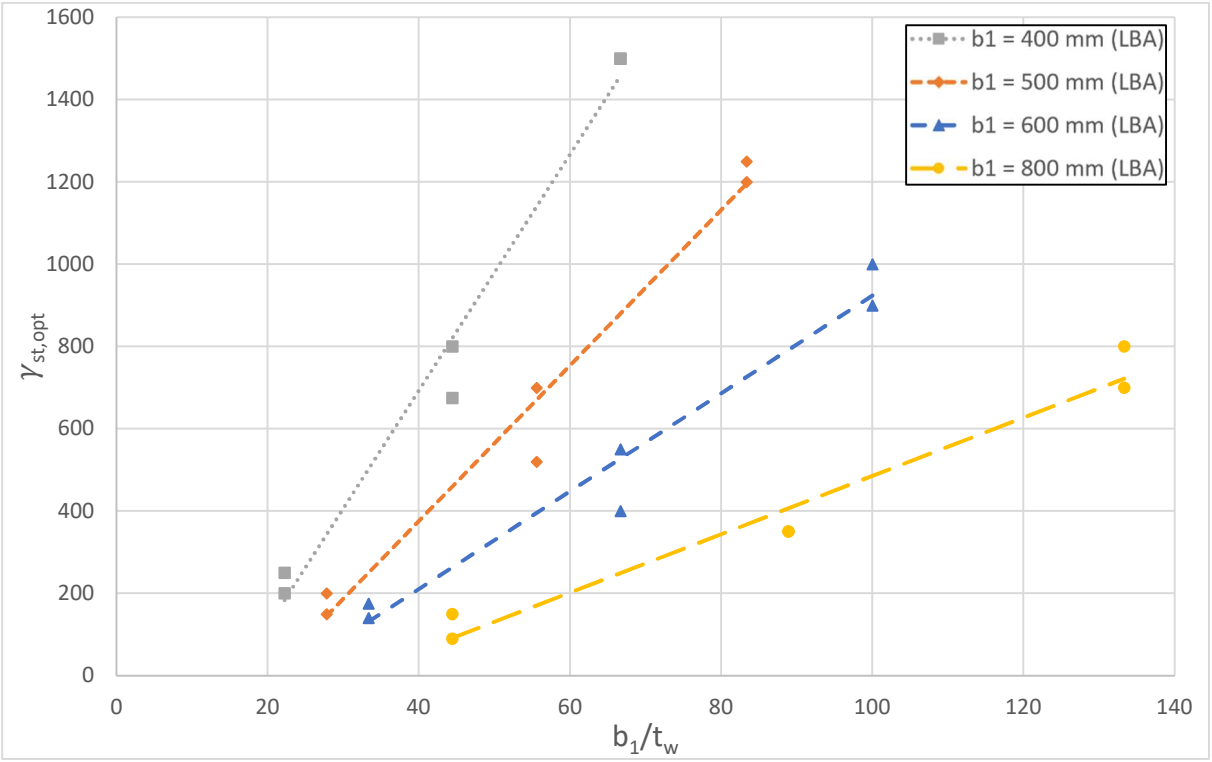

Figure 71: Link between the optimal stiffness and the ratio b_1/t_w

The next four graphs (Figure 72 until 75) shows all of the test results used for the determination of the optimal stiffness of each of the 24 cases. They are shown per value of b_1 and are set all relatively to each critical buckling load value (F_{cr}) divided by the maximum ($F_{cr,max}$) value for that specific case. The vertical lines represents each time the value of the optimal stiffness for that specific case.

As stated before, the influence of the amount of stiffeners are relatively small. This can be seen on these graphs by the fact that the straight lines per t_w value are close together. Another observation that can be made is that for a decreasing value of the thickness of the web, a higher optimum stiffness is reached.

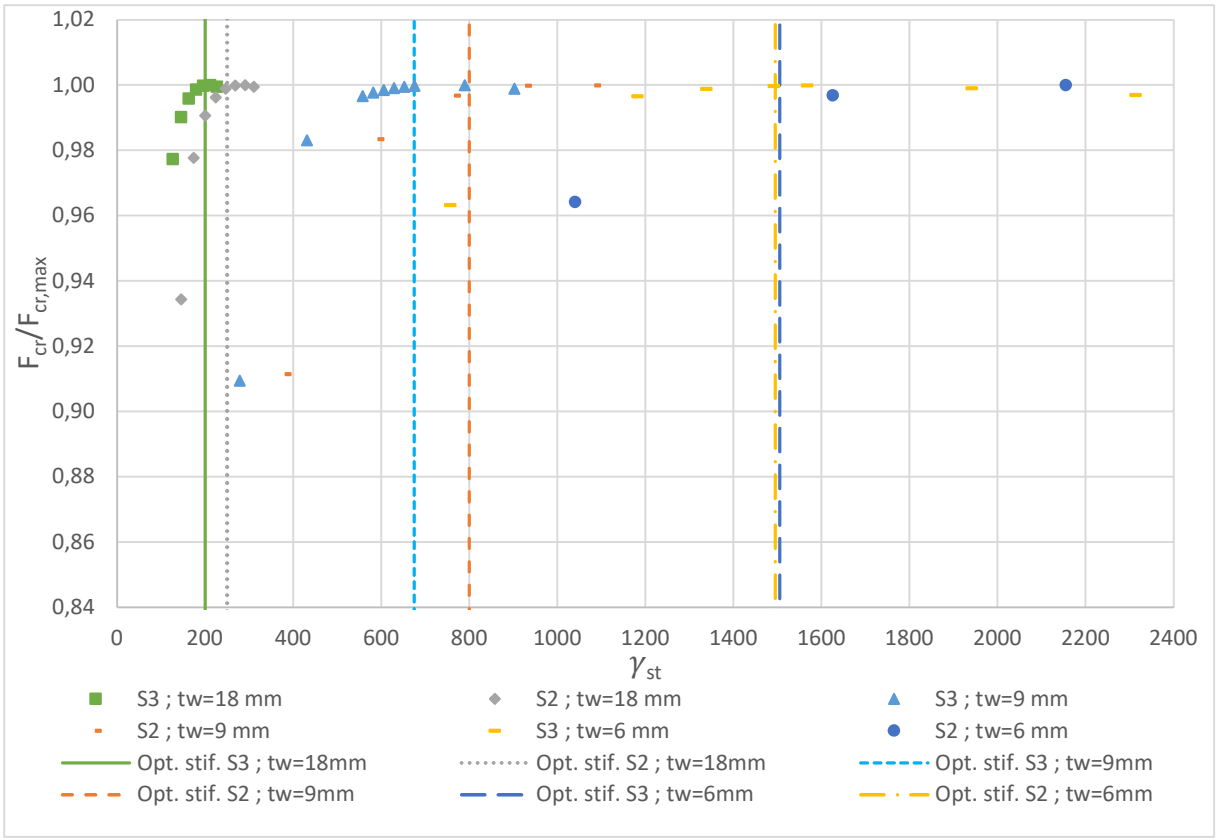

Figure 72: Critical buckling load in function of stiffness (LBA) (b_1 = 400)

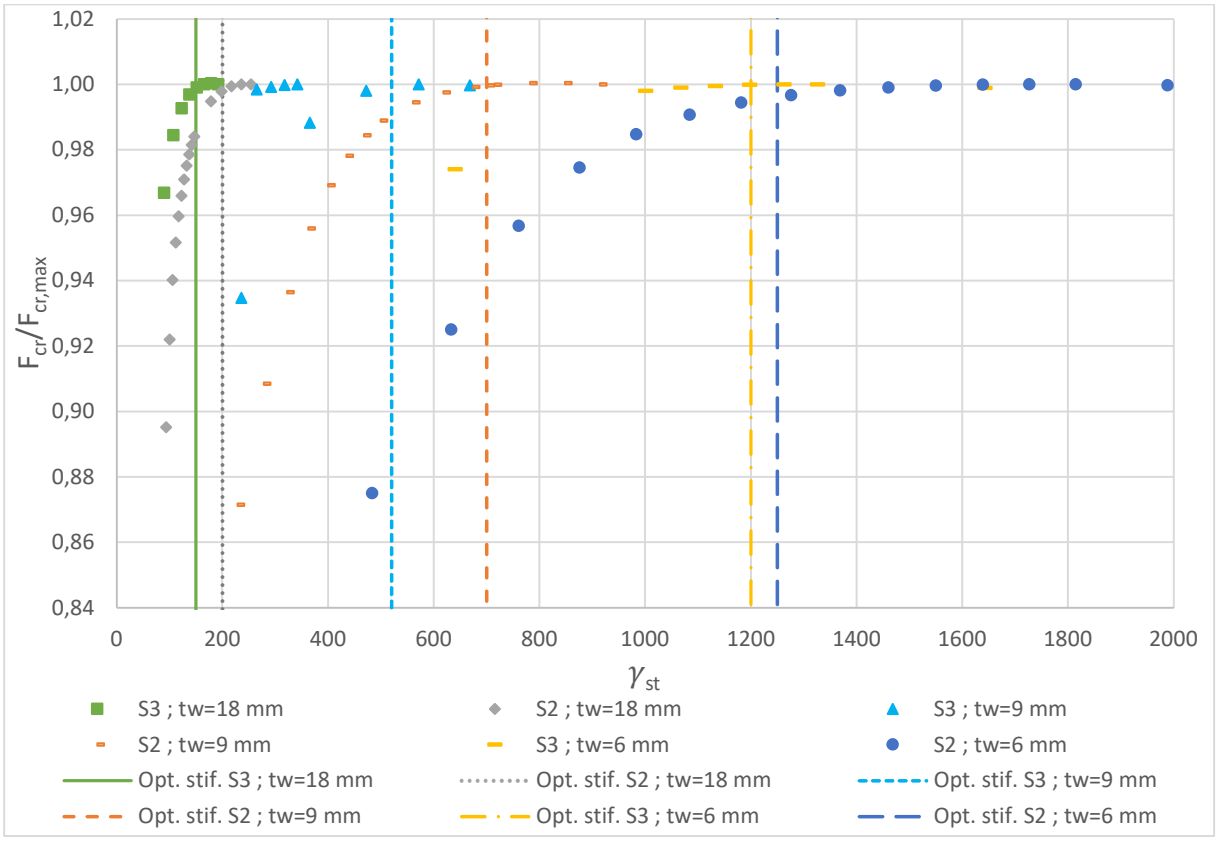

Figure 73: Critical buckling load in function of stiffness (LBA) (b_1 = 500)

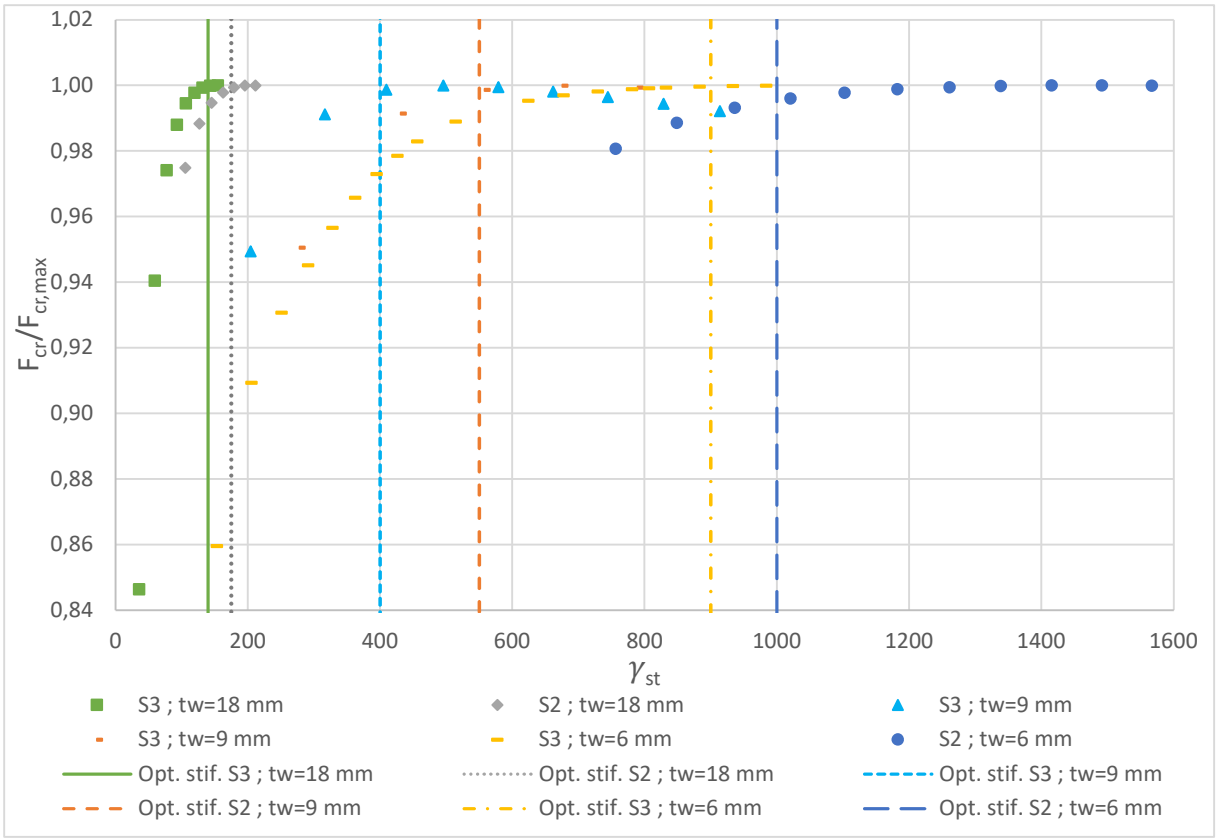

Figure 74: Critical buckling load in function of stiffness (LBA) (b_1 = 600)

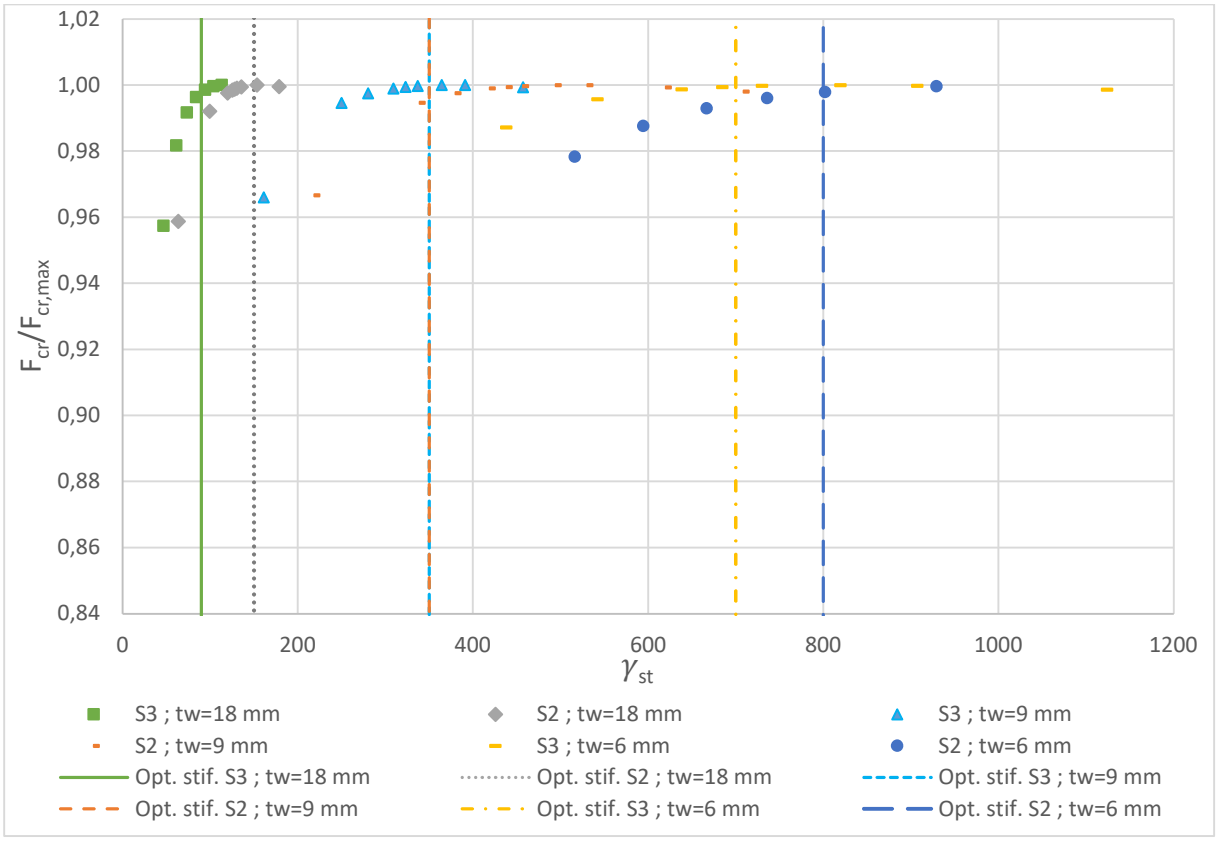

Figure 75: Critical buckling load in function of stiffness (LBA) (b_1 = 800)

4.5.4 New formulation for optimal stiffness – LBA method

The formulation that will be formed, will include both two and three stiffener cases. In order to do this, a conservative formulation will be made. This means that for every b_1/t_w-value, the highest optimal stiffness will be taken into account of the two and three stiffener cases. In this way, there will be no underestimation of the optimal stiffness. On Figure 76, these conservative points can be seen together with their corresponding trendlines.

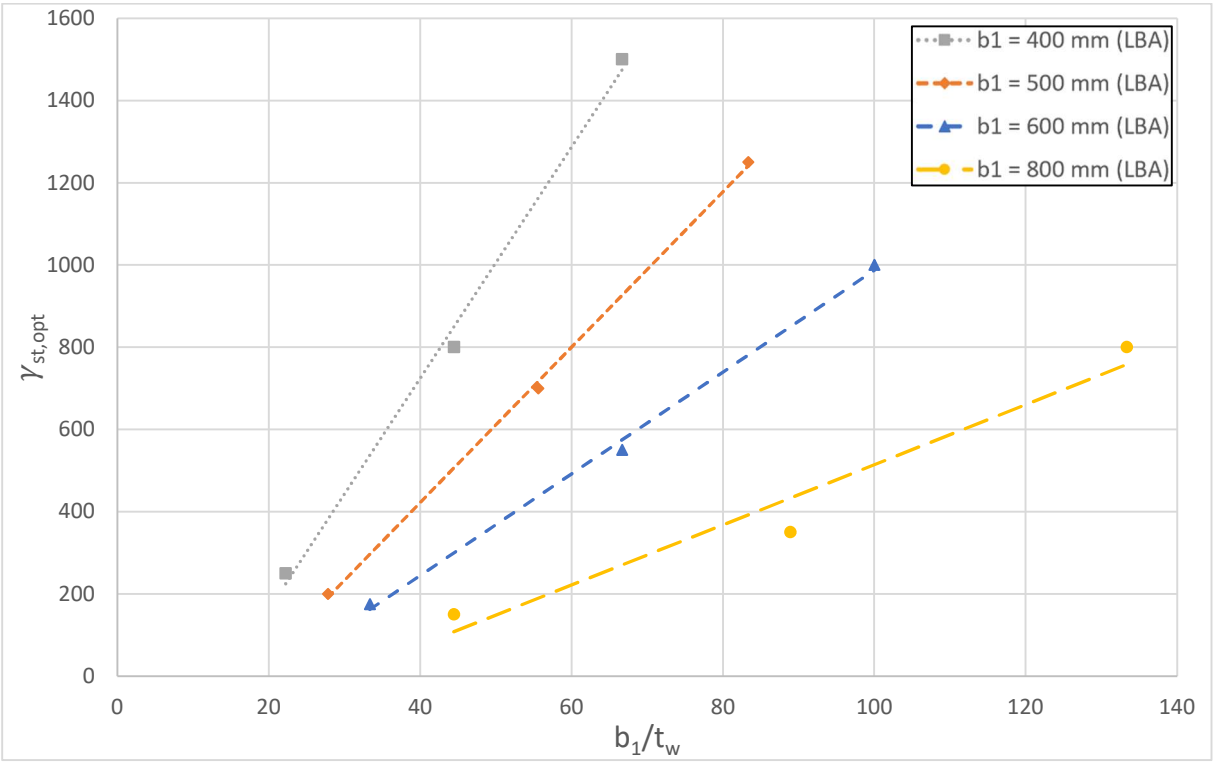

Figure 76: Optimal stiffness (LBA) in function of the ratio b_1/t_w (max values)

In order to describe the observed trends, the slopes of the four trendlines were calculated. These values can be found in Table 14. To establish a new formulation for the optimal stiffness, a link between the values of these slopes should be found. To do that, these values of the slopes were plotted together with their corresponding value of b_1. This graph can be found in Figure 77.

Table 14: Slopes of the four trendlines

b_1 (mm)	slope
400	28.1
500	18.9
600	12.4
800	7.3

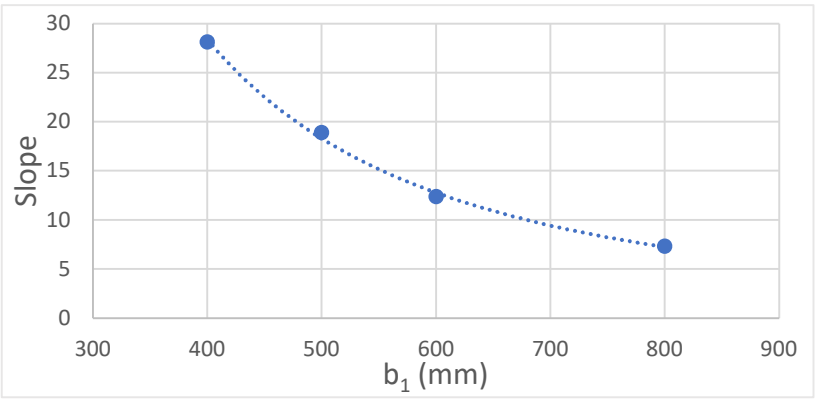

Figure 77: Slopes of the four trendlines

As can be seen in Figure 77, a clear trend can be observed to describe the slopes of each different b_1 value. This is a $\frac{1}{b1}$ – trend. This means that there is a inversely proportional connection between the depth of the loaded subpanel and the pace at which the optimum stiffness increases when the b_1/t_w ratio increases. This relation can be described by the following formula.

$$slope = \frac{4*10^6}{{b_1}^{1.968}} \tag{4.4}$$

From this relation, one can concluded that the slope gets very low for a high depth of the loaded subpanel, but never goes to zero or less. This means that an increase of the stiffness of a stiffener always has an impact. This impact becomes very small when the b_1-value is very high.

The next part of the equation is the intersection point with the y-axis. This point is searched for the four linear trendlines. The intersection points with the y-axis (b) are shown in Table 15 and plotted together with their corresponding b_1 value onto Figure 78.

Table 15: Intersection points y-axis

b_1 (mm)	b
400	-400
500	-333.33
600	-250
800	-216.67

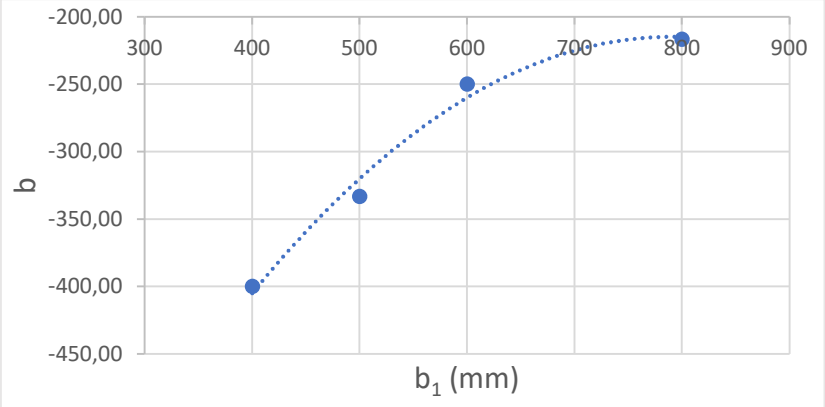

Figure 78: Intersection point with the y-axis four the four trendlines

Through these points, a polynomial function can be found. This function is described according to eq. (4.5).

$$b = -0.0013 * b_1^2 + 1.9751 * b_1 - 995.02 \tag{4.5}$$

Together with eq. (4.4), one equation can be made that describes the optimal stiffness in function of the b_1/t_w ratio.

$$\gamma_{st,opt,LBA} = slope * \frac{b_1}{t_w} + b$$

$$\gamma_{st,opt,LBA} = \frac{4 * 10^6}{{b_1}^{1.968}} * \frac{b_1}{t_w} - 0.0013 * b_1^2 + 1.9751 * b_1 - 995.02$$

$$\gamma_{st,opt,LBA} = b_1 * \left(\frac{4*10^6}{{b_1}^{1.968} * t_w} - 0.0013 * b_1 + 1.9751\right) - 995.02 \tag{4.6}$$

This formula describes the maximum values for the stiffness of a stiffener depending on the height of the loaded subpanel and on the thickness of the web. The next part is going to make a comparison between the 24 cases which were numerically found and between this formulation, described in eq. (4.6).

4.5.4.1 Verification of the new formulation

In this section, eq. (4.6) will be compared with the numerical results which were earlier obtained, in order to check the accuracy of this formula. Eq. (4.6) was filled in 12 times so that we get 12 different results. The reason that it is not done for all of the 24 cases is that in this formula, a difference has not been made between the two or three stiffener cases. This equation only depends on the height of the loaded subpanel and not on the height of the web. The obtained results for two similar cases, with only a change in the amount of stiffeners and height, remain the same. By making this formula depending on only the highest values of optimal stiffness between the two and three stiffener cases, a conservative formula is obtained which is applicable for both two and three stiffener cases. Later on, this formula will also be checked for one value of b_1 for the one stiffener case to check its validity in this area. These results can be seen in Table 16.

Table 16: Percentual difference between new formula and numerically found values

Point number	b_1 (mm)	# stiffeners	t_w (mm)	$\gamma_{st,opt,num}$	$\gamma_{st,opt,eq.(4.6)}$	Perc. Diff.
1	400	2	6	1500	1606	6.6%
2	400	3	6	1500	1606	6.6%
3	400	2	9	800	933	14.3%
4	400	3	9	675	933	27.7%
5	400	2	18	250	260	3.8%
6	400	3	18	200	260	23.1%
7	500	2	6	1250	1294	3.4%
8	500	3	6	1200	1294	7.3%
9	500	2	9	700	752	6.9%
10	500	3	9	520	752	30.9%
11	500	2	18	200	210	4.8%
12	500	3	18	150	210	28.6%
13	600	2	6	1000	1068	6.4%
14	600	3	6	900	1068	15.7%
15	600	2	9	550	631	12.8%
16	600	3	9	400	631	36.6%
17	600	2	18	175	177	1.1%
18	600	3	18	140	177	20.9%
19	800	2	6	800	785	1.9%
20	800	3	6	700	785	10.8%
21	800	2	9	350	441	20.6%
22	800	3	9	350	441	20.6%
23	800	2	18	150	97	54.6%
24	800	3	18	90	97	7.2%

In the last column, the percentual difference between the numerical obtained result and the results via eq. (4.6) are shown. This percentage is calculated as in eq. (4.7).

$$perc.diff. = \frac{\gamma_{s_{opt_{eq.4.6}}} - \gamma_{s_{op\ num.}}}{\gamma_{s_{op\ eq.4.6}}} * 100\% \tag{4.7}$$

To verify this formula that describes these 24 cases, the percentual differences are plotted according to their numerical optimal stiffness values and can be seen in Figure 79.

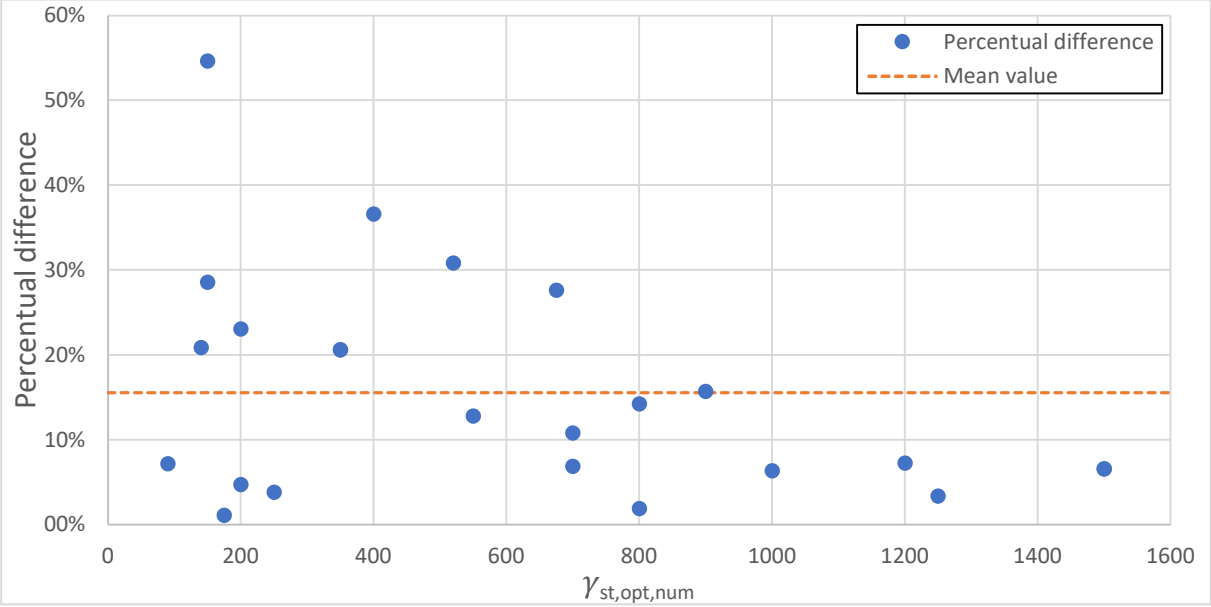

Figure 79: Absolute percentual difference between new formula and numerical values

The percentual differences are expressed in their absolute values. The mean value of these percentual differences is 15.6% .

A second way to verify the new formulation is to plot these results on the same graph which was used to start this investigation. This plot can be seen in Figure 80.

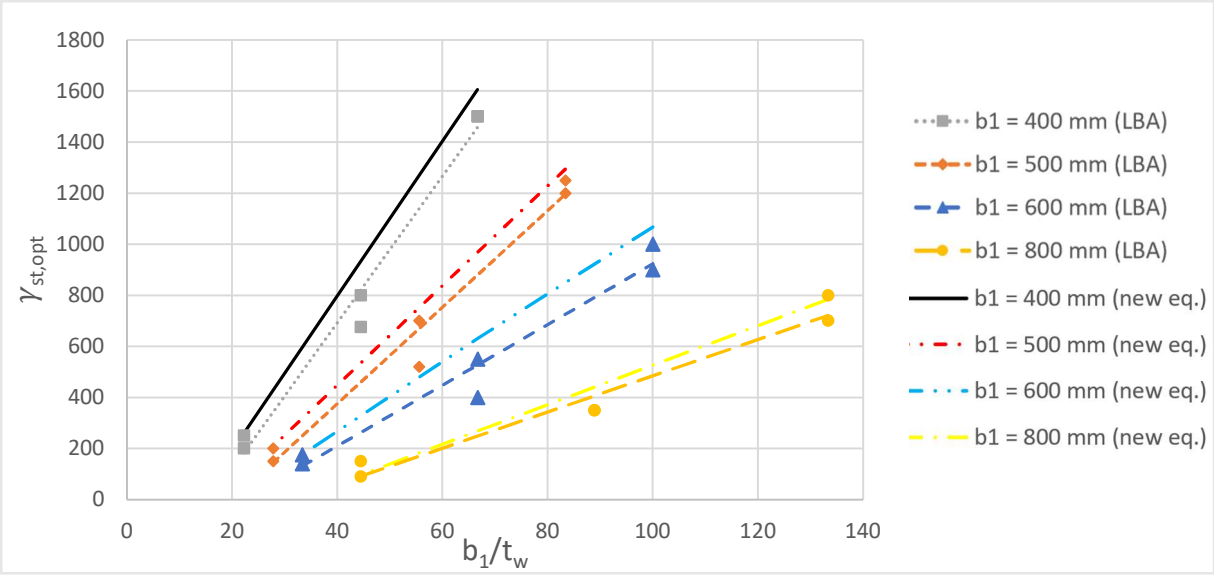

Figure 80: Optimal stiffness (LBA) in function of the ratio b_1/t_w

On this chart it is clearly visible that there is a good correlation between the numerical obtained results and the results obtained via eq. (4.6). It is also visible that the described trend of the new formulation is always on the conservative side and thus on the safe side.

To further show that the eq. (4.6) does not underestimate the optimal stiffness, the percentual difference is shown between the values obtained using eq. (4.6) and the numerically obtained values. When the points are above the x-axis, the optimal stiffness is overestimated. When the points are below the x-axis, the optimal stiffness is underestimated. This can be seen in Figure 81. The associated values can be found in Table 17.

Table 17: Percentual difference from new formulation with EC for each case

Point number	Proc. Difference	Point number	Proc. Difference	Point number	Proc. Difference
1	7.1%	9	7.4%	17	1.1%
2	7.1%	10	44.6%	18	26.4%
3	16.6%	11	5.0%	19	-1.9%
4	38.2%	12	40.0%	20	12.1%
5	4.0%	13	6.8%	21	26.0%
6	30.0%	14	18.7%	22	26.0%
7	3.5%	15	14.7%	23	-35.3%
8	7.8%	16	14.7%	24	7.8%

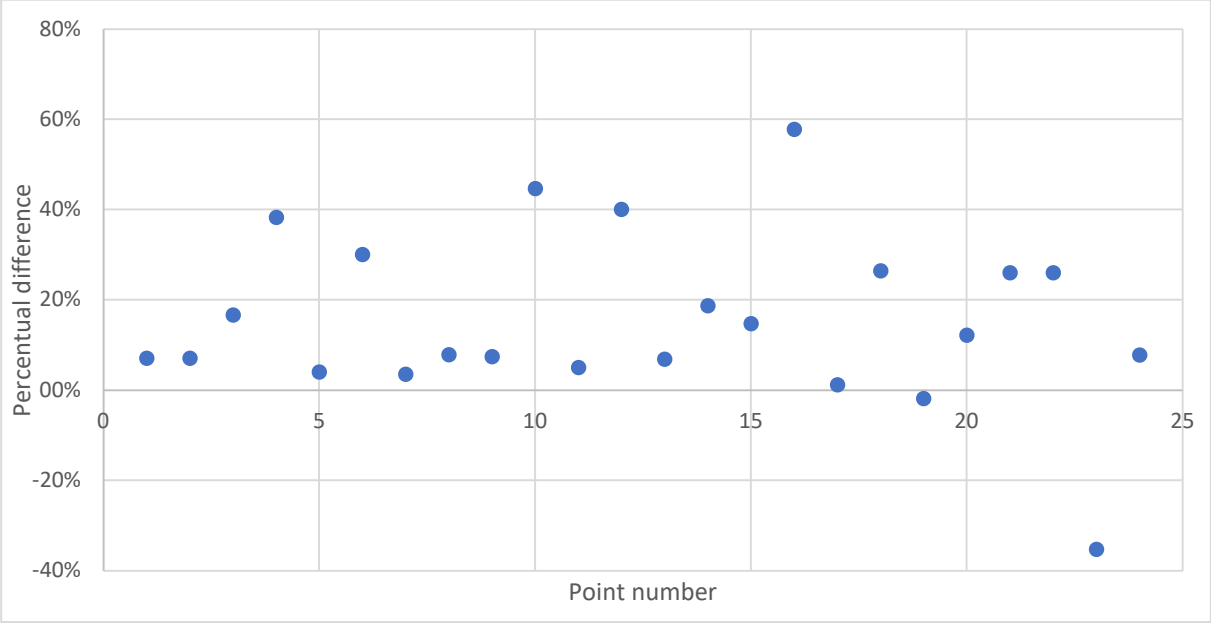

Figure 81: Percentual difference from new formulation with EC for each case (LBA)

As can be seen on Figure 81 and in Table 17, there is an overestimation made for 22 of the 24 researched points. This proves that the formulation is conservative and can be used for both two and three stiffener cases. The two points that are underestimated by eq. (4.6) are points 19 and 23. Point 19 only has an underestimation of 1.9% and can be neglected. On the other hand, point 23 has an underestimation of 35.3 %. This is not a neglectable difference. This point can be defined as an outlier because it has a significant negative deviation. This is the only point where such a significant deviation in the negative way can be observed.

4.5.4.2 Testing of validity in one stiffener case

The new formulation is now validated for the two and three stiffener cases. In this section, the validity of the formulation will be checked for the one stiffener cases. Before doing so, some remarks should be given regarding the one stiffener cases. The formulation that is created is only validated when the failure is happening in the upper subpanel. This was the case for both the two and three stiffener cases. When using this formula for the one stiffener cases, one should be careful about where the failure would take place. If the b_1 value is chosen low and the height of the web is chosen high, the failure will be situated in the lower subpanel. This kind of failure is not in the scope of this formulation. This is different in comparison to the two and three stiffener cases. This is because in those cases the stiffeners were uniformly placed along the web. This caused that the failure would always happen in the directly loaded subpanel.

The validation will therefore be done for a large b_1 value, namely b_1 = 800. This is the same case that was used in the research of the parameter t_w with the one stiffener cases. The geometrical parameters can therefore be found in Table 18. The validation will be done for the cases that were obtained using the LBA method. In Figure 82, the trend of the new formulation is visualized, together with the points of the one, two and three stiffener cases.

Table 18: Points used for validation

Point number	b_1 (mm)	# stiffeners	t_w (mm)	$\gamma_{s\_opt\_num}$	$\gamma_{s\_opt\_eq.(4.6)}$	Perc. Diff.
25	800	1	6	750	785	4.5%
26	800	1	9	400	441	9.3%
27	800	1	18	140	97	-44.2%

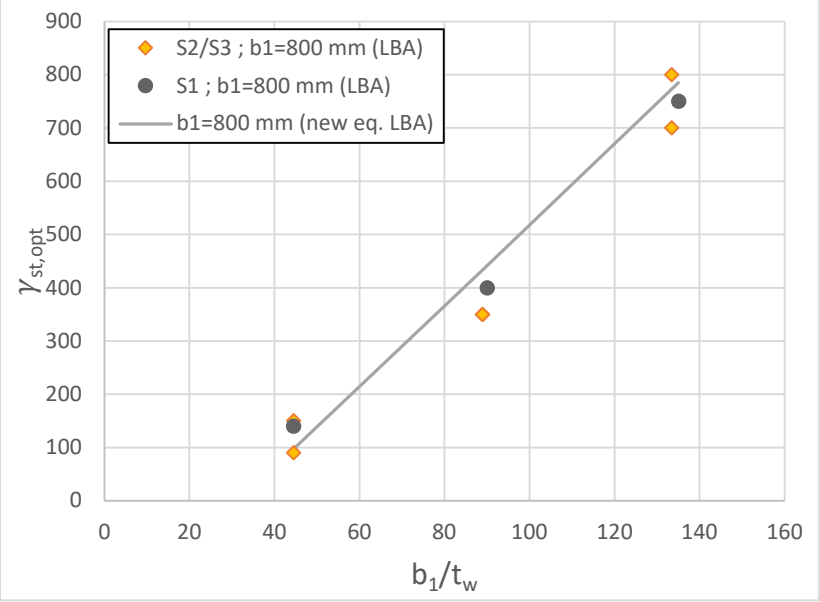

Figure 82: Points used for validation of new formulation (LBA)

The formulation for this specific case of the one stiffener is correctly described by this new formulation. For point 25 and point 26, there is a slightly overestimation of the optimal stiffness which falls within an acceptable range. Point 27 has a underestimation 44.2 %, which is significant.

4.5.5 New formulation for optimal stiffness – GMNIA method

The same process, as described above, is repeated for the GMNIA method.
Figure 83 shows the used points for determining the optimal stiffness formula. All of these points were the highest values between the two and three stiffener cases in order to make a conservative formulation.

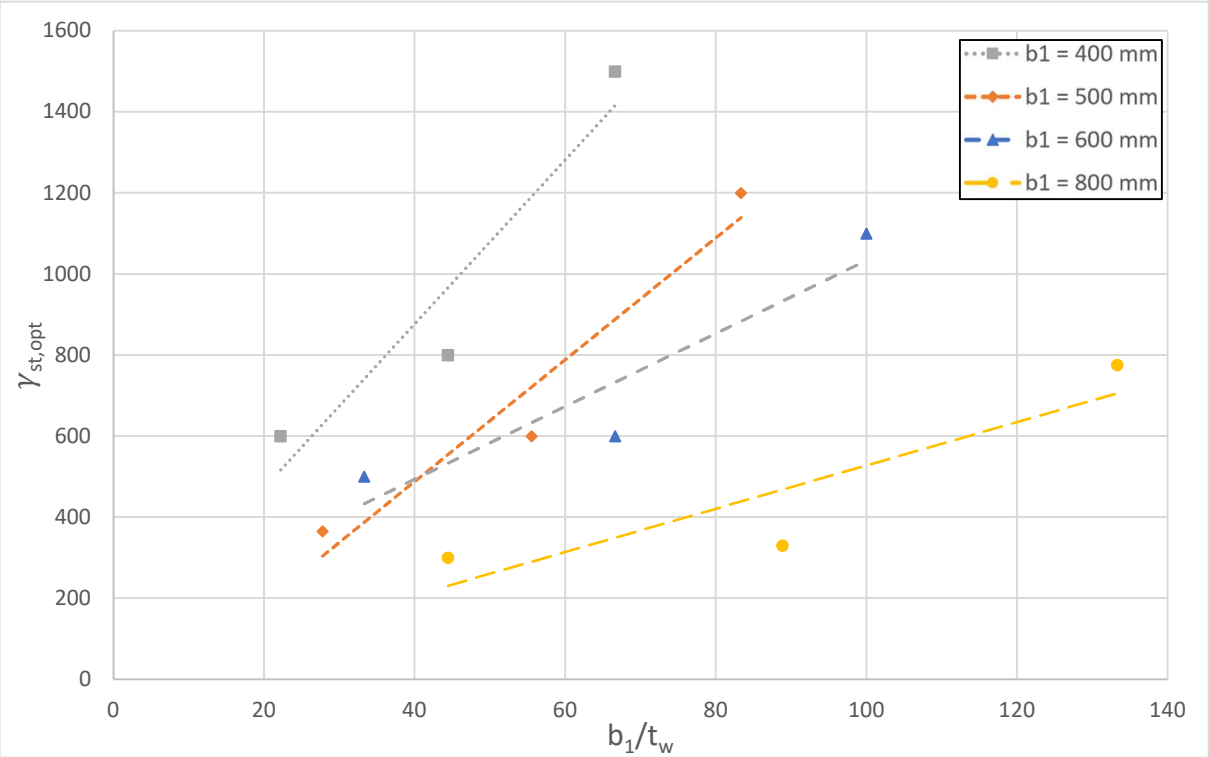

Figure 83: Optimal stiffness (GMNIA) in function of the ratio b_1/t_w (max. values)

In order to describe the observed trends, the slopes of the four trendlines were calculated. These values can be found in Table 19. To establish a new formulation for the optimal stiffness, a link between the values of these slopes should be found. To do that, these values of the slopes were plotted together with their corresponding value of b_1. This graph can be found in Figure 84.

Table 19: Slope of the four trendlines

b_1 (mm)	slope
400	20,3
500	15,0
600	9,0
800	5,3

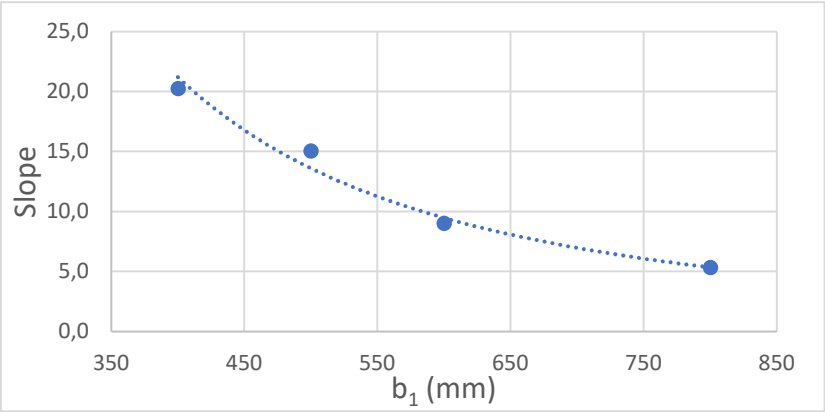

Figure 84: Slope of the four trendlines

Figure 84 shows a clear $\frac{1}{b1}$ – trend. This means there is an inversely proportional connection between the depth of the loaded subpanel and the pace at which the optimum stiffness increases when the b_1/t_w – ratio increases. This is exactly the same trend which was observed by the LBA method. The following formula was made to describe this trend.

$$slope = \frac{3*10^6}{{b_1}^{1.968}} \tag{4.8}$$

From this relation, one can concluded that the slope gets very low for a high depth of the loaded subpanel, but never goes to zero or less. This means that an increase of the stiffness of a stiffener always has an impact with smaller web thicknesses. But this impact becomes very small when the b_1 value is very high.

The next part of the equation is the intersection point with the y-axis. This point is searched for the four linear trendlines. However, a function could not be found to describe these points due to the scatter in the results from the GMNIA. Therefore, the maximum value was taken to determine the intersection point with the y-axis. The maximum value was 135. If we take this value, there is only a minor part of the researched points that are slightly underestimated (5.1%) and the average percentual difference is within proper limits (30%). The formula for the optimal stiffness, applicable on the GMNIA formulation, is given in eq. (4.9).

$$\gamma_{st,opt,GMNIA} = slope * \frac{b_1}{t_w} + b$$

$$\gamma_{st,opt,GMNIA} = \frac{3 * 10^6}{{b_1}^{1.968}} * \frac{b_1}{t_w} + 135$$

$$\gamma_{st,opt,GMNIA} = b_1 * \left(\frac{3*10^6}{{b_1}^{1.968}*t_w}\right) + 135 \tag{4.9}$$

Therefore, eq. (4.9) now describes the maximum values for the stiffness of a stiffener depending on the height of the loaded subpanel and on the thickness of the web, independently on the amount of stiffeners. The next part is going to make a comparison between the 24 cases which were numerically found and between this formulation described in eq. (4.9).

4.5.5.1 Verification of the new formulation

In this section, the new formulated formula for the GMNIA will be verified. This is done in the same way as described in section 4.5.4.1. In Table 20, all of the researched points can be seen together with their numerically obtained optimal stiffness, the optimal stiffness according to eq. (4.9) and the percentual difference between these two values. In Figure 85, the percentual differences are plotted with their corresponding point number. The mean value of all the percentual differences is also marked on this graph.

Table 20: Percentual difference between new formula and numerical values (GMNIA)

Point number	b_1 (mm)	# stiffeners	t_w (mm)	$\gamma_{s,opt,num}$	$\gamma_{s,opt,eq.(4.9)}$	Perc. Diff.
28	400	2	6	1500	1649	9.0%
29	400	3	6	1300	1649	21.2%
30	400	2	9	800	1144	30.1%
31	400	3	9	675	1144	41.0%
32	400	2	18	450	640	29.7%
33	400	3	18	600	640	6.2%
34	500	2	6	1100	1355	18.8%
35	500	3	6	1200	1355	11.4%
36	500	2	9	600	948	36.7%
37	500	3	9	400	948	57.8%
38	500	2	18	200	542	63.1%
39	500	3	18	365	542	32.6%
40	600	2	6	1100	1158	5.0%
41	600	3	6	900	1158	22.3%
42	600	2	9	600	817	26.5%
43	600	3	9	478	817	41.5%
44	600	2	18	500	476	- 5.1%
45	600	3	18	500	476	- 5.1%
46	800	2	6	747	909	17.8%
47	800	3	6	775	909	14.7%
48	800	2	9	330	651	49.3%
49	800	3	9	220	651	66.2%
50	800	2	18	300	393	23.7%
51	800	3	18	60	393	84.7%

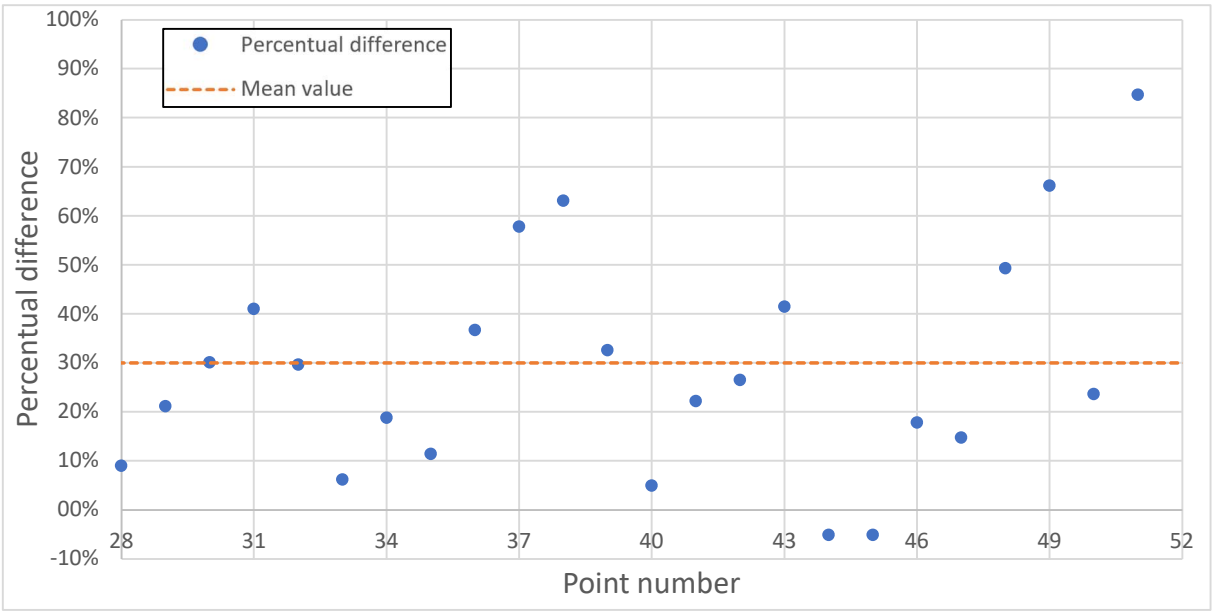

Figure 85: Percentual difference between new formula and numerical values (GMNIA)

As stated before, there are only two cases that have a slightly underestimation of both 5.1%. The rest of the points are all overestimated and thus on the conservative side. The average percentual difference is 30.0%. This is higher than the accuracy level obtained with the LBA (15.6%). This is due to the fact that the GMNIA had a lot of scatter in its data compared to the data obtained with the LBA. The newly made formulation is now again plotted together with the original obtained numerical data. This plot can be seen in Figure 86 . On this plot, it can be clearly seen that the new formulation is conservative for almost all of the observed values.

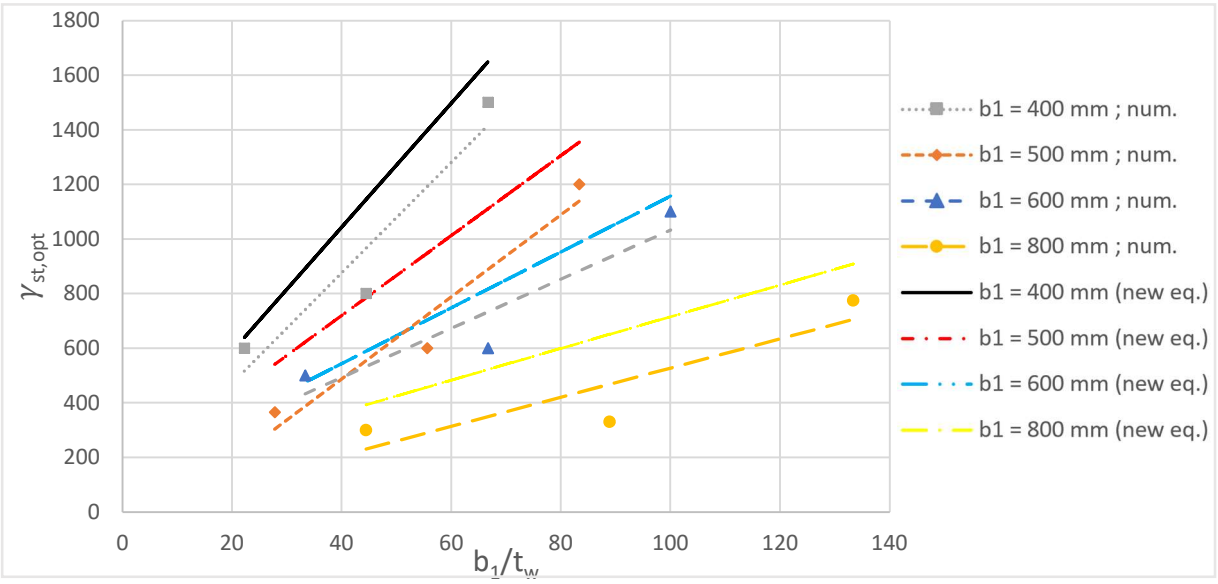

Figure 86: Optimal stiffness (GMNIA) in function of the ratio b_1/t_w

4.5.5.2 Testing of validity in one stiffener cases

In the same way as in the LBA analysis the validity of the new formulation is tested on the one stiffener cases. The same restrictions regarding the failure mode, as mentioned in section 4.5.4.2, also apply here.

Table 21: Points used for validation

Point number	b_1	# stiffeners	t_w	b_1/t_w	$\gamma_{s,opt,num}$	$\gamma_{s,opt,eq.(4.9)}$	Perc. Diff.
52	800	1	6	135	500	909	45.0%
53	800	1	9	90	300	651	53.9%
54	800	1	14	57	175	467	62.5%
55	800	1	16	50	125	425	70.6%
56	800	1	18	44	100	393	74.6%

From Table 21 and Figure 87 one can conclude that the absolute values are overestimated, this with an average of 61.3%. The trend however is correctly described by the new formulation. We can thus state that the formula is also valid for the one stiffener cases, although there has to be mentioned that there is a significant overestimation of the optimal stiffness.

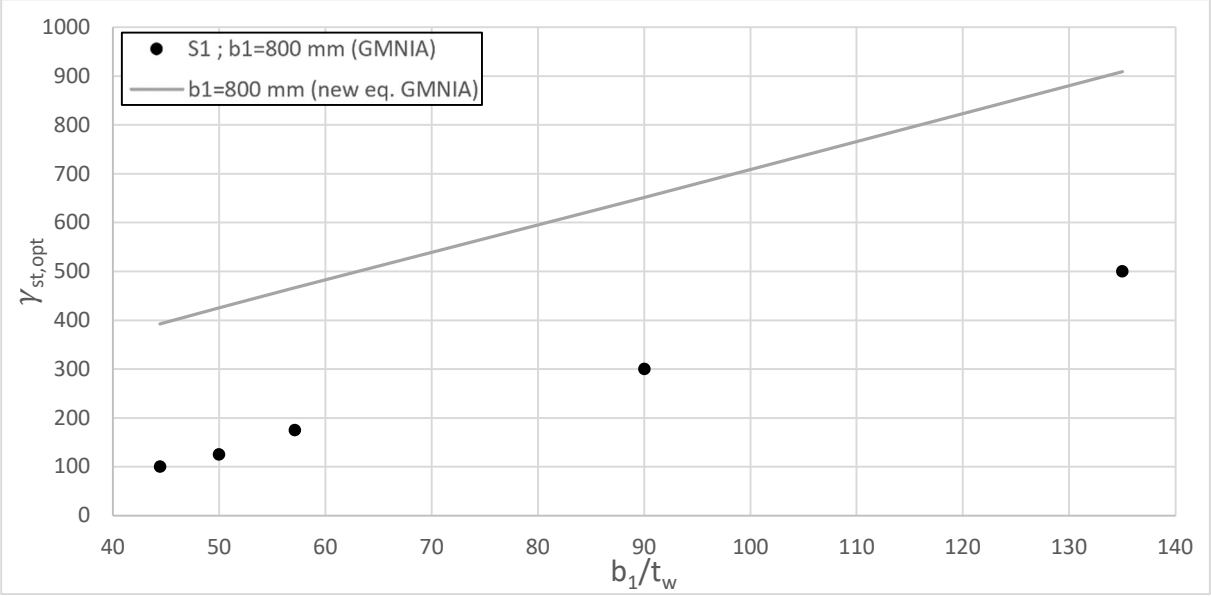

Figure 87: Points used for validation one stiffener cases (GMNIA)

4.5.6 Comparison formulation LBA vs. GMNIA

When looking at the results of Table 16 and Table 20, one can see that the values obtained with the GMNIA and the LBA numerical analysis are matching when the thickness of the web is 6mm or 9mm. However, when the thickness is 18mm, the values between the GMNIA and LBA are not corresponding to each other. The LBA underestimates the optimal stiffnesses of these points. This can be explained by the fact that the system does not fails elastically anymore when the thickness of the web is 18mm. At that thickness, the system fails plastically. Therefore, a higher stiffness of the stiffener is needed in order to let the system fail plastically. This phenomena can also be seen when observing the two new equations that were made, once based on the LBA and once based on the GMNIA. The plots of these two equations can be seen in Figure 88.

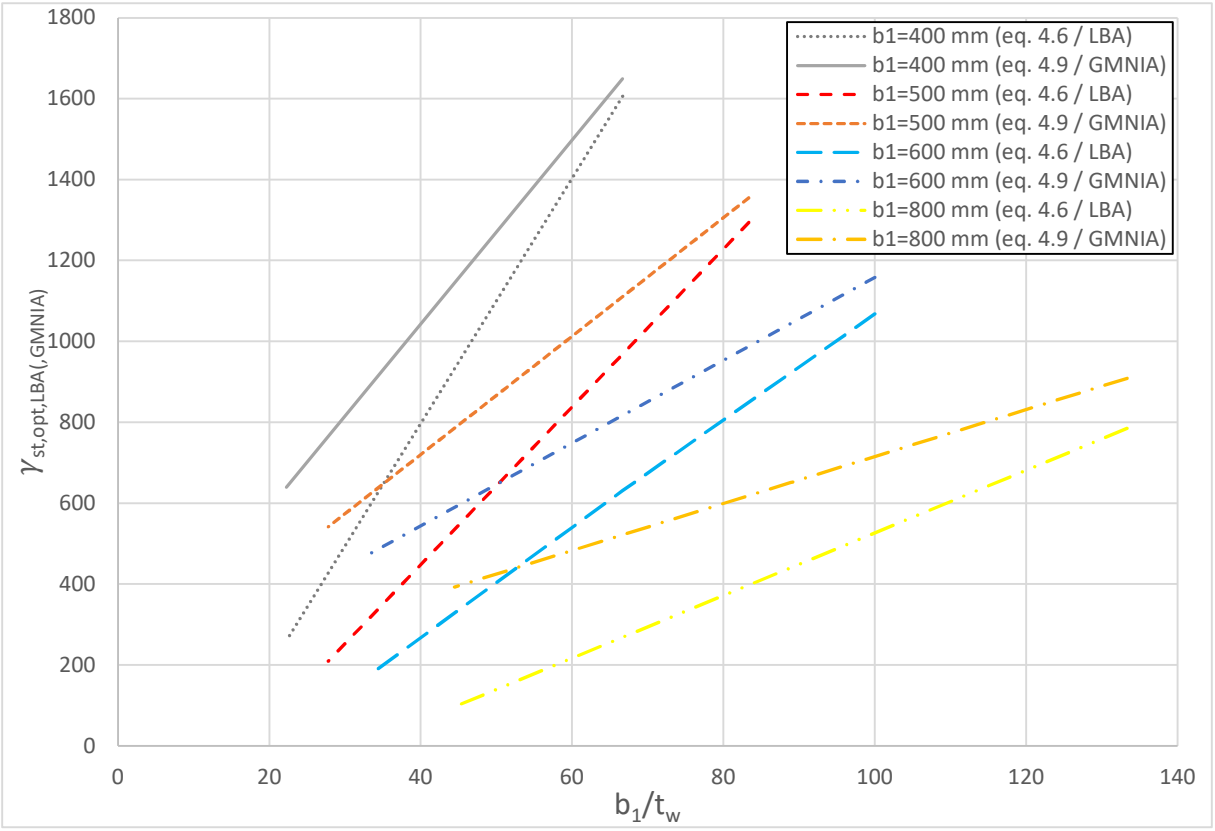

Figure 88: Plot of newly formed equations, LBA and GMNIA

For a high b_1/t_w – ratio, the LBA and GMNIA values for the optimal stiffness are close together. This is the case for all of the different b_1 – values. When decreasing the b_1/t_w– ratio, the difference between the points of the optimal stiffness of the GMNIA and LBA increases. This is applicable for all of the b_1 – values. This is in agreement with the numerical founded results, as stated before.

From this graph, one can conclude that the GMNIA based formulation gives the highest values of the optimal stiffness. This formulation will thus be chosen as the most accurate one. It can thus be stated that equation 4.9 gives the optimal stiffness in function of the b_1/t_w– ratio. This equation defines whether the stiffener can be classified as “strong”, when the stiffness is the same or higher than the one defined in equation 4.9, or “weak”, when the stiffness is lower than the one defined in equation 4.9.

5. Conclusion

In this thesis, a research related to the patch load resistance of steel girders was conducted. This phenomon is critical when installing steel bridges via the incremental launching method. The EN 1993-1-5 formulation of this problem is not efficient and underestimates the patch load resistance of steel girders. Therefore, a new and improved equation for this problem was created, which separates the different failure modes which can occur. This new equation is only applicable when the failure mode of the girder is a local buckling failure mode. In order to achieve this, criteria should be made which define what a "strong" stiffener is. The Eurocode has such a formulation, but this formulation is not precise enough and does not include all of the important parameters. Therefore, a new equation was made in this thesis to define what a "strong" stiffener is.

First of all, this thesis handles a parametric study of four relevant parameters which are: the length of the girder (a), the loaded length of the patch load (s_s), the height of the web (h_w) and the thickness of the web (t_w). These parameters were studied in function of girders with one stiffener. There were also two different failure modes tested. First, the stiffener was placed high on the web so that the failure would happen in the lower subpanel. Afterwards, the stiffener was placed lower on the web so that the failure would happen in the upper subpanel. Each parameter and failure mode was tested using the linear buckling analysis (LBA) and using the geometrically and material non-linear imperfection analysis (GMNIA). s_s and a were observed as having no influence on the optimal stiffness. For s_s, this was in agreement with the Eurocode formulation for the optimal stiffness. For the length of the girder, this finding is in contradiction with the Eurocode. The Eurocode formulation stated that the length of the girder had an $1/a$ increasing type of influence. Thus the length of the girder should be excluded from the formulation since it has no influence according to the numerically founded results. The next investigated parameter was h_w. Here, a linear decreasing type of influence was founded in the numerical results. The Eurocode however suggests a $1/h_w$ decreasing type of influence. The height of the web has an influence on the optimal stiffness according to the Eurocode formulation, which is true, but is wrongfully described. The last of the four parameters is the thickness of the web. According to the Eurocode formulation, the thickness of the web has no influence. This is in contradiction with the numerical found results. The thickness of the web was found to have a $1/t_w$ decreasing type of influence on the optimal stiffness of the stiffener. Therefore this parameter should be included in the formulation of the optimal stiffness. This founding was the base for the next step in the research.

In the next part of the research, a relationship was founded to describe the optimal stiffness independent of the amount of stiffeners and depending on the thickness of the web. Therefore, the ratio of the length of the loaded subpanel (b_1) over the thickness of the web (t_w) was researched in function of the optimal stiffness. This was done for cases with two and three stiffeners. Using this ratio, similar numerically obtained optimal stiffnesses were found for the two and three stiffener cases. Therefrom was concluded that, using this ratio, the optimal stiffness could be described independent of the amount of stiffeners. This relationship was researched for different values of b_1. This research discovered that if the height of the loaded subpanel is low, increasing the thickness of the web has a higher influence on the optimal stiffness than when the height of the loaded subpanel was high. The influence between the optimal stiffness and between the ratio is increasing linearly when keeping the

$b_1$value constant. This relationship was converted into a formula, once for the LBA and once for the GMNIA. The GMNIA formulation gives the highest optimal stiffnesses and thus was chosen as the formula to describe the optimal stiffness of a stiffener. Using this formula, one can describe if a stiffener is “weak” or “strong” . This is important to predict the failure mode that will happen. If a stiffener is “weak”, a global buckling failure mode will occur. If a stiffener is “strong”, with a stiffness equal or higher than the optimal one, a local buckling failure mode will happen. This classification helps to further improve the design method of determining the patch load resistance.

Even though this thesis gives a new proposal for the classification of stiffeners, a lot of further research needs to be done. The trends observed for the b_1/t_w ratio in function of the optimal stiffness are determined using only three different values for the thickness of the web and four different values for the height of the loaded subpanel. The proposed equation (eq. 4.9) ,for determining the optimal stiffness of a longitudinal stiffener, could be improved if more points would be investigated. When doing this, the trends will be more clear and more accurate which would improve the accuracy of the proposed equation. There is also a second observation that could be clarified by adding more points into the investigation. There is a change in failure mode noticeable between the cases where t_w = 18mm and between the cases where t_w = 6mm or 9mm. For the 6mm and 9mm cases, there is an elastic failure mode visible. This can be seen by the fact that the optimal stiffness points for the LBA and GMNIA methods are almost identical for these thicknesses of the web. When reviewing the thickness of the web for 18mm, the GMNIA method points gives a higher optimal stiffness than the LBA method points. This can be explained by the fact that there is a plastic failure happening when the thickness of the web becomes thicker. The point where this failure mode changes could be determined more precisely, when more points are investigated. This could also help to further predict the precise failure mode which will occur.

It is verified in this study that the presented equation is valid for one, two and three stiffeners. However, when using only one stiffener the presented equation overestimates the optimal stiffness which shows that the equation could still be improved in this case, despite the fact that most bridges are built using more than one stiffener. It could also be verified in further research if the equation is usable for girders having more than three longitudinal stiffeners. Another limitation that is applicable on this formulation is that it is only valid for one stiffener cases when the failure is happening in the upper subpanel. This limitation could be researched more in depth and criteria could be made to specify this domain.

This investigation also proved that h_w had an impact on the patch loading resistance of longitudinally stiffened girders. Here it may be concluded that the formulation now presented in the Eurocode describes this influence correctly, but gives a gross underestimation of its optimal stiffness. This parameter should be investigated more in depth to make a new formulation based on this parameter.

References

[1] "Eurocode 3: Design of steel structures, Part 1-5: General Rules, Supplementary rules for planar plated structures without transverse loading," 2006.

[2] B. Kövesdi and L. Dunai, *Patch loading resistance of girders with longitudinally stiffened webs (powerpoint),* Munich, Germany, 2019.

[3] M. Clarin, *Plate buckling resistance - Patch loading of longitudinally stiffened webs and local buckling,* Lulea university of technology, 2007.

[4] M. R. Hirmand, E. Rahimi, A. Moghadam and H. T. Riahi, "A Mathematical Investigation on the Optimum Design of the Nose-Deck System in Incrementally Launched Bridges," *European Journal of Scientific Research,* vol. 1, no. 108, pp. 38-52, 8 2013.

[5] M. Seitz, *Tragverhalten längsversteifter Blechträger unter quergerichteter Krafteinsleitung,* Germany, 2005.

[6] Á. László, *MSc diplomamunka: Hosszbordával merevített acél szekrény keresztmetszetű tartó beroppanási vizsgálata,* Budapest: Budapesti Műszaki és Gazdaságtudományi Egyetem, 2012.

[7] S. Aleksic, M. Rogac and D. Lucic, "Analysis of locally loaded steel plate girders Model for patch load resistance," *Elsevier,* no. 89, pp. 153-164, 2013.

[8] A. Cevik, "A new formulation for longitudinaly stiffened webs subjected to patch loading," *Elsevier,* no. 63, pp. 1328-1340, 2007.

[9] J. Gozzi, *Patch loading resistance of plated girders - ultimate and serviceability limit state (PhD thesis),* Lulea University of Technology - Sweden, 2007.

[10] R. Chacon, M. Bock and E. Real, "Longitudinally stiffened hybrid steel plate girders subjected to patch loading," *Elsevier,* no. 67, pp. 1310-1324, 2011.

[11] C. Graciano, "Ultimate resistance of longitudinally stiffened webs subjected to patch loading," *Elsevier,* no. 41, pp. 529-541, 2003.

[12] C. Graciano and B. Johansson, "Resistance of longitudinally stiffened I-girders subjected to concentrated loads," *Elsevier,* no. 59, pp. 561-586, 2003.

[13] B. Kövesdi, *Patch loading resistance of slender plate girders with longitudinal stiffeners,* Hungary: Budapest University of Technology and Economics.

[14] British Standard Institution, *BS 5400-3: Steel, concrete and composite bridges,* London: BSI, 2000.

[15] K. Janus, I. Karnikova and M. Skaoud, "Experimental investigation into the ultimate load behaviour of longitudinally stiffened steel webs under partial edge loading," *ACTA Technica CSAV,* no. 2, pp. 158-195, 1986.

[16] C. Graciano, "Patch loading resistance of longitudinally stiffened girders - A systematic review," *Elsevier,* no. 95, pp. 1-6, 2015.

[17] SIA, *SIA 161: Construction métalliques,* Zurich: Société suisse des ingénieurs et des architects, 1991.

[18] J.-P. Lebet and M. A. Hirt, *Conceptual and Structural Design of Steel and Steel-Concrete Composite Bridges,* Lausanne, Switzerland: CRC Press, 2013.

[19] Aermican Association of State Highway and Transportation Officials, *LFRD Brdige Design Specifications,* Wachingon, D.C, USA: AASHTO, 2012.

[20] O. Lagerqvist and B. Johansson, "Resistance of I-girders to concentrated loads," *J. Constr. Steel Res. 39 (2),* pp. 87-119, 1996.

[21] L. Davaine, Formulation de la résistance au lancement d'une âme métalliaue de pontraidie longitudinalement, 2005.

[22] C. Graciano and O. Lagerqvist, "Critical buckling of longitudinally stiffened webs subjectoed to compressive edge loads," *J. Constr. Steel Res. 59 (9),* pp. 1119-1146, 2003.

[23] B. Kövesdi, B. Mecséri and L. Dunai, "Imperfection analysis on the patch loading resistance of girders with open section longitudinal stiffeners," *Elsevier,* pp. 195-205, 2017.

[24] C. Graciano and B. Edlund, "Failure mechanism of slender girder webs with longitudinal stiffener under patch loading," *Journal of constructional Steel Research,* no. 59, pp. 27-45, 2003.

[25] C. Graciano, "Patch loading resistance of longitudinally stiffened steel girder webs," 2002.

[26] S. Walbridge and J.-P. Lebet, "Patch loading test of bridge girders with longitudinal web stiffeners.," *Rapport d'essais Ecole Polytechnique Fédérale de Laussane, ICOM 447,* 2001.

[27] C. Graciano and J. Mendes, "Elatic buckling of longitudinally stiffened patch loaded plate girders using factorial design," *Elsevier,* no. 100, pp. 229-236, 2014.

[28] C. Graciano and B. Edlund, "Nonlinear FE analysis of longitudinally stiffened girder webs under patch loading," 2001.

[29] ANSYS®v17.2, *ANSYS Inc.,* Canonsburg, USA.

[30] C. Graciano and A. Felipe Uribe-Henao, "Strength of steel I-girders subjected to eccentric patch loading," *Elsevier,* no. 79, pp. 401-406, 2014.